Design Optimization of Cable-Stayed Bridges

by

Georgios Bessas

Diploma in Civil Engineering (2005)

National Technical University of Athens

Submitted to the Department of Civil and Environmental Engineering
in Partial Fulfillment of the Requirements for the Degree of
Master of Engineering in Civil and Environmental Engineering

at the

Massachusetts Institute of Technology

June 2006

Signature of Author.....
Department of Civil and Environmental Engineering
May 12, 2006

Certified by .....
Jerome J. Connor
Professor of Civil and Environmental Engineering
Thesis Supervisor

Accepted by .....
Andrew J. Whittle
Chairman, Departmental Committee for Graduate Students

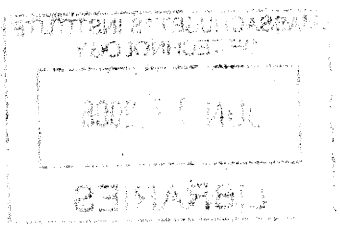

DESIGN OPTIMIZATION OF CABLE-STAYED BRIDGES

by

GEORGIOS BESSAS

Submitted to the Department of Civil and Environmental Engineering
on May 12, 2006 in partial fulfillment of the
requirements for the Degree of Master of Engineering in
Civil and Environmental Engineering

ABSTRACT

The goal of this thesis is to achieve a basic understanding of cable-stayed systems. Issues to be treated are the diachronic evolution of cable-stayed bridges, including the advantages, the limitations and the basic design concepts of these indeterminate systems.

During this project, the design of typical cable-stayed bridges is optimized with computer-based simulation capabilities contained within the SAP2000 computer software system. The analysis strategy starts with the analyses of ten different 3D models under earthquake loading. The numerical results of the analyses form the basis for the optimization of the bridges' designs.

This study has indicated that for the specific design examined, the optimum cable spacing is: 13.2m and 12.39m for equivalent steel decks with bending rigidities of IEequiv=3.25*105 kN*m2 and IEequiv=2.25*105 kN*m2 respectively. The procedure also identified the advantage of using bracing on the top half of the towers.

The final part of this thesis concerns a case-study of the Rion-Antirion cable-stayed bridge. This includes the creation of an appropriate computer model as well as the proper examination of the quasi-static behavior of the bridge.

Thesis Supervisor: Jerome J. Connor

Title: Professor of Civil and Environmental Engineering

Acknowledgments

I am greatly indebted to Professor Jerome Connor for his invaluable assistance and counsel during the time of research, preparation and writing of this thesis. He has been most helpful since the first day of this difficult process. His wisdom and knowledge have been very instructive.

I would also like to thank my parents, who have been very supportive for all my years of education. Their encouragement and their moral support throughout the academic years have been endless.

Furthermore, I would like to thank Anna-Maria for her precious help in editing the text and her support through the entire duration of my studies abroad, Charis for supplying valuable information that facilitated the fulfillment of this thesis and a number of others who contributed either a little or a lot.

Finally, I would like to mention that I am grateful to my MEng classmates and all the new people I met here, in my new life, for making the time we passed together this year exceptionally pleasant and a really unique experience which I would never wish to have missed.

TABLE OF CONTENTS

LIST OF TABLES

LIST OF FIGURES

LIST OF IMAGES

CHAPTER 1
INTRODUCTION

In this chapter, the objective of the thesis is presented at the very beginning. The definition of the basic terms and the methodology of the thesis subject are analyzed and finally, a brief presentation of the next chapters is given.

1.1 Objective of the thesis

The goal of this research is the optimization of the design of a typical cable-stayed bridge. An overview of cable-stayed bridges and the basic concepts for their design are presented. Afterwards, a model of a typical cable-stayed bridge with a main span of 500m is created and, through structural analysis with computer simulation models, an optimum design for the cables arrangements and the stiffness of the deck is obtained.

1.2 Definition of a cable-stayed bridge

Two piers and one beam form the simplest bridge. This design concept currently can achieve a maximum single span of 250 meters.

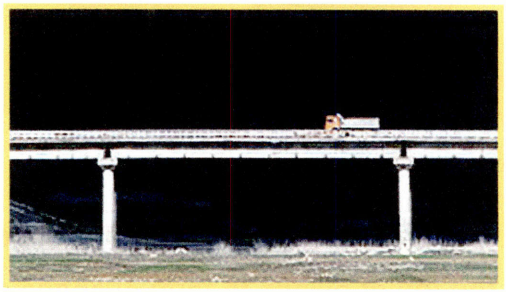

Image 1.1 Beam bridge example[1]

[1] Capture by http://www.gefyra.gr

When necessary, piers and beams are added to form a continuous span viaduct without limited length, the world record being the Lake Ponchartrain causeway in the United States with about 38 km length (Image 1.2).

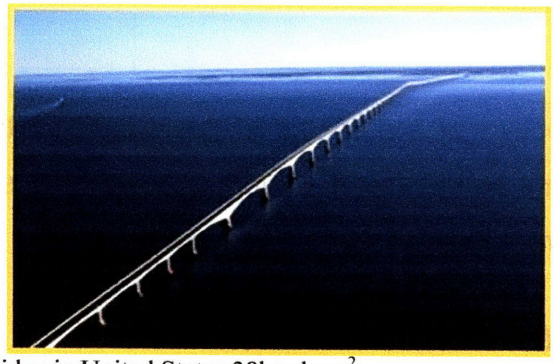

Image 1.2 Lake Ponchartrain Bridge in United States 38km long[2]

Another traditional technique consists in suspending the bridge from two cables anchored at the ends. It results in a simple structure that is used to cross deep gorges where no pier can be built (see Image 1.3).

Image 1.3 Traditional bridge suspended by ropes[3]

In the nineteenth century, men were seeking to span longer distances and devised ways to raise the cables to the top of pylons to form suspension bridges. This technique

[2] Capture by http://www.gefyra.gr
[3] Capture by http://www.gefyra.gr

achieves the longest single span, the world record being the Akashi Kaikyo in Japan with a single span of 1,991 meters (Image 1.4).

Image 1.4 Akashi Kaikyo suspension bridge in Japan with a single span of 1,991 meters[4]

However, when sufficient anchorage for the suspension cables is not available at crossing ends or for economical reasons, the cable-stayed technique developed in Europe during the fifties, may be used (Image 1.5). The deck is then suspended through stay cables to a pylon in a balanced and aesthetic way.

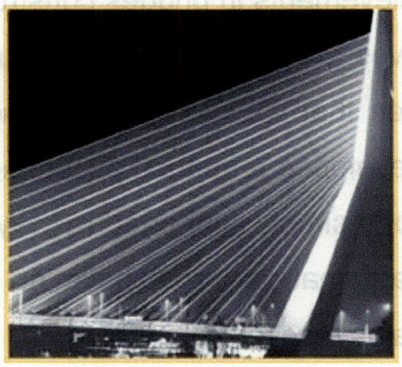

Image 1.5 Typical cable-stayed bridge[5]

The equilibrium of the structure lies independently on each and any pylon and thus, cable-stayed bridges may indifferently have one, two, or more pylons, as for the four-pylon Rion-Antirion cable-stayed bridge.

---

[4] Capture by http://www.gefyra.gr
[5] Capture by http://www.gefyra.gr

Image 1.6 Normandy Cable-Stayed Bridge[6]

Bridge Type	Main Span	Longest bridge
Simple Beam	Up to 250m	
Steel Box/Plate Girder	Up to 300m	Ponte Costa e Silva, Rio de Janeiro, Brazil (300m)
Prestressed Concrete Girder	Up to 330m	Shibanpo, Chongqing, China (330m)
Concrete arch	Up to 420m	Wanxian, Wanzhou, China (420m)
Steel Arch	Up to 550m	Lupu, Shanghai, China (550m)
Steel Truss Girder	Up to 550m	Pont de Quebec, Quebec City, Canada (549m)
Cable-stayed	200m-1100m	Sutong Bridge, China (in progress 1088m)
Suspension	700m-2000m	Akashi Kaikyo Bridge, Japan (1991m)

Table 1.1 Types of bridges and typical spans

Table 1.1 summarizes the achievements in bridges construction today. It is clear that as technology of materials improves those numbers will go up. Already, the active control application to structures proves that we can increase the spans by much more. For example, Sobek (2006) has developed a method according to which by only measuring the reactions at the supports of a simply supported railway beam bridge it is possible to adjust the deck's geometry automatically and have no deflection even with a very slender deck at the time the trains crosses its opening.

[6] Capture by http://www.gefyra.gr

1.3 Methodology

During the present study, a brief research of the evolution of cable-stayed bridges has been conducted. The design concepts of cable-stayed bridges are discussed and these concepts are used in order to create the layout of a typical cable-stayed bridge.

This design was used to create a computer simulation model for simulating the structural behavior of the bridge subjected to a specific earthquake. The response of the bridge was evaluated carefully. Then several different models were generated and they were used to optimize the behavior of the bridge with respect to the vertical displacements of its deck.

1.4 Structure of the thesis

Basically, the thesis consists of three parts. The first part, which consists of chapters 2 and 3, includes a research on the topic of cable-stayed bridges. The evolution of cable-stayed bridges over the centuries up to the most recent designs of the twenty first century is examined.

The second part of the thesis treats the design optimization of cable-stayed bridges. A typical cable-stayed bridge is designed and several modifications of the basic design are created. After running computer simulations using SAP2000 structural analysis software it was possible to optimize the behavior of the bridge with respect to vertical displacements. Optimum values were found for both the spacing of the stays and the stiffness of the deck.

1.5 Next chapters guide

In the second chapter it is presented an analysis of the evolution of cable-stayed bridges. The research starts from the conception of the idea of cable-stayed structures even B.C. from the Egyptians and ends with the twenty first century's cable-stayed bridges.

Chapter number three presents the design concepts for cable-stayed bridges. All the possible designs for cable-stays and the bridge deck are evaluated. Advantages and disadvantages for each one are listed, and finally, the most promising designs are pointed out.

In chapter four, the design of typical cable-stayed bridges is optimized with computer-based simulation capabilities contained within the SAP2000 computer software system. The analysis strategy is defined initially, and then analytical results for optimum cable spacing and stiffness are derived and presented.

Chapter five cable-stayed bridge, the Rion-Antirion Bridge. A finite element model has been created in order to study the behavior of the bridge, through static structural analysis. The loads applied to the model are dead loads, live loads and the design earthquake response spectrum.

Finally, the last chapter summarizes the results of the analysis and concludes to ideas that can lead to further research in the field cable-stayed bridges.

CHAPTER 2
DIACHRONIC DEVELOPMENT OF CABLE-STAYED BRIDGES

The purpose of this chapter is to present an analysis of the evolution of cable-stayed bridges. The research starts from the conception of the idea of cable-stayed structures from the years B.C. by the Egyptians and ends with the twenty first century's cable-stayed bridges.

2.1 The first stayed structures

The idea of cable-stayed system has been conceived by engineers a very long time ago. The earliest application can be tracked back to the ancient Egyptian period when inclined ropes were running from the ship mast to support a beam as shown in Image 2.1. Primitive types of cable-stayed bridges were found B.C. in Borneo and Laos. These small pedestrian bridges were supported by inclined vines attaching to trees on both sides of the abutment (Troitsky, 1988). Even though these primitive structures suggested an early understanding of the stayed system, records of stayed bridges did not appear again before the 17th century (Amornvivat, 1996).

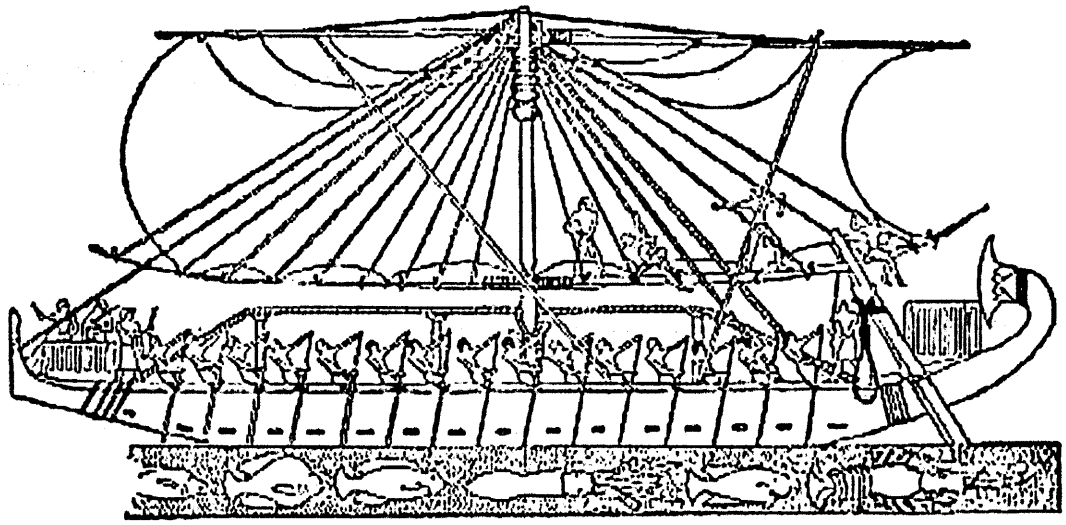

Image 2.1 Egyptian Queen Halshepsut's expedition ship in 1493 B.C.[1]

In Europe, the interest in bridges with stays was initiated in 1617, when Faustus Verantius, a Croatian engineer, proposed a bridge supported by several chain stays but it was not until the late 18th Century that such bridges were actually built (ESDEP Lecture, 2006). The first cable-stayed system ever built was by C.J. Loscher, a German carpenter, in 1784. His design consisted of a wooden deck supported by a wooden tower and stays.

[1] Capture by http://www.unb.ca

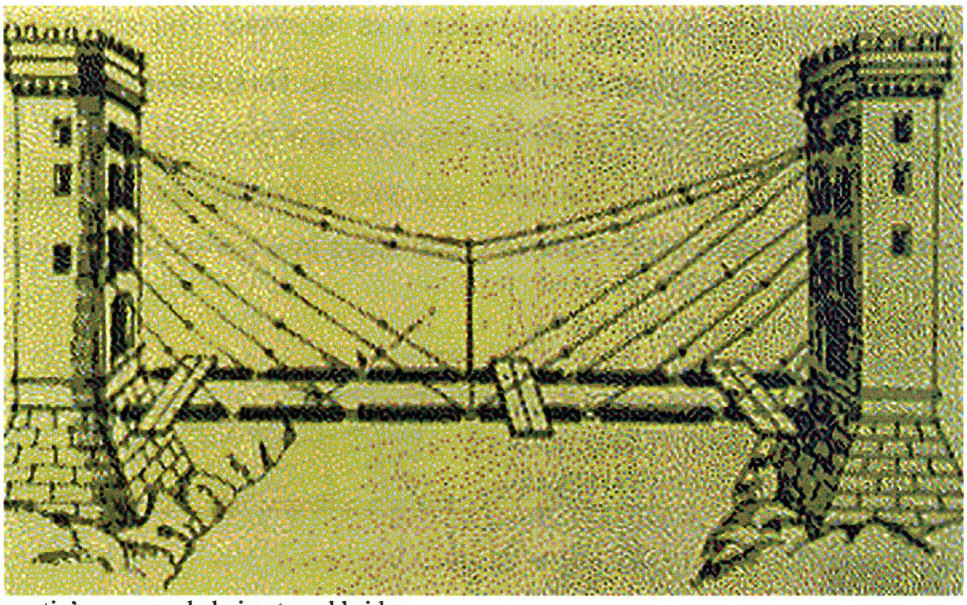

Image 2.2 Verantiu's proposed chain-stayed bridge

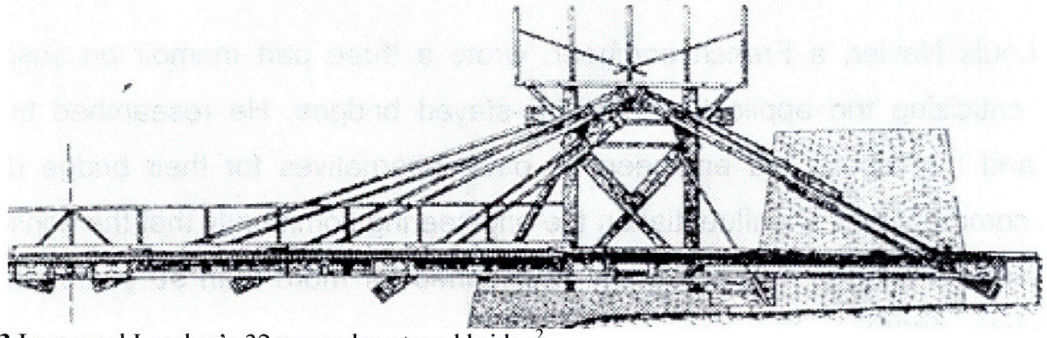

Image 2.3 Immanuel Loscher's 32m wooden-stayed bridge[2]

Further development took place in 1817, with the English engineers, Redpath and Brown, who designed the Kings Meadow footbridge with a span of 33.6m. In 1821 Poyet, a French architect, suggested a very steep fan-type (radial) steel bar-stayed bridge for a prestigious French undertaking. These bridges were the first signs of a burgeoning cable-stayed revolution. This revolution in cable-stayed bridges would have continued but for the collapse of two bridges in 1818 and in 1824. The first one, the 79m pedestrian Tweed River bridge near, Dryburgh-Abbey, England, collapsed six months after completion due to fatigue failure of the chain stays subjected to severe wind

[2] Captured by http://www.lmc.ep.usp.br/

oscillations (Troitsky, 1988), for which no cause was reported. The second, 78m Saale River bridge in Nienburg, Germany, collapsed in 1824. This collapse was reported to have been caused by an unusual crowd loading during a river festival, a load that was not expected (Ponaldy, 1986). The first harp-type stayed bridge was proposed by Hatley in 1840, an English engineer, which utilized chain stays in a parallel configuration.

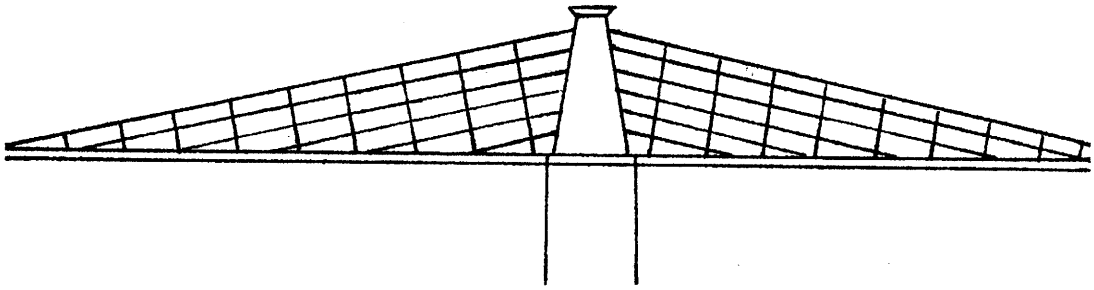

Figure 2.1 Harp configuration by Hatley (1840)

Claude Louis Navier, a French engineer, wrote a three part memoir on suspension bridges, criticizing the application of cable-stayed bridges. He researched the early failures and his reports led engineers to other alternatives for their bridge designs. Navier's comment was so influential on the engineering community that the construction of cable-stayed bridges was practically abandoned for more than 50 years (Billington and Deodatis, 1991).

The lack of technical knowledge in the theoretical analysis of the internal forces in the stays, the inappropriate materials and the inability of the engineers to understand the behavior of this type of bridges, lead the structures to fail miserably. High stiffness materials, unavailable in those early constructions, were later introduced and, finally, made it feasible to construct a safe cable-stayed system.

2.2 Nineteenth Century

Even though cable-stayed bridge constructions were absent due to adverse criticism from Navier, the principle of using the stays to support a bridge superstructure was still

practiced in the nineteenth century. This was due to a great American bridge engineer named John Roebling who incorporated the stays concept into his designs of suspension bridges. These types of bridges were named later stayed-suspension bridges (Buonopane, 2006). Roebling's motivation came following the tragic collapse of the suspension bridge across the Ohio River at Wheeling, due to wind reaction in 1854.

Roebling and Sons Company understood the need of a stiff deck to prevent oscillations from the wind. Niagara Falls Railroad Bridge (Image 2.4), made by Roebling, was the first stayed-suspension bridge carrying railway loads. In 1855, the First Minneapolis (Image 2.5) stayed-suspension bridge, made by Thomas Griffith, had stays that were not designed to carry any load.

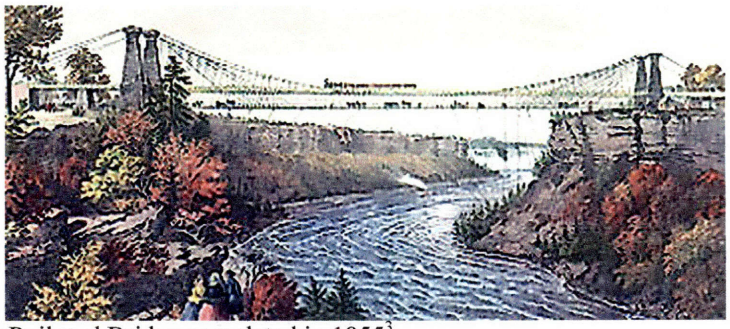

Image 2.4 Niagara Falls Railroad Bridge completed in 1855[3]

[3] Captured by http://home.pcisys.net/~ronkrob/currier2.htm

Image 2.5 First Minneapolis suspension bridge[4]

Near the end of the nineteenth century, the Brooklyn Bridge (Image 2.6), which has a main span of 486m, was one of the most impressive structures of this time when it opened to traffic, in 1883. Roebling used the stays to add rigidity to the span and also took advantage of the additional load carrying capacity which the stays supplied. There were also a few stayed-suspension bridges in France in the late nineteenth century made by a famous engineer named Arnodin. His work included the bridge over the Saone River at Lyons, completed in 1888, with a main span of 121m as well as the Rhone River Bridge at Avignon, completed in 1888.

[4] Captured by Buonopane Paper (2006)

Image 2.6 East River (now called Brooklyn Bridge) completed in 1883[5]

2.3 Twentieth century

It was time for the technological evolution and the advancement of analytical theories for statically indeterminate structures to overcome the problems associated with cable-stayed bridges and to make this type of bridges a viable alternative for bridge design.

2.3.1 France

At the early part of the twentieth century, a French engineer named Gisclard proposed a new system consisting of inclined and horizontal cables. The system represented three-hinged arch, having the diagonals made of cable trusses. This is known as the Gisclard system and found wide application in France and its former colonies. An example of a Gisclard system bridge is the Cassagne Bridge (Image 2.7) completed in 1907 and having a main span of 156m. In 1925, another French engineer, named Leinekugel le Cocq, further developed the Gisclard system and proposed the Lezardrieux Bridge

[5] Captured by Reis (2006)

(Image 2.8) which has stays from both towers overlapping. This system proved to be very economical and also gave only small deflections (Troitsky, 1988). This bridge became the prototype of the contemporary cable-stayed bridges, which have a fan-system (radial) of cables.

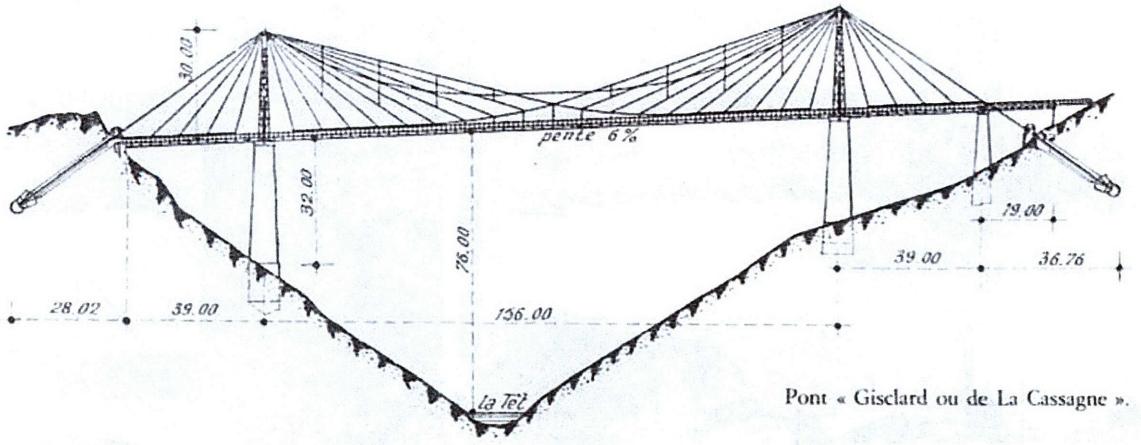

Image 2.7 Cassagne bridge completed in 1907[6]

Image 2.8 Lezardrieux Bridge completed in 1925[7]

[6] Captured by Prade (1988)
[7] Captured by Structurae website (2006)

The plane steel-deck cellular cross-section, promoted by Leonhardt in 1936, was also a major factor which made the re-introduction of cable-stayed bridge possible. These steel plates acted as an upper chord of the transverse girders and also of the longitudinal main girders. With these plates, the entire deck would act as one continuous unit, including the towers supports. The continuous deck became a requirement for cable-stayed bridge. (Leonhardt, 1991)

In 1938, Franz Dischinger, a German engineer, discovered that the incorporation of cable-stays significantly reduce the bridge deflection under railroad loading (Ponaldy, 1986). He also pointed out that cables made of high-stiffness steel wire must be pre-stressed in order to minimize the softening effect of the sag in long cables (Leonhardt, 1991). His findings marked a significant step toward the modern era for cable-stayed bridges.

2.3.2 Germany

After the Second World War, 15,000 bridges in Germany had been destroyed. The need to rebuild these crossings provided the opportunity for engineers and builders to apply new concepts of design and construction. The cable-stayed bridge system was the most economical type of structure available, because of its lighter weight and the quick construction. Therefore, cable-stayed bridges became the favorite type of structure chosen for crossing spans, especially in Germany.

In 1952, Leonhardt designed the world's first modern cable-stayed bridge across the Rhine River in Dusseldorf (Image 2.10), but this bridge was not constructed until 1958. In 1955, the German firm Demag, in collaboration with Dischinger, ultimately erected the first contemporary cable-stayed bridge in the world, the Stromsund Bridge (Image 2.9), which has a main span of 183m (Podolny and Fleming, 1972). At present, cable-stayed bridges can be found in every country in Europe.

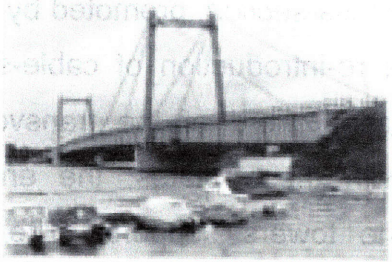

Image 2.9 Stromsund Bridge, the first modern cable-stayed bridge, completed in 1955[8]

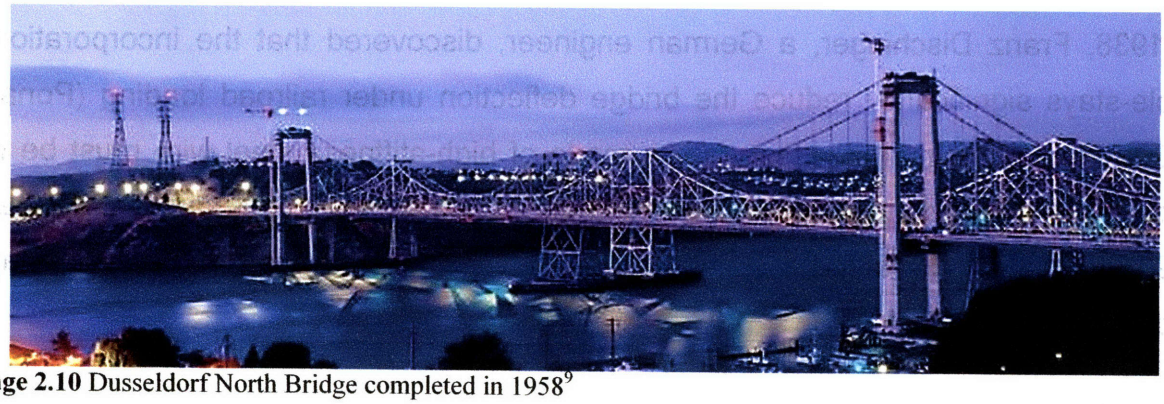

Image 2.10 Dusseldorf North Bridge completed in 1958[9]

2.3.3 Japan

In Japan, the engineers began to take cable-stayed bridges seriously in the 1960s (Amornvivat, 1996). The first Japanese's' attempt at modern cable-stayed bridge was the Kutsuse Bridge, which has a single span of 128m. The Kutsuse Bridge, completed in 1960, was the first contemporary cable-stayed bridge constructed outside of the sphere of the pioneering German technology. The number of cable-stayed bridge constructions in Japan has increased tremendously since the 1970s. As of 1991, Japan has one third of the total number of the world cable-stayed bridges (Ito, 1991). Most of the cable-stayed bridges in the country are constructed with steel for two reasons: the structures have to be able to withstand severe earthquake and steel is marketed at a reasonable price (Ito, 1991).

---

[8] Captured by Caprani thesis
[9] Captured by Structurae website, 2006

2.3.4 North America

The first contemporary cable-stayed bridge to be constructed in North America is the Menomonee Falls Pedestrian Bridge in Wisconsin. This bridge, designed by the Wisconsin Division of Highways Bridge Section with a center span of 66m, was built in 1971. The first vehicular cable-stayed bridge in North America was the Sitka Harbor Bridge, completed in 1972 in Alaska (Image 2.11) (Ponaldy, 1986). In North America, the number of cable-stayed bridge constructions has increased greatly in the past three decades (Tang, 1991).

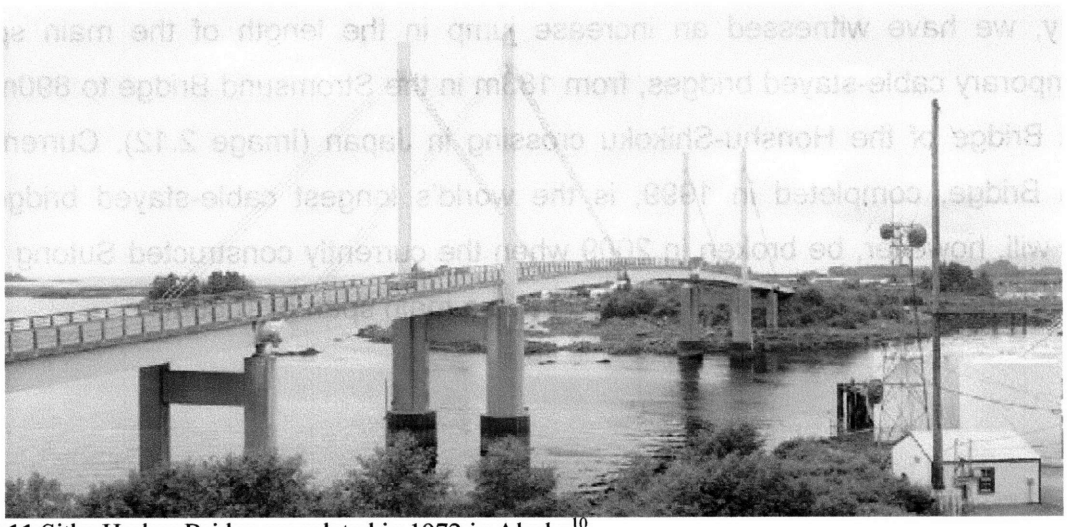

Image 2.11 Sitka Harbor Bridge completed in 1972 in Alaska[10]

2.4 Conclusions

Contemporary cable-stayed bridges have been constructed all over the world. Early iron bridge constructions assumed similar forms to those traditionally used for masonry and timber bridge constructions. Significant developments in iron and subsequently steel bridge construction have enabled longer spans, have improved the efficiency and, have offered greater elegance. These developments are associated with an improved understanding of structural behavior and material properties. Equally critical in this

[10] Captured by Structurae website, 2006

development has been the engineers' ability to create new design concepts and to perform sophisticated analyses. Developments in bridge construction have not been without failures though.

As the technology of bridge construction keeps improving, the engineers stand before a variety of options concerning the selection of the suitable materials and the design of each of the major bridge components. The design and construction of longer span becomes possible. The twenty first century will witness bridges with main span over the psychological limit of 1000m.

Already, we have witnessed an increase jump in the length of the main span for contemporary cable-stayed bridges, from 183m in the Stromsund Bridge to 890m in the Tatara Bridge of the Honshu-Shikoku crossing in Japan (Image 2.12). Currently, the Tatara Bridge, completed in 1999, is the world's longest cable-stayed bridge. This record will, however, be broken in 2009 when the currently constructed Sutong Bridge, China (Image 2.13) is completed as it will have a main span of 1088m.

Image 2.12 Tatare bridge, Japan is currently the longest cable-stayed bridge in the world with a main span of 890m[11]

These massive cable-stayed bridge structures suggest that constructions of an even longer span will occur in the future. There have already been several proposals for a possible construction of 1,100 to 3,000m long cable-stayed bridges (Endo, 1991). Even though those extreme lengths seem to be impractical for a cable-stayed bridge, it is clear that the future of cable-stayed bridges is very promising.

[11] Captured by http://en.wikipedia.org

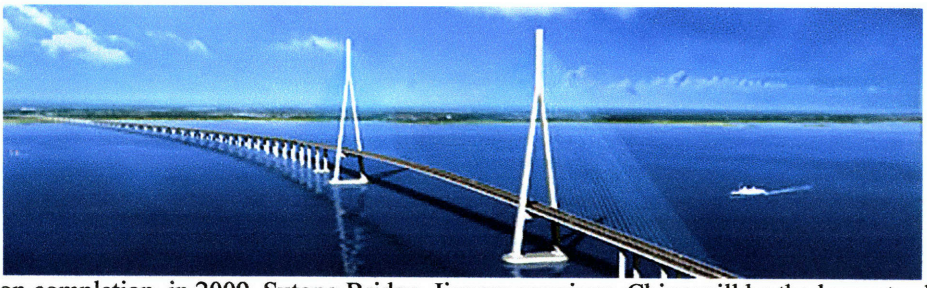

Image 2.13 Upon completion, in 2009, Sutong Bridge, Jiangsu province, China will be the longest cable-stayed bridge in the world with a main span of 1088m[12]

The summary of the evolution of cable-stayed bridges is illustrated in Table 2.1.

Evolution of cable-stayed bridges	
BC	Egyptian used ropes to support beam from their ship mast Primitive bamboo pedestrian bridges found in Laos and Borneo
1617	Verantius's chain-stayed bridge in Italy
1784	Loscher designed an all-timber-stayed bridge in Germany (32m main span)
1817	Redpath and Brown constructed the King's Meadow Bridge (34m main span)
1818	Tweed River Bridge constructed with inclined chains in England
1819	Tweed River Bridge collapsed under wind oscillation
1823	Navier published "Memoir on Suspension Bridge"
1824	Poyet designed a steep fan-type steel-bar-stayed bridge. Saale River Bridge was constructed (78m main span)
1825	Saale River Bridge collapsed under a crowd of people
1854	Suspension bridge at Wheeling Ohio collapsed due to wind reaction
1855	Roebling constructed the Niagara Falls Bridge, first railroad suspension bridge
1872	Albert Bridge was built by Ordish and Le Fleuve (122m main span)
1883	Roebling's Brooklyn Bridge opened to traffic. The contribution of cable-stays was realized
1888	Arnodin's Saone River Bridge completed in Lyons
1904	The Bonhomme Bridge in Marbihan was completed (163m main span)
1907	Gisclard system bridge was built in the Cassagne Bridge
1925	Lezardrieux Bridge employed overlapping cable stays
1936	Leonhardt introduced the use of orthotropic steel plate
1938	Dischinger realized that cables must be highly pre-stressed in order to minimize the sag
1952	Leonhardt designed the Rhine River cable-stayed bridge (not built until 1958)
1955	Stromsund Bridge, the first contemporary cable-stayed bridge, was completed in Sweden (183m main span)

[12] Captured by http://www.roadtraffic-technology.com

Evolution of cable-stayed bridges	
1960	Kutsuse Bridge, the first cable-stayed bridge in Japan, was built (single span of 128m)
1971	Menomonee Bridge, first contemporary cable-stayed bridge in the United States (main span of 66m)
1972	Sitka Harbor Bridge was completed in Alaska (first vehicular CSB in N. America)
1978	Parana Bridge was completed in Argentina (330m main span)
1984	Barrios de Luna Bridge was completed in Spain (440m main span)
1986	Annacis Bridge was completed in Vancouver (465m main span)
1990	Rama IX Bridge was completed in Bangkok, Thailand (450m main span)
1991	Ikushi Bridge was completed in Japan (490m main span) Skamsundet Bridge was completed in Norway (530m main span)
1993	Yangpu Bridge in Shanghai with the span of 602m
1995	Normandy Bridge was completed in France (856m main span)
1998	Tatara Bridge was completed in Japan (890m main span)
2004	Completion of Rion-Antirion bridge in Greece (the longest cable-stayed deck in the world of 2,250 meters in five spans)
2008	Stonecutters, Hong Kong, China (main span 1018m)
2009	Projected completion of Sutong Bridge in China (main span of 1088m)

Table 2.1 Evolution of cable-stayed bridges design (adapted by the author from Amornvivat, 1996)

CHAPTER 3
DESIGN CONCEPTS FOR CABLE-STAYED BRIDGES

This chapter presents the design concepts for cable-stayed bridges. All the possible designs for cable-stays and the bridge deck are evaluated. Advantages and disadvantages for each one are listed, and finally, the most promising designs are pointed out.

3.1 Cable stays

The cables can be arranged in various configurations both in longitudinal and transverse directions. As they determine the behavior of the bridge, the cable stays are the most distinguishing feature of the bridge (White, 1975).

As previously mentioned, the stiffness of the structure is highly dependent on the stiffness of the cables, but deficiencies in cable stiffness can be compensated for by various methods. An alternative is to fix the top cable on the side spans to abutments. This would greatly reduce the horizontal deflection of the tower and thereby increase the stiffness of the structure.

At this point, it is appropriate to mention that the major advantage of the cable-stayed system over suspension bridges is that there is no requirement for massive foundations to anchor the cables at each end of the span[1]. Therefore, it is possible that site requirements may not allow anchoring the top cable to side abutments or even it is not

[1] Although, recently the design of the replacement of the San Francisco-Oakland Bay Bridge east span by T.Y. Lin International expands the horizons of the suspension bridges design. It's the first bridge incorporating a self-anchored suspension section but with only 160m length is not very long.

preferred economically to do so. An excellent solution is to anchor each of the cables on the side spans to piers.

In the following paragraphs the different arrangements are outlined both in the longitudinal and transverse direction.

3.1.1 Longitudinal Arrangements

Historically, the longitudinal arrangement has been categorized into two main types, the fan (radial) and the harp type. Most bridges to date employ either one of these systems or a combination of the two. Other systems such as the star pattern and other asymmetrical shapes have been successfully utilized to enhance the appearance of the structure as well as to satisfy various site requirements.

The major criterion in determining the most appropriate arrangement of the stays is the provision of sufficient stiffness to the main bridge girder in an efficient and aesthetically pleasing manner. It is a common knowledge that the cables work more effectively when they form angles between 25°-65° with the deck.

3.1.1.1 Fan (radial) shape

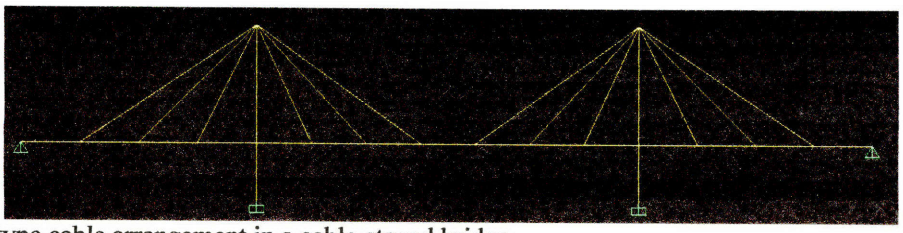

Figure 3.1 Fan-type cable arrangement in a cable-stayed bridge

In the fan cable-stayed bridge design, the cables fan outwards from the tower to the deck as if from the handle of a fan (Figure 3.1). From the engineering point of view, the fan shape is most efficient since it transfers the vertical load from the deck to the towers with the minimum amount of steel and with the lowest horizontal thrust to the girder. Structurally, this system is ideal because it minimizes the bending moment established in the towers.

In addition, with all the cables attached to the tower at one point, the fan type has the advantage of requiring only one cable anchorage in the tower. However, this system is not practical for a multiple stay bridge because cables connection at the top of the tower can become very congested. Usually, radial bridges would have at most two to three stays.

Unfortunately, the fan type does not offer the best solution in terms of aesthetics. In the event that towers and cable supports are required on both sides of the deck, the cable lines intersect when the bridge is viewed from most angles. This detracts a great deal from the appearance of the structure and has led many designers to lower the interior anchorages from the top of the tower. In fact, only two radial type cable-stayed bridges have been built since 1980.

3.1.1.2 Harp system

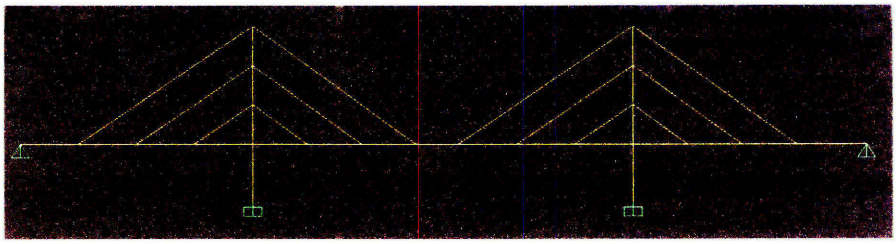

Figure 3.2 Harp cable arrangement in a cable-stayed bridge

In this design, cables radiate at a uniform distance from each other throughout their length (see Figure 3.2). The cables are spaced uniformly along the tower height and also along the girder, giving an excellent stiffness to the main span (Troitsky, 1988). The connection of the cables to the towers is much easier than it is in the radial system. It is generally more aesthetically pleasing but has one major disadvantage. Large bending moments are produced in the towers by anchoring the cables at different levels.

These bending moments can be greatly reduced by allowing the cables' horizontal movement at the tower connection. Due to the friction at the anchorages and the eccentricity of loads applied to the towers, the bending moment produced cannot be

neglected. Also, by allowing the movement of the cables, the stiffness of the overall structure is reduced. Even with the disadvantage of high bending moments in the tower, the harp configuration is still very appealing to bridge designers, because of its aesthetic pleasure due to the minimization of the visual intersection of cables from oblique angle.

3.1.1.3 Semi-fan arrangement

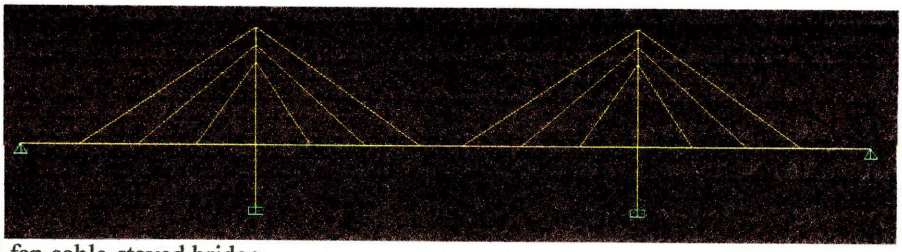

Figure 3.3 Semi-fan cable-stayed bridge

This is a style of cable-stayed bridge (Figure 3.3) which combines the fan and the harp. To minimize the bending moment which occurs in the harp system, the semi-fan arrangement has all the cables concentrated on the top half of the tower, making these cables unparalleled. The appeal of this configuration lays to the fact that multiple stays systems have steadily become more popular than systems with only a few stays (where the radial system would be most appropriate). Moreover, the semi-fan bridge is easier to design than the harp system, especially when there are many cables involved along the tower. The semi-fan has become the most popular choice among the engineers, especially when the main span of the cable-stayed bridge exceeds the 200m.

3.1.2 Cable plane and towers

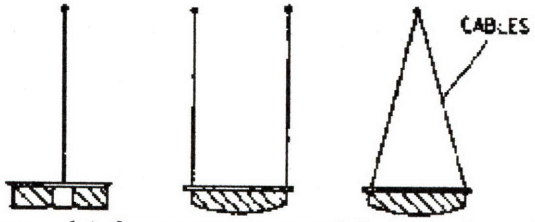

Figure 3.4 Single plane, double plane and A-frame arrangement of the cables in a cable-stayed bridge

In the transverse direction, there are three basic configurations for the cables; the single plane, the double plane and the A-frame (Figure 3.4). There are also few cases where arrangements that are more complicated or even a combination of the possibilities above apply (Image 3.1).

Image 3.1 The cable-stayed bridge over Charles River in Boston, MA[2]

It is a common practice to create bridge with ratios between main span and tower height from five to six. This design offers the most economical solution. However, in concrete deck bridges it is possible to design with a little higher ratio in order to take advantage of the concrete beneficial behavior under compression.

3.1.2.1 Single plane

In a single plane system, a plane of cables passes through the median of the bridge's cross-section. The single plane system has been used in many recent designs. This system offers great aesthetical advantages due to the overall impression of lightness and the unobstructed view obtained for the motorists by locating the towers in the center of the deck. Any visual crossing of the cables is therefore avoided.

[2] Captured by http://www.massturnpike.com

This arrangement is most suitable for divided highways for which the required central meridian strip is an excellent location for the towers and cable anchorages. The major disadvantage of this system is that the cables do not supply any rotational restraint to the deck and therefore the deck must have high torsional rigidity in order to carry the torsional moments induced by eccentric loadings. Due to this requirement, an excessive amount of material may be needed, either for reinforcement or stiffening of the deck structure.

The Sunshine Skyway bridge (Image 3.2) is an example of one of the first single-plane bridges that in 1988 won the prestigious Presidential Design Award of the National Endowment for the Arts.

Image 3.2 Sunshine skyway bridge in Tampa, FL[3]

3.1.2.2 Double plane

The double plane system has been used the most, especially for spans greater than 400m because of its high torsional rigidity. The minimum dimension of the deck is governed by the transverse moment and by the considerable point load introduced at the anchorages.

The A-frame is more appropriate for very long-spans (see Image 2.13) because it supplies more torsional restraint to the deck and it has much more lateral resistance

[3] Capture by http://www.fhp.state.fl.us

both from the cables and from the frame action in the towers. An A-frame or even a delta frame of the towers, applies an inclined fashion for the cables which offers more lateral and torsional rigidity to the deck. This way a transverse bracing may be considered as redundant.

3.1.3 Conclusions

As can be seen from the precedent analysis, the more typical cable-stayed bridges constructed nowadays are based on a semi-fan cable arrangement with a double plane for the cables. For openings greater than 500m A or delta frame for the towers are often chosen. It is a common knowledge that the deflections for the towers should be limited to H/80.

The spacing of the cables in cable-stayed bridges is a very important factor when determining the cables' arrangements. Early structures such as the Papineau Bridge in Quebec and the Knie Bridge in Germany, which were both constructed in 1969, only had a few cables at large spacing. Thick and stiff girders were required to support the local bending moments between the cables in these bridges. The advantages of closely-spaced cables were first recognized by H. Homberg in 1964, when he designed the Bonn Bridge using a cable spacing of only 2.24m across 280m main span. Close cable spacing also allows smaller individual cables and more slender deck. Nowadays, common practice is the use of a cables spacing between 8m and 15m.

3.2 Deck

Generally throughout the world, steel is the most popular material used in cable-stayed bridges deck. More specifically, in case of spans of more than 450m, in areas with frequent severe earthquakes or in an area with soft ground, steel girders are preferred as they perform better under dynamic excitations (Ito, 1991). Concrete sections are a viable alternative, although they are much heavier and therefore are not often used in long-span bridge design. The deflections for bridges' deck are set by AASHTO

(American Association of State Highway and Transportation Officials) to be less than L/800m.

The continuous support that the cables provide along the deck allow for a much shallower and lighter deck support system, as compared to other bridge designs. The total depth of the cable-stayed bridge deck usually ranges from 2 to 4 meters for highway bridges and from 4 m to 6.5 m for railroad bridges. The depth is almost independent of the length of the main span and is basically a function of the dead to live load ratio and of the side to main span ratio. Experience gained from past designs indicates that for an optimum use of cable stiffness, a side to main span ratio of approximately four tenths is desirable (White, 1975).

It has been the practice of many engineers to limit the deflection to span ratio on bridge designs. This may prove to be a harsh restriction for the cable-stayed bridge system. Although the total deck deflection may be substantial under large distributed loadings, the cables are in a high stress state and therefore the stiffness of the structure is at a maximum. Due to the cable supports and the continuous main girder, the deflection under concentrated loads is much smaller for the cable-stayed system than for other systems. Therefore, another important criterion for the design is the change in slope of the deflection curve and the resultant bending moments. The present limitations on deflection to span ratio may place unjust restrictions on design.

The main girder must carry large axial loads, transmitted by the cables, in addition to the vertical deck loadings. For all bridge designs to date, the axial load is compression which requires that the non-linear beam-column effects be taken into account in the final analysis. The anchorage of the deck at the ends of the side spans with the placement of expansion joints in appropriate positions has been proposed (Grimsing and Neils, 1966) in order to decrease the horizontal thrust transmitted to the girder. In this scheme, either part or the entire main girder will be in tension. Increased stiffness and material savings in the deck structure are the major advantages of this system.

3.3 Conclusions

The application of the cable-stayed system as a bridge design has come into prominence in recent years. Many of the problems that arise in the design are associated with the major advantages of the system. The multiple cable supports and the continuous deck constitute a high degree of indeterminacy and together with the non-linear cable stiffness and beam-column effects they lead to a very laborious analysis. Fortunately the computer power today can easily handle those difficulties. The material and construction savings far outweigh the disadvantages pf detailed computations. Also, the aerodynamic problems associated with long-span bridge design are minimized by the use of the shallow, streamlined deck.

It is essential that the engineer recognizes the interdependence of the structural components and the behavior of the entire system. The behavior of the overall structure is dependent on the stiffness of the individual components. A change in the design of the towers, cables or deck may significantly affect the response of all three of the major bridge components. Therefore, it is most important that all options are considered in the design.

The study of cable-stayed bridges is an excellent field for the application of innovative techniques in design, detailing and construction. The practical bridge designer must first satisfy the functional requirements and, on this basis, produce an aesthetically pleasing structure.

CHAPTER 4
OPTIMIZATION OF TYPICAL CABLE-STAYED BRIDGES

In this chapter, the design of typical cable-stayed bridges is optimized with computer-based simulation capabilities contained within the SAP2000 computer software system. The analysis strategy is the first to be defined and described in this chapter. The derived analytical results concerning the determination of the optimum cable spacing and deck stiffness naturally follow the analysis procedure and provide the necessary conclusions.

4.1 Analysis strategy

The analysis attempts to determine an optimal correlation between the spacing of the stays in a bridge and the stiffness of the deck. This chapter presents sensitivity studies of different models of cable-stayed bridges with the help of the structural analysis software SAP2000.

This effort includes the examination of different bridge designs, all of which share the same span length. What varies is the cable spacing as well as the deck stiffness. More specifically, the process includes two different deck structures and five different layouts of the cables spacing.

In the following sections different models of cable-stayed bridges are created, based on the design constants that are established from the very beginning. Afterwards, computer analyses are conducted, using SAP2000 software, in order to find an optimum correlation between the spacing of the cables and the deck stiffness in a typical cable-stayed bridge.

The optimum performance of the cable-stayed bridge model is evaluated by analyzing the following measures:

- The maximum vertical deflection of the deck
- The maximum cable tension in the cable anchored at the center of the main span
- The maximum bending moment in the girder

4.2 General design constants

The goal of the design is to come up with a typical cable-stayed bridge that needs to be generic, in order for this research to be applicable to the greatest possible number of newly constructed cable-stayed bridges.

4.2.1 Geometry

The structure is a cable-stayed bridge, doubly symmetrical about both the longitudinal (X) and transverse (Y) axes (see Figure 4.1 and Figure 4.2). There are four towers, two at each side of the deck, one middle span and two equal side spans.

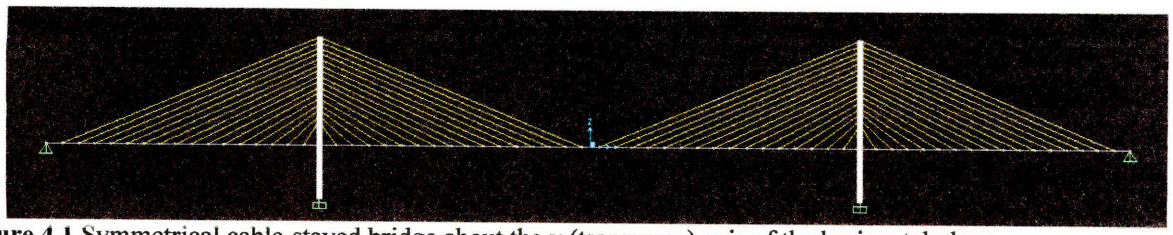

Figure 4.1 Symmetrical cable-stayed bridge about the y (transverse) axis of the horizontal plane

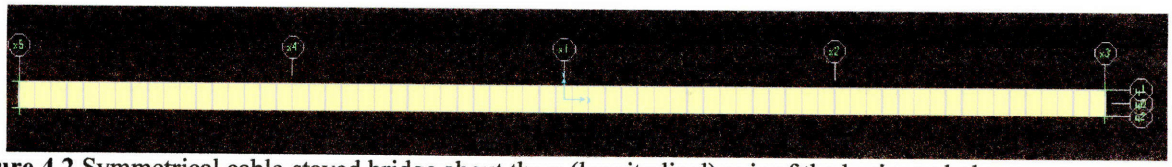

Figure 4.2 Symmetrical cable-stayed bridge about the x (longitudinal) axis of the horizontal plane

The length of the main span is 500m. Because of the fact that cable-stayed layouts are optimal for a span between 200m to 1100m, a 500m span can be considered a middle

span cable-stayed bridge. Consequently, the symmetrical design requires the existence of two side-spans of 250m wide each.

4.2.2 Deck

The deck is 25m wide, which can accommodate two traffic lanes plus safety lanes in each direction as well as a pedestrian walkway, on one of the sides. In the longitudinal direction, the deck is perfectly horizontal[1]. It is a composite construction the top slab of which, is made of precast concrete panels, 25cm thick and the steel frame has variations according to the different designs.

The support conditions for the deck are simulated as pins to both ends in the longitudinal direction as well as to the points of intersection with the towers[2].

4.2.3 Towers

The structure is a twin-tower bridge. All four towers are identical and their height, which is related to the main span of the bridge, is 100m above the deck level. So, the ratio of height to main span has a magnitude of 5 and offers an economical solution for the design.

There are 50m-high piers below the level of the deck. This height was selected to avoid the need for a different cross section between the piers and the pylons. This produces a ratio of 2:1 between the heights of the pylons and piers, which is within typical design range.

The material used for the towers is conventional concrete C30, and the cross-section tends to be 3.5mx5.5m. This design requires longitudinal reinforcement of around 1.2m^2, in the tower. Each of the towers is supported at the base with a fixed connection and is pinned at the deck level.

---

[1] In the longitudinal direction the deck is perfectly horizontal. A grade is needed to the transverse direction for drainage purposes.

[2] The need for expansion joints is neglected in the present analysis.

4.2.4 Cables

The cable arrangement for this model is the double-plane system which is applied to the majority of cable-stayed bridges in the world. The chosen longitudinal arrangement of the cables is the semi-fan system, as it provides better support to the deck. This system has become the most preferred especially for constructions after 1980.

The material used for the cables is steel T15S 1770; the cable diameter is 20cm. The constant of thermal expansion for the cables equals to α=0.0000117/Celcius while the modulus of elasticity is E=165000000kPA.

4.3 First model

As already mentioned, there are five different models created in order to be analyzed in SAP2000. Every model has different spacing for the cables. Each one of these five models, though, is analyzed twice, each time having different properties assigned to the deck section. This way, five unique geometries exist, with two different deck cross-sections each. In total, these combinations create ten different analysis models.

4.3.1 Deck section type A

4.3.1.1 Description of the finite element model

Geometry

Spacing between 10m to 13m for the cables is very common for cable-stayed bridges. Therefore, in the first place it was decided that 22 cables should be used on each side of every tower. This requires a spacing of 11.11m at the main span (176 cables in total). The geometry of the model can be seen in Figure 4.3. This specific arrangement leads to a minimum angle of the cables equal to 22.7°[3] and a maximum angle of 66°.

[3] Although this angle is a little low, thanks to the composite deck and the advantages of concrete under compression we prefer to keep low towers because of the economy.

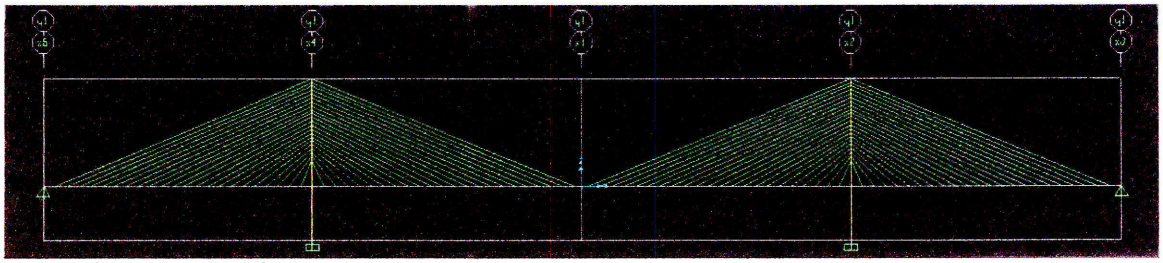

Figure 4.3 Side view of model 1

Deck

The cross-section of the deck for type A structure consists of three I-beams with dimensions shown in Figure 4.4. The layout of those beams along the transverse direction of the deck is shown in Figure 4.5. This type of cross-section from now on will be referred to as section of type A.

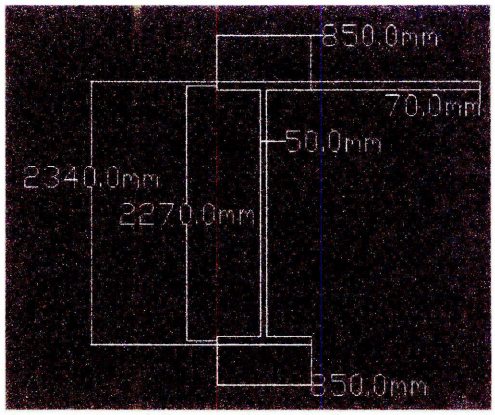

Figure 4.4 One of the I-beams that form the steel frame of the deck

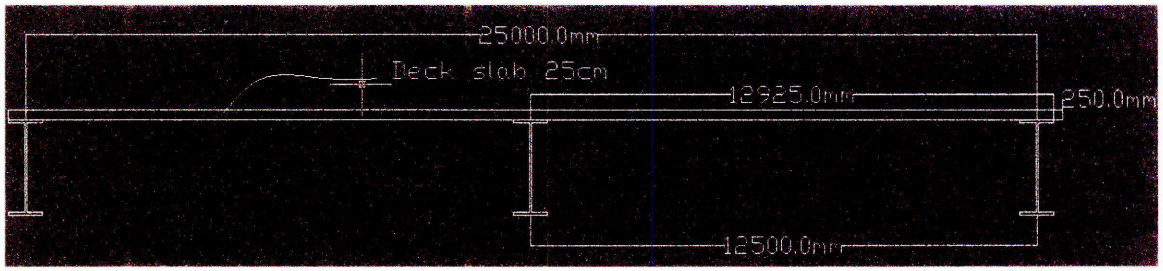

Figure 4.5 Deck cross-section type A

The way that the deck has been modeled is shown in Figure 4.6. In the longitudinal direction, there is a beam running in the middle of the deck. This beam represents the

steel frame of the deck. It is a single frame section which has the equivalent properties of the three parallel I-beams shown in Figure 4.5. The exact properties of the equivalent beam are listed in Figure 4.7[4]. In the transverse direction, this beam is connected with the stays through rigid links. Finally, the deck slab is modeled with shell elements which have been assigned with the properties of concrete as well as with a thickness of 25cm. These shell elements are simply supported on each corner on the deck's equivalent beams at one side and on the cable-stays at the other side. In the transverse direction, they are divided in half by the beam of the equivalent steel frame.

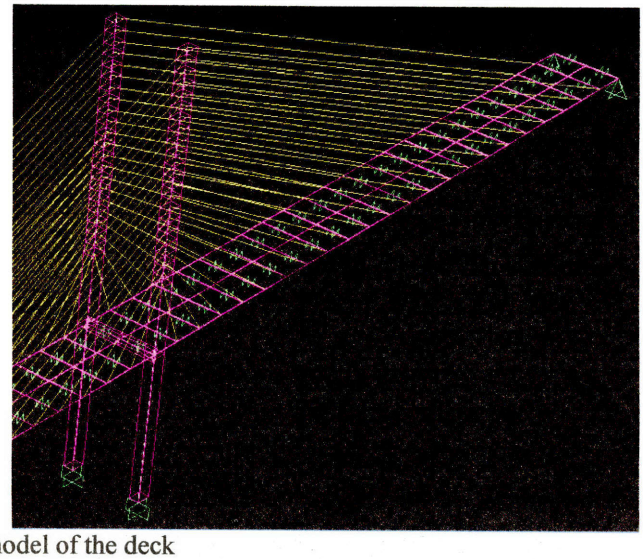

Figure 4.6 Finite element model of the deck

[4] More details on the way to fill the form in Figure 4.7 are given in APPENDIX A.

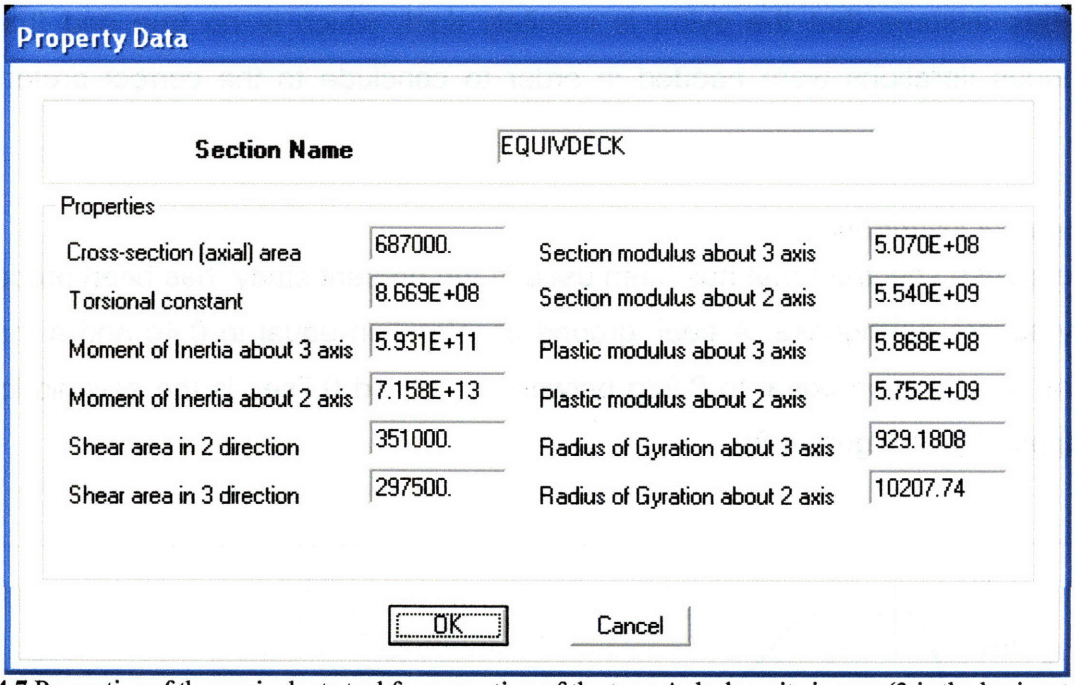

Figure 4.7 Properties of the equivalent steel frame section of the type A deck, units in mm (3 is the horizontal axis and 2 is the vertical axis)

Pretensioning

Prestress was applied to all the cables in order to ensure small deformations of the deck after the application of the the structure's factored self-weight. The initial displacements were gradually reduced after five iterations. The pretensioning was applied to each cable through temperature load.

The equations that explain the temperature loading of the cables follow:

$$\delta = \alpha * \Delta T * \ell \qquad (4.1)$$

$$F = \frac{E * A}{\ell} * \delta \qquad (4.2)$$

$$\Delta T = \frac{F}{\alpha * A * E} \qquad (4.3)$$

where α is the constant of thermal expansion for the cables, ΔT is the temperature difference, F is the pretensioning force and δ the shrinkage of the cable. These

equations assume that the pylon is infinitely rigid, which is no true and that's why continuous iterations were needed in order to conclude to the correct pretensioning force.

Earthquake excitation

The response spectrum that has been used in the present study, has been produced by a very severe earthquake. A peak ground acceleration equal to 0.4g and a maximum spectral acceleration equal to 0.92g between 0.15 and 0.7sec is the seismic load that was applied (see Figure 4.8).

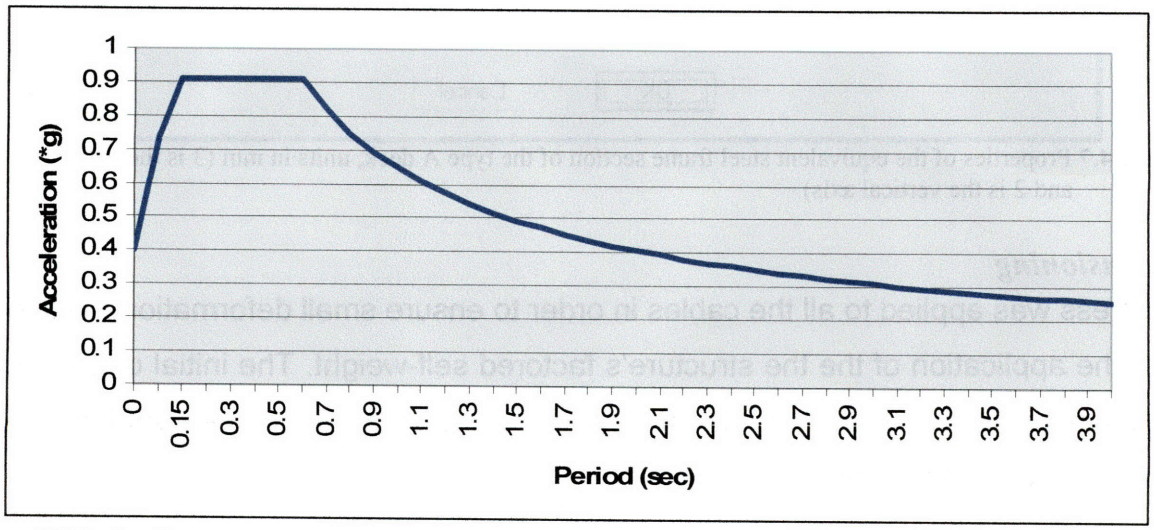

Figure 4.8 Design Response spectrum

This excitation corresponds to the most severe design earthquake response spectrum of the Greek aseismic code (EAK, 2000) and has a return period of 475 years. Considering that Greece is a seismically active area, where the tectonic zones cause severe earthquakes, it is clear that a similar earthquake will never occur in areas like Massachusetts. This fact makes the design really conservative.

For this reason, it was redundant to apply wind loads to the structure, since the earthquake loading will govern the design. The static traffic loads applied were 1.8kPa over the entire area of the deck.

4.3.1.2 Static characteristics of the model

After running the analysis of the model the results are derived and presented below.

The model's deformed shape, due to the dead and live loads of the bridge, is as shown in Figure 4.9. The condition of the bridge at this state has as follows:

Max vertical deflection of the deck:	1.752m
Max cable tension at the center of the main span:	5.2MN
Max bending moment in the deck girder:	37MN-m at the tower supports

Table 4.1 Performance of model 1 type A under static loads before pretensioning

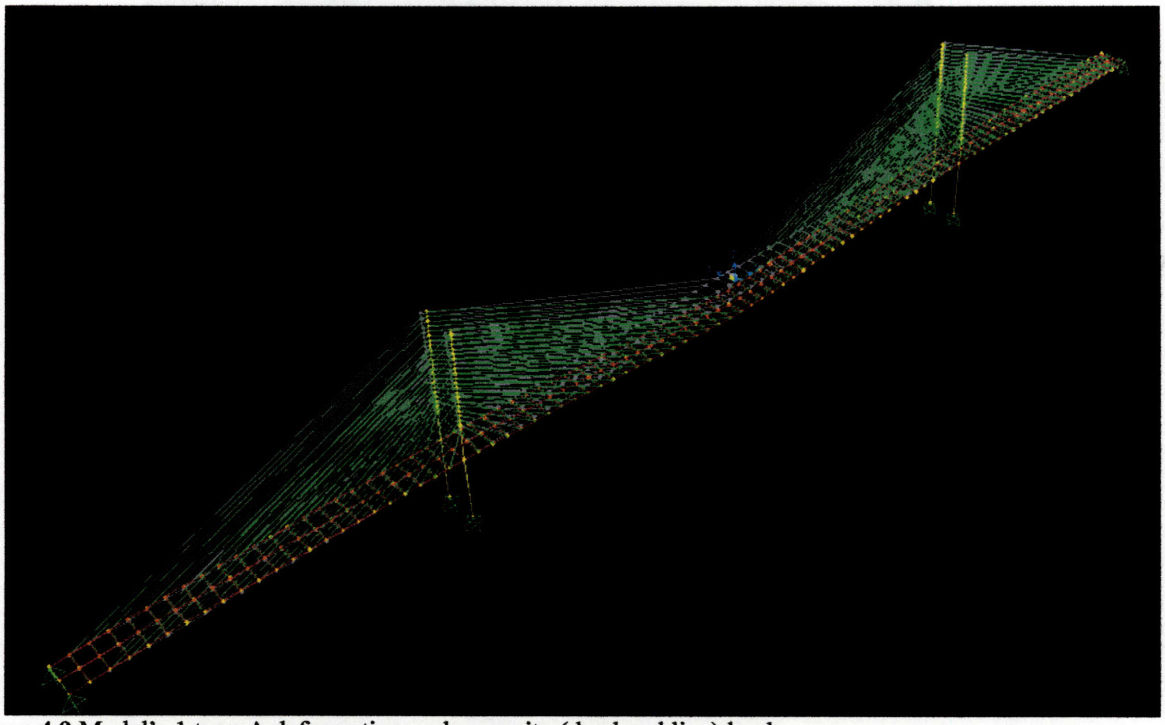

Figure 4.9 Model's 1 type A deformation under gravity (dead and live) loads

Finding the appropriate pretensioning force requires five iterations. The reduction of the deflections under the static loading of the bridge is shown in Figure 4.10 and Figure 4.11. In this case, huge bending moments are generated in the towers because of the

continuous beam[1] behavior of the deck (see Figure 4.12). The specific results are listed in Table 4.2.

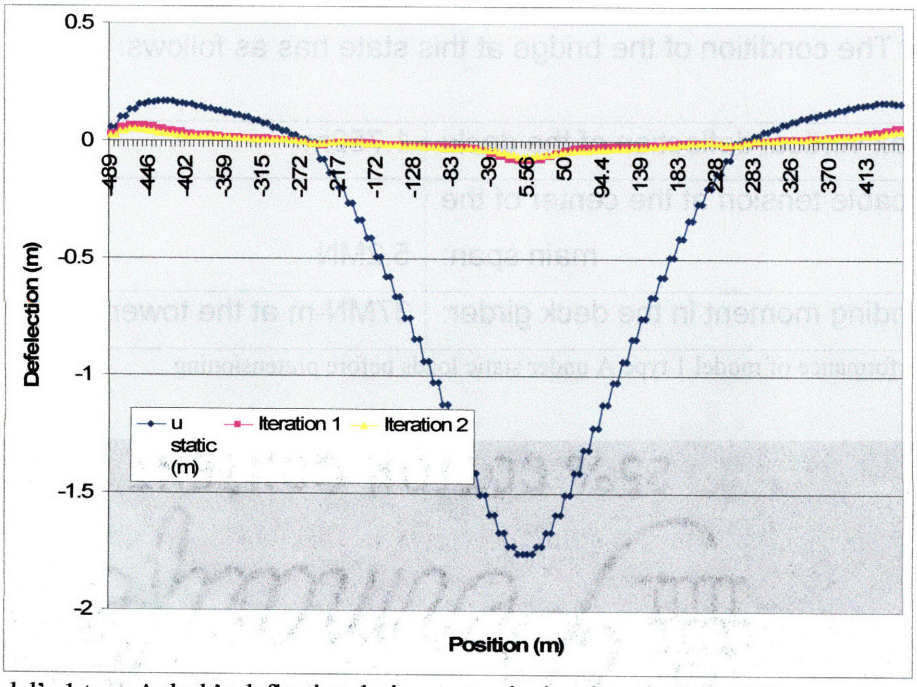

Figure 4.10 Model's 1 type A deck's deflection during pretensioning, iterations 1 and 2

[1] There are two alternatives to avoid the continuous beam problem. Either not to connect the deck with the towers but in this case the towers would be very flexible as they would act as a cantilever beam 150m high. Or try connecting the deck to the towers but as a discontinuous beam with a hinge.

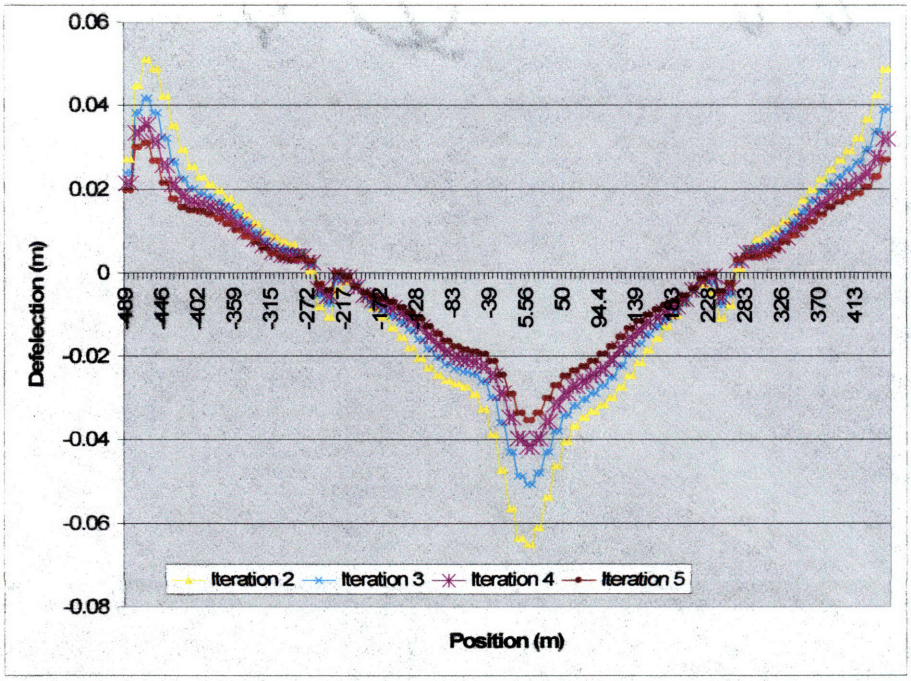

Figure 4.11 Model's 1 type A deck's deflection during pretensioning iterations 2 and 5

Max vertical deflection of the deck:	0.0353m
Max cable tension at the center of the main span:	5.6MN
Max bending moment in the deck girder:	34.12MN-m at the tower supports

Table 4.2 Performance of model 1 type A under static loads after pretensioning

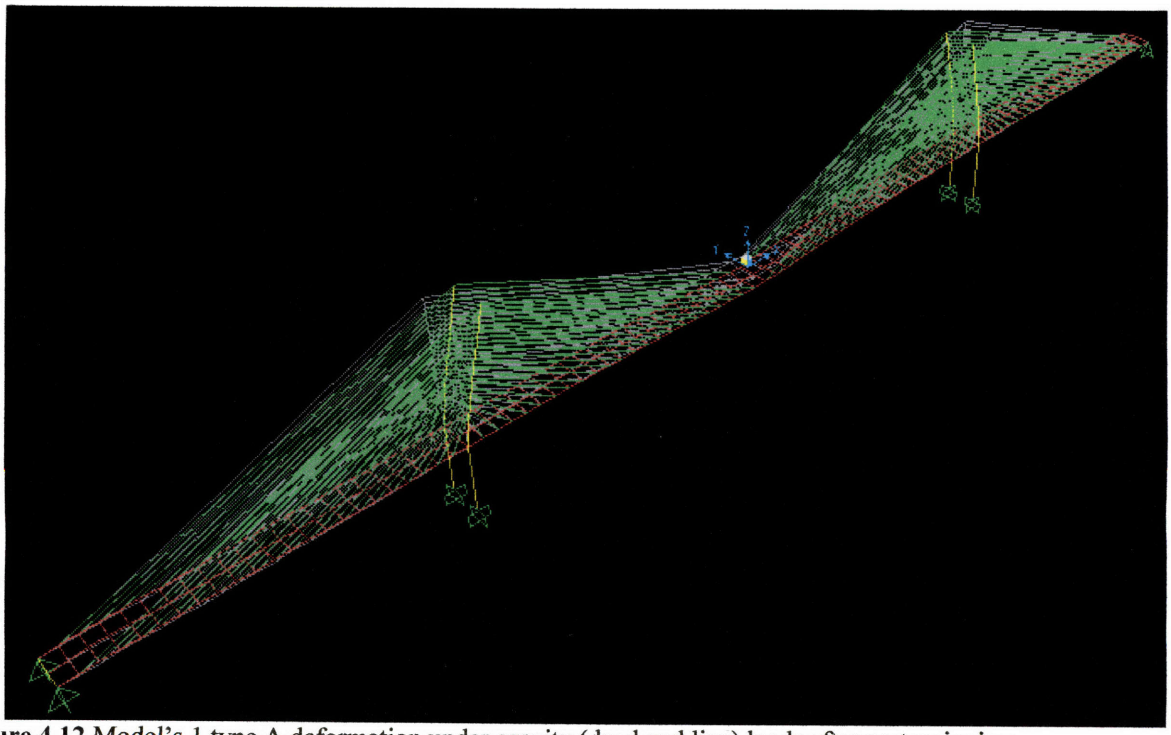

Figure 4.12 Model's 1 type A deformation under gravity (dead and live) loads after pretensioning

4.3.1.3 Dynamic characteristics – modal analyses

The modal analysis of the bridge revealed the model's fundamental weaknesses. Mode 1 is shown in Figure 4.13. Due to the flexibility of the towers, the fundamental period of the structure is boosted to 7.047sec. This corresponds to the fundamental mode, which represents symmetrical lateral movement of the towers. The first 7 modes of the bridge are shown in the following figures (Figure 4.13 to Figure 4.19) while Table 4.3 contains information on the first 12 modes.

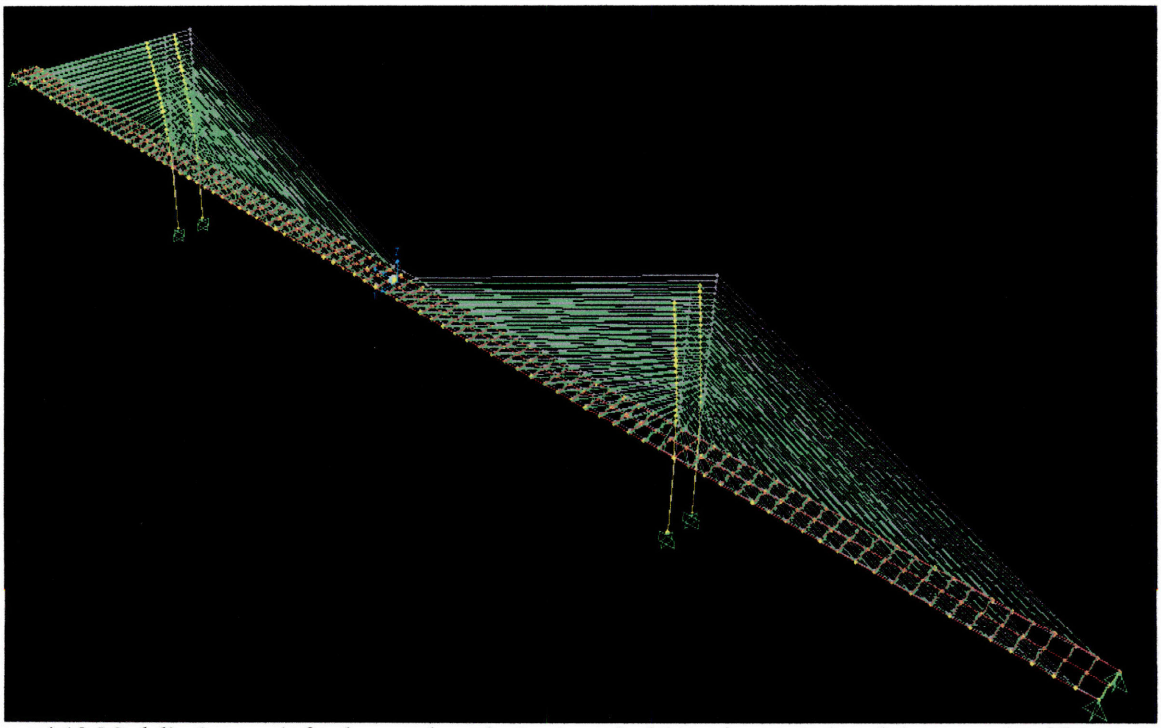

Figure 4.13 Model's 1 type A fundamental mode (symmetrical lateral movement of the towers) with a period of T_1=7.047sec

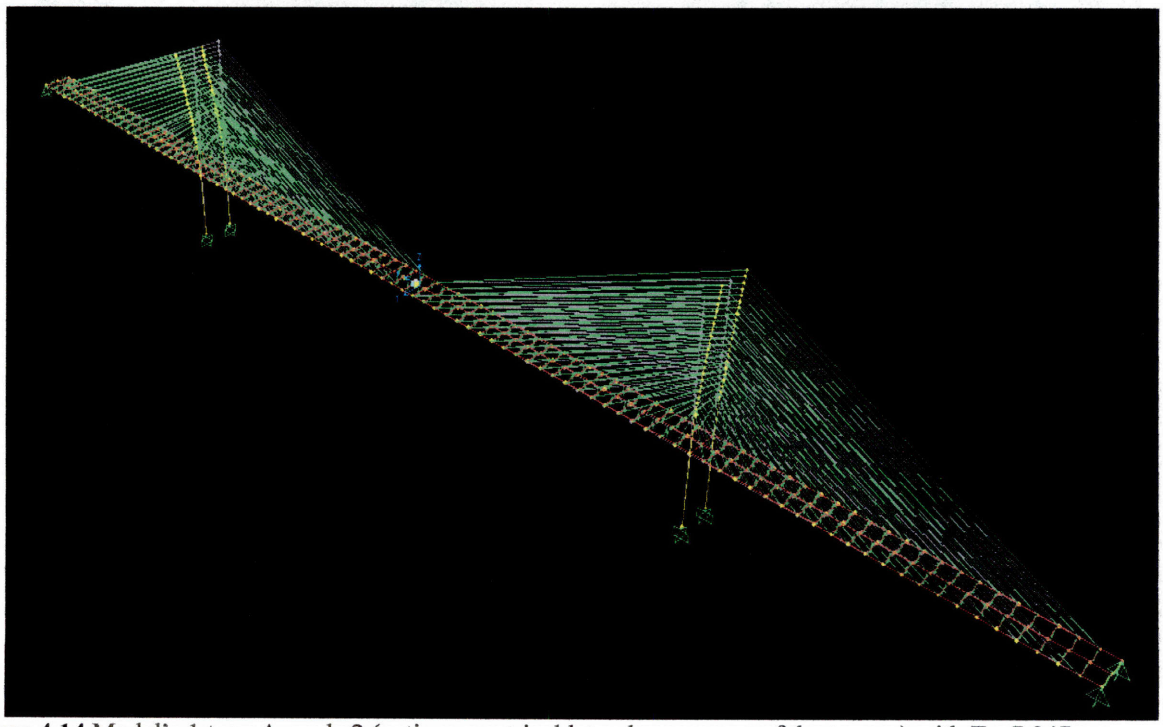

Figure 4.14 Model's 1 type A mode 2 (anti-symmetrical lateral movement of the towers) with T_2=7.047sec

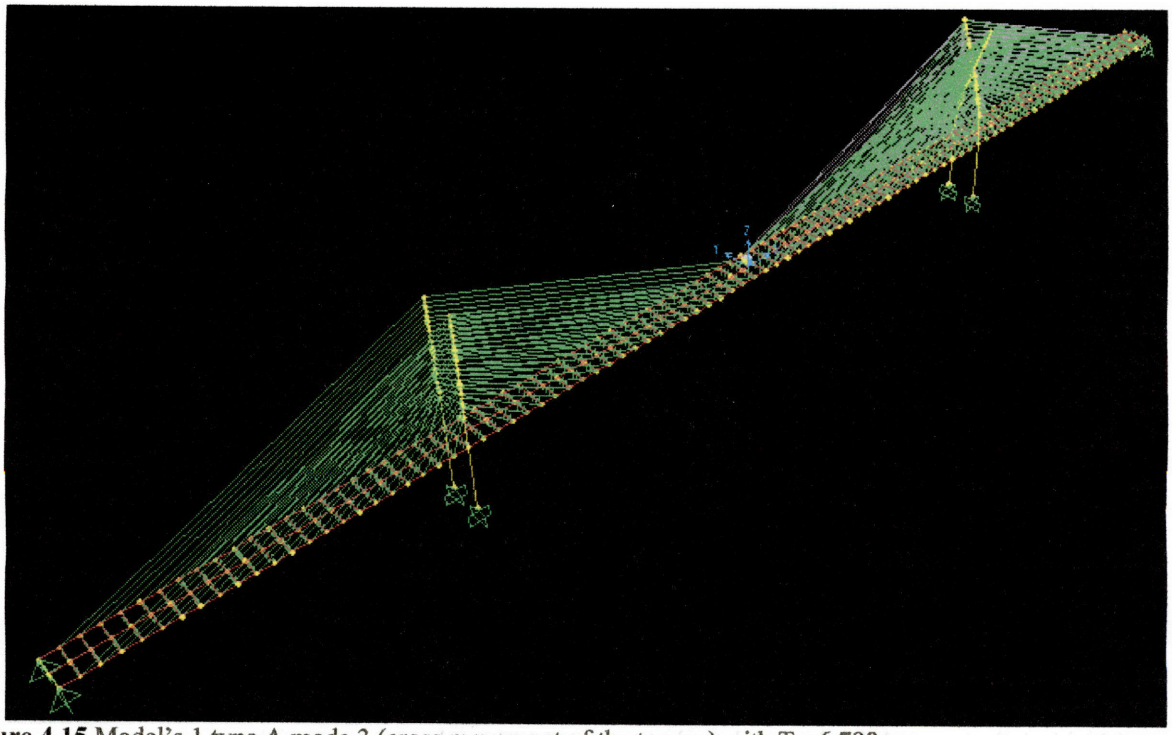

Figure 4.15 Model's 1 type A mode 3 (cross movement of the towers) with T_3=6.798sec

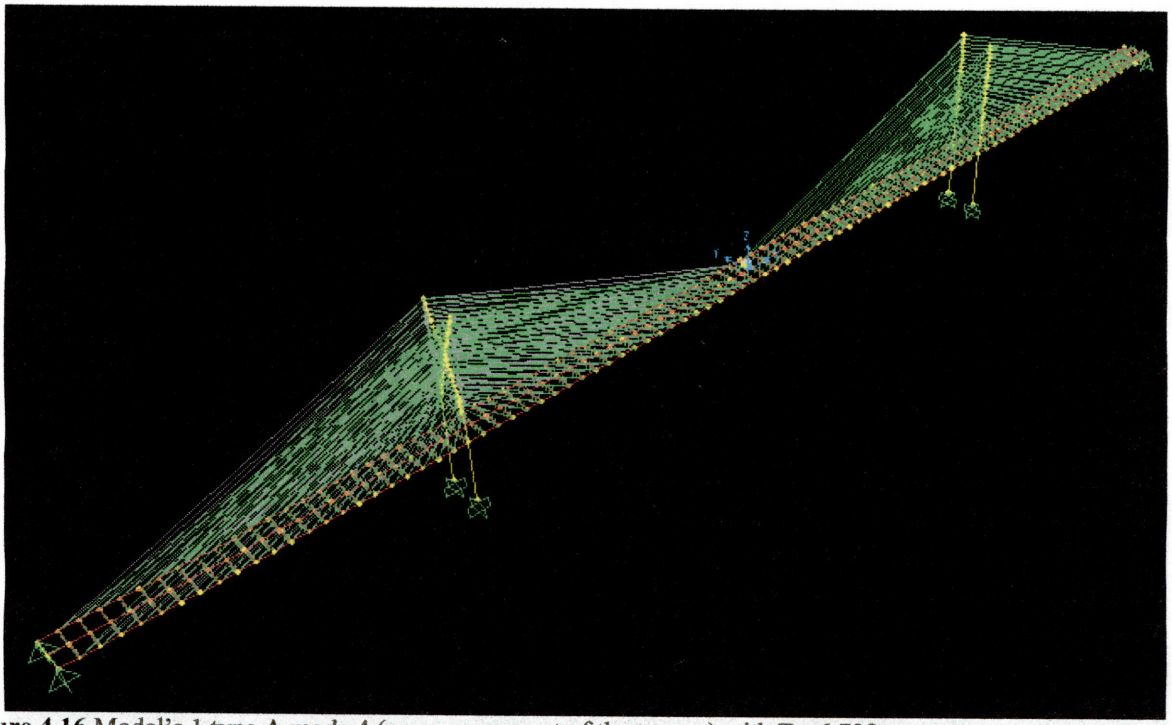

Figure 4.16 Model's 1 type A mode 4 (cross movement of the towers) with T_4=6.798sec

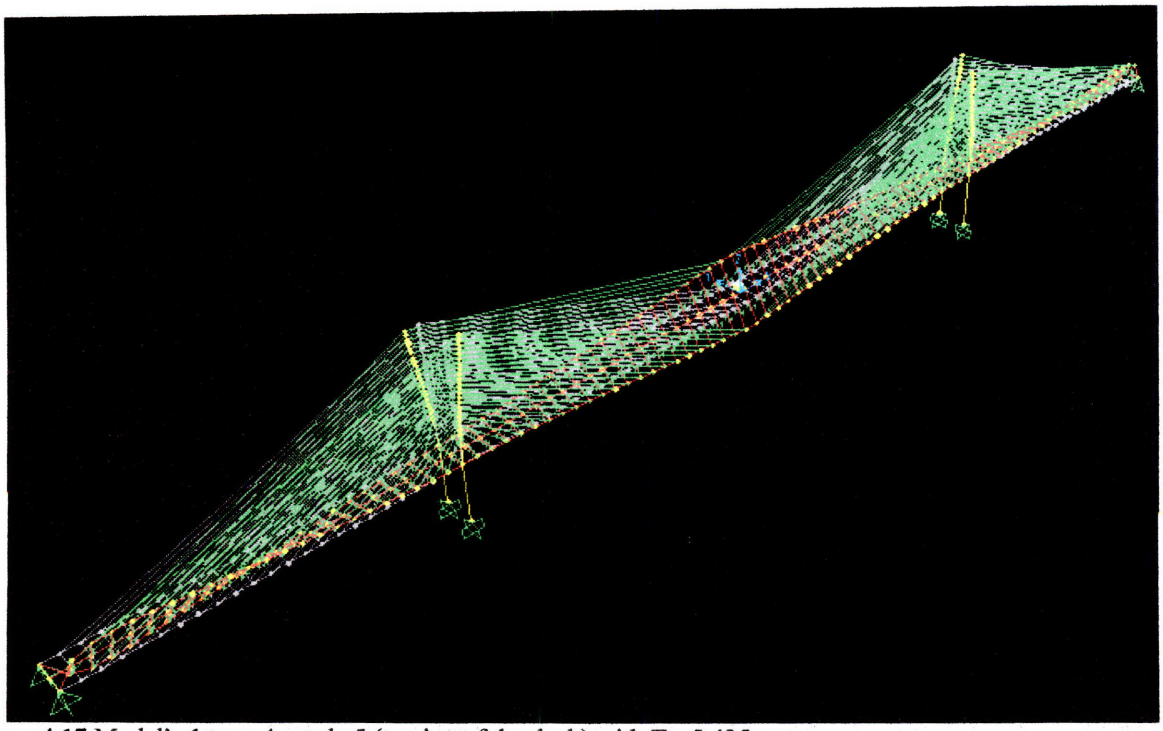

Figure 4.17 Model's 1 type A mode 5 (torsion of the deck) with T_5=5.435sec

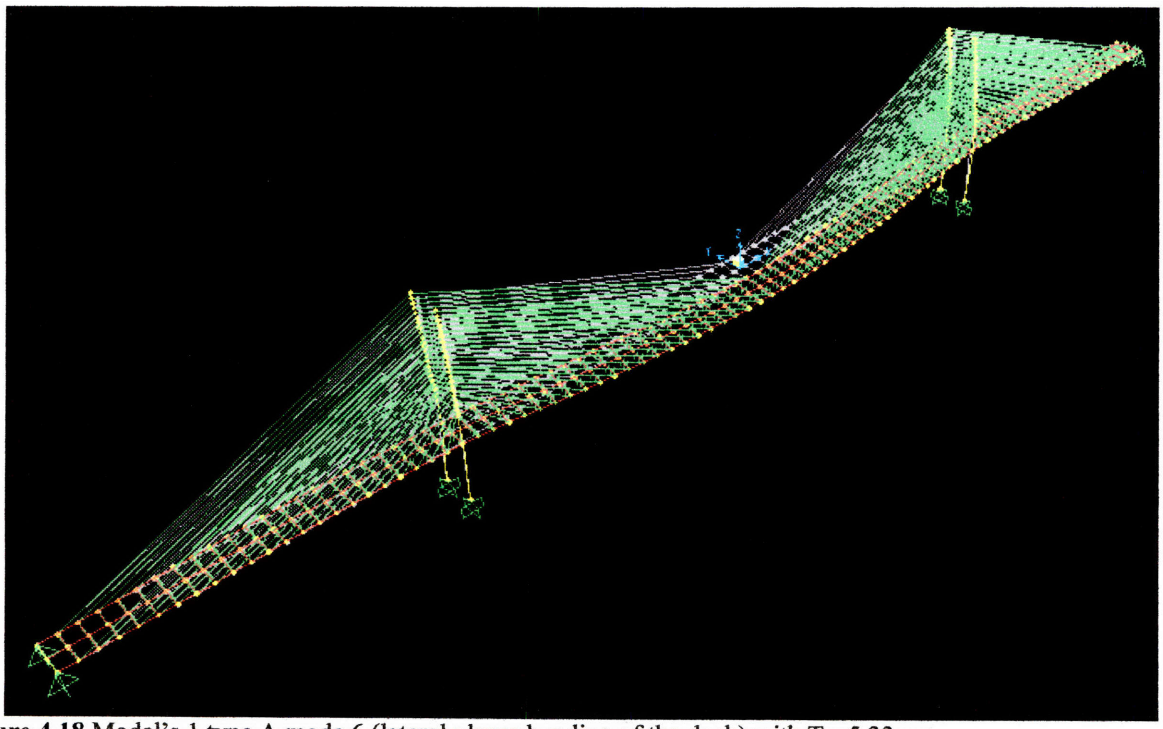

Figure 4.18 Model's 1 type A mode 6 (lateral planar bending of the deck) with T_6=5.33sec

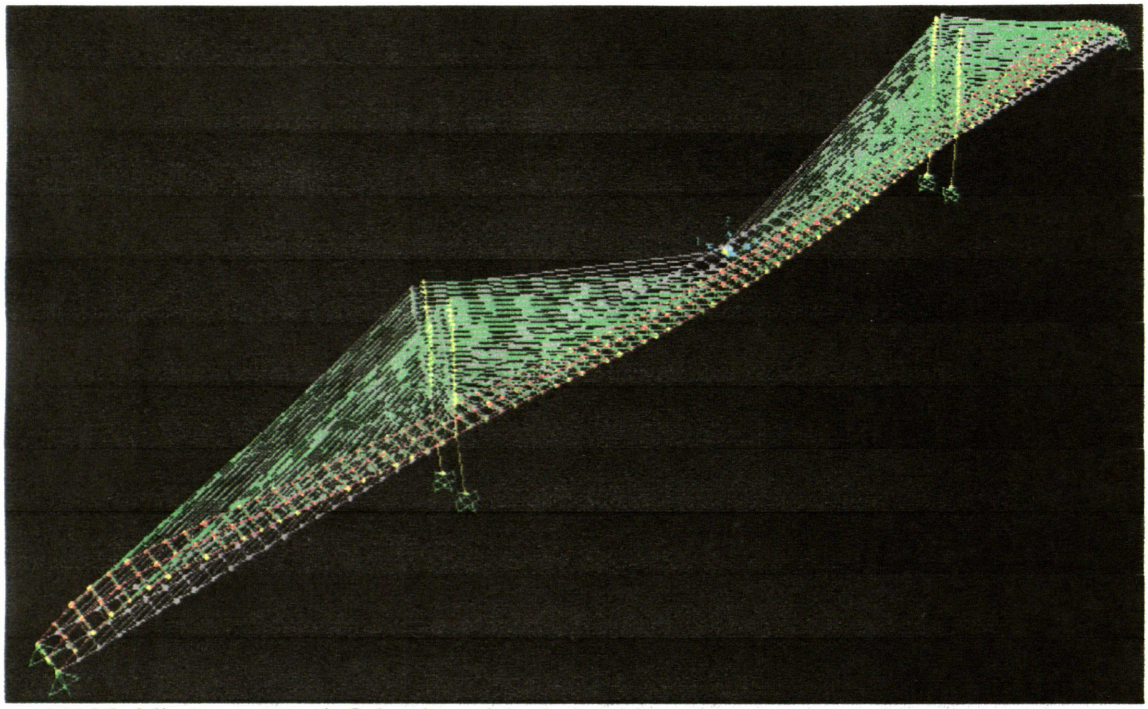

Figure 4.19 Model`s 1 type A mode 7 (bending of the deck) with T-=3.94sec

Mode No.	T (sec)	Nature	Direction
1	7.047345	Symmetrical lateral movement of the towers	Y
2	7.047345	Anti-symmetrical lateral movement of the towers	Y
3	6.798179	Cross movement of the towers	Y
4	6.798168	Cross movement of the towers opposite of mode 3	Y
5	5.434757	Torsion of the deck	X
6	5.32986	Lateral (planar) bending of the deck	Y
7	3.935782	Bending of the deck	Z
8	3.860966	Anti-symmetrical torsion of the deck	X
9	1.821474	Anti-symmetrical bending of the deck	Z
10	1.512381	Lateral anti-symmetrical bending of the deck with torsion	Y
11	1.456266	Lateral symmetrical bending of the deck	Y
12	1.36681	Lateral anti-symmetrical bending of the deck	Y

Table 4.3 First 12 modes for model 1 type A

In the present study the performance of the bridge is evaluated according to the vertical deflections of the deck under seismic excitation so it is not of major importance to improve the overall response of the cable-stayed bridge. Such a goal could be achieved with the application of x-braces to the towers above the deck level. This would make the

structure much more rigid and would make mode 6 and mode 7 become mode 1 and mode 2 in the case of the braced bridge (see §4.7).

4.3.1.4 Earthquake response

After analyzing the above characteristics of the bridge. the response spectrum of paragraph 4.3.1.1 is applied to the bridge as an excitation in both longitudinal and transverse direction. The equations representing the loading for the seismic excitation case are the following:

$$1.3*DL+1.6*LL+1*Temp+1.0*EQx+0.3*EQy \qquad (4.4)$$

$$1.3*DL+1.6*LL+1*Temp+0.3*EQx+1.0*EQy \qquad (4.5)$$

where equation (4.4) corresponds to the earthquake load of the bridge in the longitudinal direction (X axis) and equation (4.5) to the loading in the transverse direction (Y axis).

The quasi-static behaviors of the structure under each loading condition due to the seismic excitation are shown in Figure 4.20 and Figure 4.21. The most critical loading condition for the criteria set in §4.1 appears to be the case of an earthquake load in the longitudinal direction.

The overall performance of model 1 under seismic excitation is summarized in Table 4.4.

Max vertical deflection of the deck:	0.444m
Max cable tension at the center of the main span:	7.5MN
Max bending moment in the deck girder:	39.6MN-m at the tower supports

Table 4.4 Performance of model 1 type A under earthquake in the longitudinal direction

The 0.444 m vertical deflection of the deck corresponds to a deflection of $\frac{L}{1100}$ which satisfy the criteria set by AASHTO for a deflection less than $\frac{L}{800}$=0.625m.

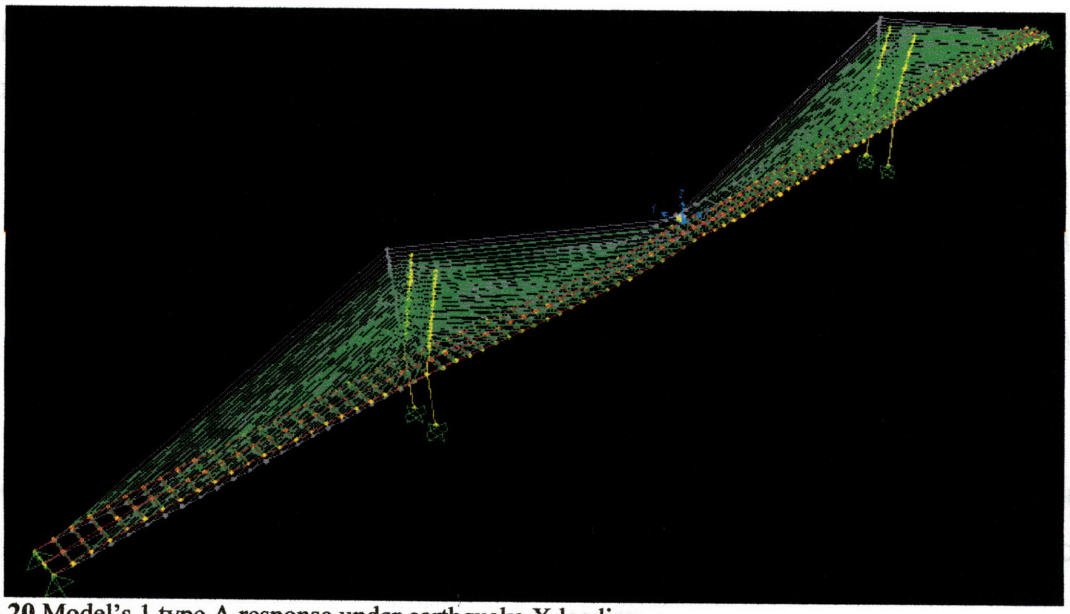

Figure 4.20 Model's 1 type A response under earthquake X loading

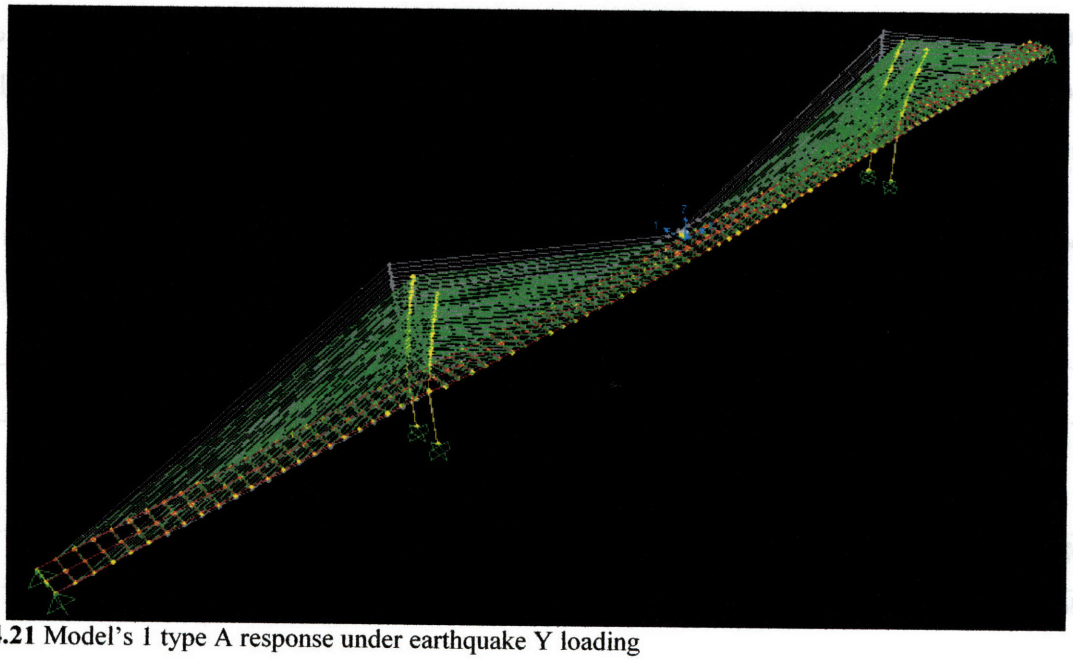

Figure 4.21 Model's 1 type A response under earthquake Y loading

4.3.2 Deck section type B

4.3.2.1 Description of the finite element model

The geometry of the model remains exactly the same as in deck section type A model. Both the pretensioning and the earthquake excitation methods are applied according to the section 4.3.1.1 of page 48. The only difference that appears concerns the properties of the deck's steel frame.

Deck

The cross-section of the deck for type B structure consists of only two of the I-beams used for the type A structure. The dimensions are the ones shown in Figure 4.4 but the layout of those beams along the transverse direction of the deck is shown in Figure 4.22. From now on, this type of deck cross-section will be referred to as type B.

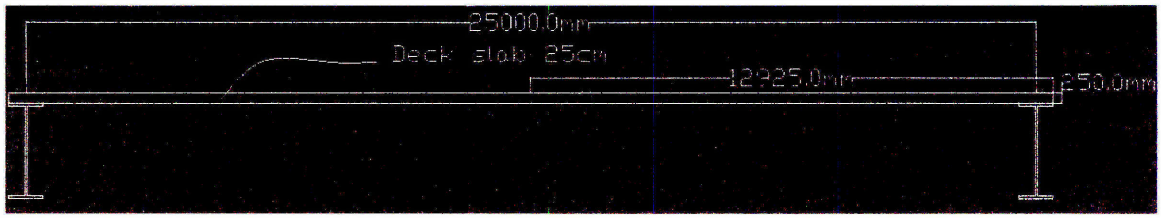

Figure 4.22 Deck cross-section type B

The deck has been modeled again as described in paragraph 4.3.1.1. This time, though, the equivalent properties of the deck steel frame are those of the two parallel I-beams shown in Figure 4.22. The details of the properties are shown in Figure 4.7.

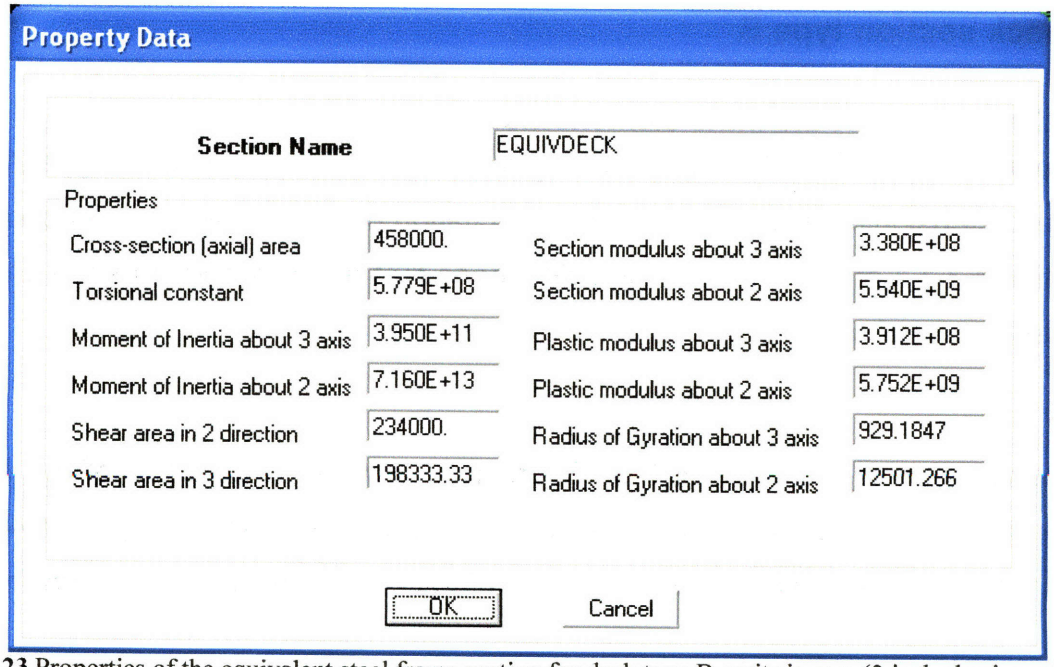

Figure 4.23 Properties of the equivalent steel frame section for deck type B, units in mm (3 is the horizontal axis and 2 is the vertical axis)

4.3.2.2 Static characteristics of the model

The numerical results for type B model are presented in Table 4.5.

	Before pretensioning	After pretensioning
Max vertical deflection of the deck:	1.69m	0.043m
Max cable tension at the center of the main span:	4.7MN	5.6MN
Max bending moment in the deck girder at the tower supports:	39.3MN-m	33.7 MN-m

Table 4.5 Performance of model 1 type B under static loads

4.3.2.3 Dynamic characteristics – modal analyses

The modal analysis of the type B bridge revealed that each shape of the first 12 modes of the bridge coincides with the respective type of modes in type A bridge. Table 4.6 shows information on the first 12 modes.

Mode No.	T (sec)	Nature	Direction
1	7.203313	Symmetrical lateral movement of the towers	Y
2	7.203313	Anti-symmetrical lateral movement of the towers	Y
3	6.92012	X movement of the towers	Y
4	6.920112	X movement of the towers opposite of mode 3	Y
5	5.450186	Torsion of the deck	X
6	5.435504	Lateral (planar) bending of the deck	Y
7	3.970109	Bending of the deck	Z
8	3.862102	Anti-symmetrical torsion of the deck	X
9	1.806047	Anti-symmetrical bending of the deck	Z
10	1.530414	Lateral anti-symmetrical bending of the deck with torsion	Y
11	1.455075	Lateral symmetrical bending of the deck	Y
12	1.366008	Lateral anti-symmetrical bending of the deck	Y

Table 4.6 First 12 modes for model 1 type B

4.3.2.4 Earthquake response

Table 4.7 shows the results that derive from the subjection of the type B bridge to the response spectrum of paragraph 4.3.1.1, in the longitudinal direction.

Max vertical deflection of the deck:	0.5086m
Max cable tension at the center of the main span:	7.7MN
Max bending moment in the deck girder:	39.4MN-m at the tower supports

Table 4.7 Performance of model 1 type B under earthquake in the longitudinal direction

The 0.5086m vertical deflection of the deck corresponds to a deflection of $\frac{L}{1000}$ which satisfies the criteria set by AASHTO for a deflection less than $\frac{L}{800}$=0.625m.

4.4 Type A and type B Models 2 to 5

Models 2-5 were loaded the same way as model 1 in terms of pretension, deck cross-section and seismic load, in order to have a basis for a proper comparison of the results.

The cables were prestressed in this case as well, and 5 iterations were performed in order to find the correct pretension force for each cable. The cross-section of the deck is exactly the same as in model 1 for type A and type B sections (see pages 49 and 63 respectively). In order to evaluate the performance of the structure, the same earthquake with model 1 (see page 52) was applied as a loading case, in both the longitudinal and transverse direction of the bridge.

4.4.1 Model 2

4.4.1.1 Geometry

A design with more appropriate angles for the cables ($25° \leq \varphi \leq 65°$). was attempted to be created during the process of the design evolution. In order to increase their minimum angle, all the cables that were forming the minimum angles in model 1, eight in total, are removed and every one of the other cables is anchored to the towers higher. The anchorage of the cables to the deck did not change place. The resulting design is shown in Figure 4.24. That means that the design has 168 cables with a minimum angle of 23° and a maximum angle of 66°.

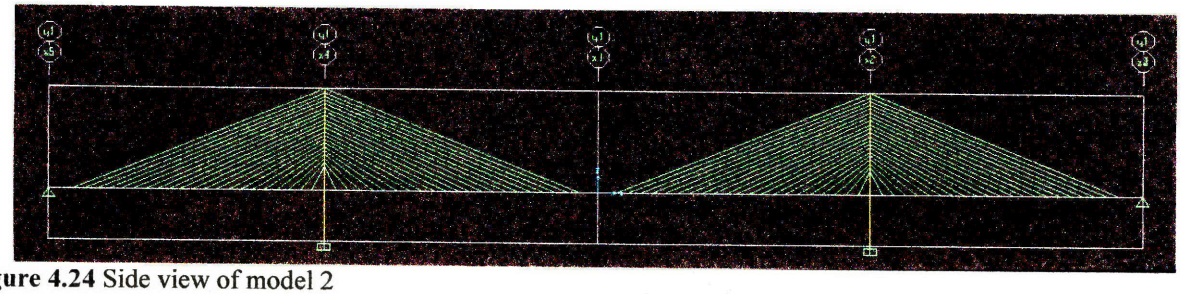

Figure 4.24 Side view of model 2

4.4.1.2 Results

After running this analysis, the results are not encouraging. This specific model does not perform better than model 1 and it is failing under the earthquake excitation.

The model's deformation due to the dead and live loads of the bridge, is as shown in Table 4.8. The numbers are much higher compared to those of model 1.

Max vertical deflection of the deck:	2.45m
Max cable tension at the center of the main span:	6.5MN
Max bending moment in the deck girder:	64.252MN-m at the mid span

Table 4.8 Performance of model 2 under static loads before pretensioning

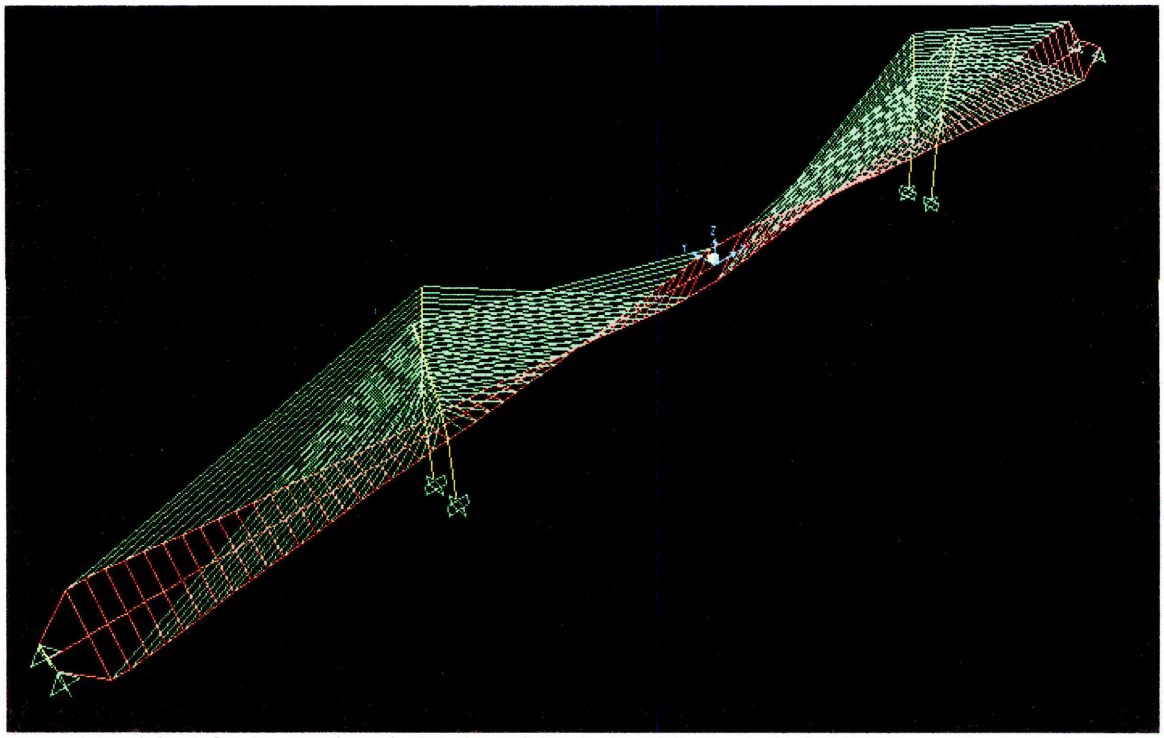

Figure 4.25 Model's 2 fundamental mode (torsion of the deck) with a period of T_1=7.46sec

Figure 4.25 shows the fundamental mode of this model. It is made clear that this arrangement of the cables makes the deck much more flexible. Table 4.9 shows the performance of the bridge after pretension. Looking at the bending in the deck girder it can easily help predict what happens afterwards.

The deck of the bridge fails under the earthquake load close to the mid-span where there is an absence of elastic supports (stays). For this reason Model 2 should be excluded from this research.

After such results, it was considered that modeling a type B structure with this geometry would be useless as it would have an even more flexible deck and it wouldn't be able to resist the applied loads.

Max vertical deflection of the deck:	0.15m
Max cable tension at the center of the main span:	7.5MN
Max bending moment in the deck girder:	75MN-m at the tower supports

Table 4.9 Performance of model 2 under static loads after pretensioning

4.4.2 Model 3

4.4.2.1 Geometry

After the inapplicability of Model 2, the next model is again a bridge with evenly spaced cables along the whole length of the deck. This time, 23 cables run from every side of each tower, in order to create a cable-stayed bridge, with 184 cables in total. This arrangement shown in Figure 4.26 requires a 10.63m spacing between the cables in the main span with a minimum cable angle of 22.65° and a maximum cable angle of 63.4°.

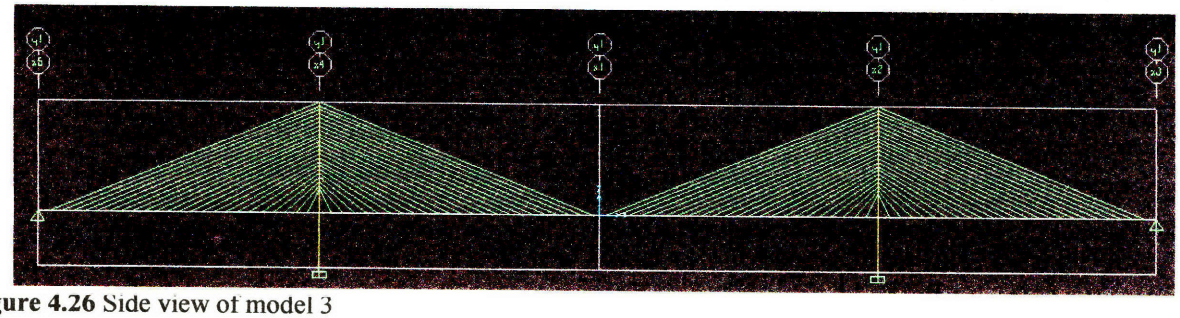

Figure 4.26 Side view of model 3

4.4.2.2 Results

Type A structure

The modes of this bridge have exactly the same form as the ones of Model 1. Table 4.10 summarizes the modal analysis for Model 3 type A while Table 4.11 contains the performance criteria for the exact same model.

Mode No.	T (sec)	Nature	Direction
1	7.052916	Symmetrical lateral movement of the towers	Y
2	7.052916	Anti-symmetrical lateral movement of the towers	Y
3	6.805112	X movement of the towers	Y
4	6.805101	X movement of the towers opposite of mode 3	Y
5	5.305236	Torsion of the deck	X
6	5.294051	Lateral (planar) bending of the deck	Y
7	3.957769	Bending of the deck	Z
8	3.783558	Anti-symmetrical torsion of the deck	X
9	1.852524	Anti-symmetrical bending of the deck	Z
10	1.532708	Lateral anti-symmetrical bending of the deck with torsion	Y
11	1.482417	Lateral symmetrical bending of the deck	Y
12	1.384919	Lateral anti-symmetrical bending of the deck	Y

Table 4.10 First 12 modes for model 3 type A

	Static before pretensioning	After pretensioning	Longitudinal earthquake
Max vertical deflection of the deck:	1.699m	0.029m	0.48m
Max cable tension at the center of the main span:	4.96MN	5MN	6.8MN
Max bending moment in the deck girder:	34.2MN-m at the tower supports	41.3MN-m at the tower supports	46.6MN at the tower supports

Table 4.11 Overall performance of model 3 type A

The vertical deflection 0.48m of the deck corresponds to a deflection of $\frac{L}{1050}$ which satisfy again the criteria set by AASHTO for a deflection less than $\frac{L}{800}$=0.625m.

Type B structure

The modes of this bridge have exactly the same shape as the ones of Model 1. Table 4.12 summarizes the modal analysis for Model 3 type B while Table 4.13 contains the performance criteria for the exact same model.

Mode No.	T (sec)	Nature	Direction
1	7.056425	Symmetrical lateral movement of the towers	Y
2	7.056425	Anti-symmetrical lateral movement of the towers	Y
3	6.805112	X movement of the towers	Y
4	6.805101	X movement of the towers opposite of mode 3	Y
5	5.4074	Torsion of the deck	X
6	5.311056	Lateral (planar) bending of the deck	Y
7	3.985731	Bending of the deck	Z
8	3.787557	Anti-symmetrical torsion of the deck	X
9	1.839214	Anti-symmetrical bending of the deck	Z
10	1.552247	Lateral anti-symmetrical bending of the deck with torsion	Y
11	1.482739	Lateral symmetrical bending of the deck	Y
12	1.385429	Lateral anti-symmetrical bending of the deck	Y

Table 4.12 First 12 modes for model 3 type B

	Static before pretensioning	After pretensioning	Longitudinal earthquake
Max vertical deflection of the deck	1.636m	0.031m	0.512m
Max cable tension at the center of the main span:	4.7MN	4.6MN	6.6MN
Max bending moment in the deck girder:	24.8MN-m at the tower supports	33.6MN-m at the tower supports	38.4MN at the tower supports

Table 4.13 Overall performance of model 3 type B

4.4.3 Model 4

4.4.3.1 Geometry

At this stage, it is important to create a model with significant differences from the previous cases. 32 cables were placed in each side of every tower in order to create the geometry shown in Figure 4.27. This model consists of 256 cables that require a 7.69m

spacing between the cables in the main span, with a minimum cable angle of 22.5° and a maximum cable angle of 68.67°.

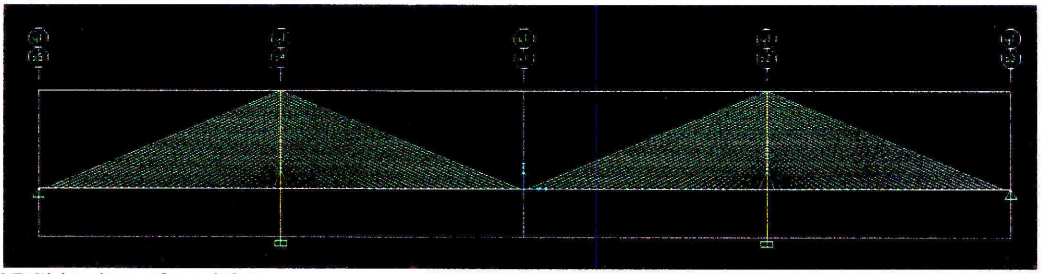

Figure 4.27 Side view of model 4

4.4.3.2 Results

Type A structure

The modes of this bridge have once again the same shape as the ones of Model 1. Table 4.14 summarizes the modal analysis for Model 3. Table 4.15 contains the performance criteria for Model 4.

Mode No.	T (sec)	Nature	Direction
1	7.366752	Symmetrical lateral movement of the towers	Y
2	7.366752	Anti-symmetrical lateral movement of the towers	Y
3	7.119531	X movement of the towers	Y
4	7.119515	X movement of the towers opposite of mode 3	Y
5	4.981112	Torsion of the deck	X
6	4.535568	Lateral (planar) bending of the deck	Y
7	3.857442	Bending of the deck	Z
8	3.315918	Anti-symmetrical torsion of the deck	X
9	1.82834	Anti-symmetrical bending of the deck	Z
10	1.499802	Lateral anti-symmetrical bending of the deck with torsion	Y
11	1.477534	Lateral symmetrical bending of the deck	Y
12	1.343352	Lateral anti-symmetrical bending of the deck	Y

Table 4.14 First 12 modes for model 4 type A

	Static before pretensioning	After pretensioning	Longitudinal earthquake
Max vertical deflection of the deck:	1.33m	0.013m	0.47m
Max cable tension at the center of the main span:	4.1MN	4.3MN	5.9MN
Max bending moment in the deck girder:	27.1MN-m at the tower supports	43.3MN-m at the tower supports	48.7MN at the tower supports

Table 4.15 Overall performance of model 4 type A

Type B structure

The modes of this bridge have exactly the same form as the ones of Model 1. Table 4.16 summarizes the modal analysis for Model 4 type B while Table 4.17 offers the performance criteria for the exact same model.

Mode No.	T (sec)	Nature	Direction
1	7.371256	Symmetrical lateral movement of the towers	Y
2	7.371256	Anti-symmetrical lateral movement of the towers	Y
3	7.119532	X movement of the towers	Y
4	7.119515	X movement of the towers opposite of mode 3	Y
5	5.06926	Torsion of the deck	X
6	4.5385	Lateral (planar) bending of the deck	Y
7	3.869831	Bending of the deck	Z
8	3.317793	Anti-symmetrical torsion of the deck	X
9	1.82132	Anti-symmetrical bending of the deck	Z
10	1.521232	Lateral anti-symmetrical bending of the deck with torsion	Y
11	1.477807	Lateral symmetrical bending of the deck	Y
12	1.343747	Lateral anti-symmetrical bending of the deck	Y

Table 4.16 First 12 modes for model 4 type B

	Static before pretensioning	After pretensioning	Longitudinal earthquake
Max vertical deflection of the deck:	1.286m	0.014m	0.493m
Max cable tension at the center of the main span:	3.88MN	4MN	5.89MN
Max bending moment in the deck girder at the tower supports:	19.87MN-m	34.8MN-m	39.7MN

Table 4.17 Overall performance of model 4 type B

4.4.4 Model 5

4.4.4.1 Geometry

This final model was selected in such a way that it lies on the extreme situation where the cable-stayed bridge is supported by the least number of cables possible. 16 cables were placed in each side of every tower in order to create the geometry shown in Figure 4.28. This model consists of only 128 cables that require a spacing of 15.15m with a minimum cable angle of 23.02° and a maximum cable angle of 57°.

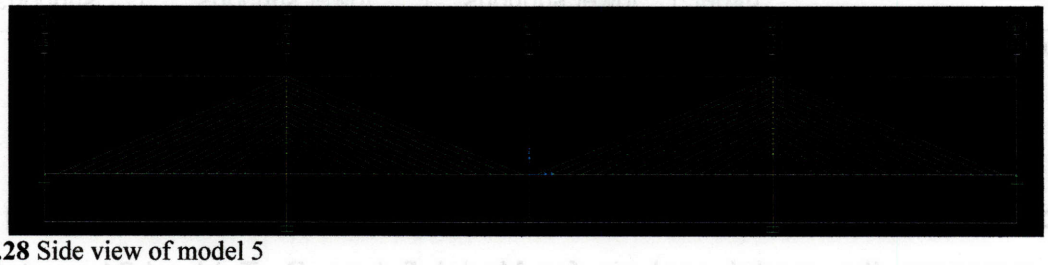

Figure 4.28 Side view of model 5

4.4.4.2 Results

Type A structure

The modes of this bridge have exactly the same shape as the ones of Model 1. Table 4.18 summarizes the modal analysis for Model 5 type A while Table 4.19 contains the performance criteria for the same model.

Mode No.	T (sec)	Nature	Direction
1	6.79463	Symmetrical lateral movement of the towers	Y
2	6.79463	Anti-symmetrical lateral movement of the towers	Y
3	6.546487	X movement of the towers	Y
4	6.546472	X movement of the towers opposite of mode 3	Y
5	6.259553	Torsion of the deck	X
6	5.761706	Lateral (planar) bending of the deck	Y
7	4.487933	Bending of the deck	Z
8	4.150584	Anti-symmetrical torsion of the deck	X
9	1.908252	Anti-symmetrical bending of the deck	Z
10	1.586934	Lateral anti-symmetrical bending of the deck with torsion	Y
11	1.498141	Lateral symmetrical bending of the deck	Y
12	1.429529	Lateral anti-symmetrical bending of the deck	Y

Table 4.18 First 12 modes for model 5 type A

	Static before pretensioning	After pretensioning	Longitudinal earthquake
Max vertical deflection of the deck:	2.24m	0.048m	0.517m
Max cable tension at the center of the main span:	6.7MN	7.2MN	9.3MN
Max bending moment in the deck girder:	39.66MN-m at the tower supports	39.1MN-m at the tower supports	44.3MN-m at the tower supports

Table 4.19 Overall performance of model 5 type A

Type B structure

The modes of this bridge have exactly the same shape as the ones of Model 1. Table 4.20 summarizes the modal analysis for Model 5 type B. Table 4.21 contains the performance criteria for the exact same model.

Mode No.	T (sec)	Nature	Direction
1	6.797203	Symmetrical lateral movement of the towers	Y
2	6.797203	Anti-symmetrical lateral movement of the towers	Y
3	6.546488	X movement of the towers	Y
4	6.546472	X movement of the towers opposite of mode 3	Y
5	6.269992	Torsion of the deck	X
6	5.911755	Lateral (planar) bending of the deck	Y
7	4.496341	Bending of the deck	Z
8	4.201298	Anti-symmetrical torsion of the deck	X
9	1.889099	Anti-symmetrical bending of the deck	Z
10	1.605759	Lateral anti-symmetrical bending of the deck with torsion	Y
11	1.498517	Lateral symmetrical bending of the deck	Y
12	1.430164	Lateral anti-symmetrical bending of the deck	Y

Table 4.20 First 12 modes for model 5 type B

	Static before pretensioning	After pretensioning	Longitudinal earthquake
Max vertical deflection of the deck:	2.18m	0.053m	0.56m
Max cable tension at the center of the main span:	6.4MN	6.8MN	9.1MN
Max bending moment in the deck girder at the tower supports:	28.1MN-m	30.7MN-m	35.4MN

Table 4.21 Overall performance of model 5 type B

4.5 Optimization

The following paragraphs describe the process of determining the optimum spacing of the cables, separately for type A and B models, given the stiffness of the deck.

4.5.1 Type A models

All of the above results, for type A, models are summarized in Table 4.22.

	Model 1	Model 3	Model 4	Model 5
Max vertical deflection of the deck (units in m):	0.444	0.48	0.467	0.517
Max cable tension at the center of the main span (MN):	7.5	6.8	5.9	9.3
Max bending moment in the deck girder (MN-m):	39.6	46.6	48.7	44.3

Table 4.22 Performance of models 1-5 type A under longitudinal earthquake

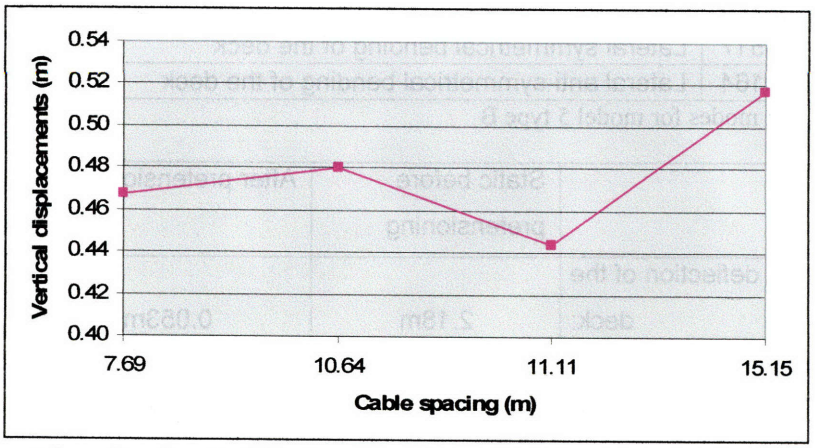

Figure 4.29 Experimental results of vertical displacements for deck section type A

The relationship between the cable spacing and the vertical displacements of the deck can be approximated as:

$$u(x) = a * x^3 + \beta * x^2 + \gamma * x + \delta \qquad (4.6)$$

where u represents the vertical displacements of the deck and x equals to the spacing of the cables' anchoring at the deck.

Using the values of Table 4.23 we solve for the constant parameters α, β, γ and δ of equation (4.6).

u	x
0.443938	11.11111
0.479933	10.6383
0.467496	7.692308
0.51717	15.15152

Table 4.23 Vertical displacements for each cable spacing with deck section type A

The values for the constants were determined using MATLAB and are shown in Table 4.24. The derived function is equation (4.7), which is plotted in Figure 4.30. After differentiating once, we find that for a cable spacing of 13.2m the function appears to have a local minimum, u3=0.3345m. Looking closer at Figure 4.29 we should expect a minimum of the function between 10.64m and 15.15m. Translated in terms of bridge design, this means that 19 cables are needed on each side of every tower. This calls for a cable spacing of 12.82m in the main span. For this value equation (4.7) gives a vertical displacement of u_3=0.34m.

Constant	Value
α	0.006
β	-0.1987
γ	2.134
δ	-6.8989

Table 4.24 Constants of equation (4.6) for deck section type A

$$u(x) = 0.006 * x^3 - 0.1987 * x^2 + 2.134 * x - 6.8989 \qquad (4.7)$$

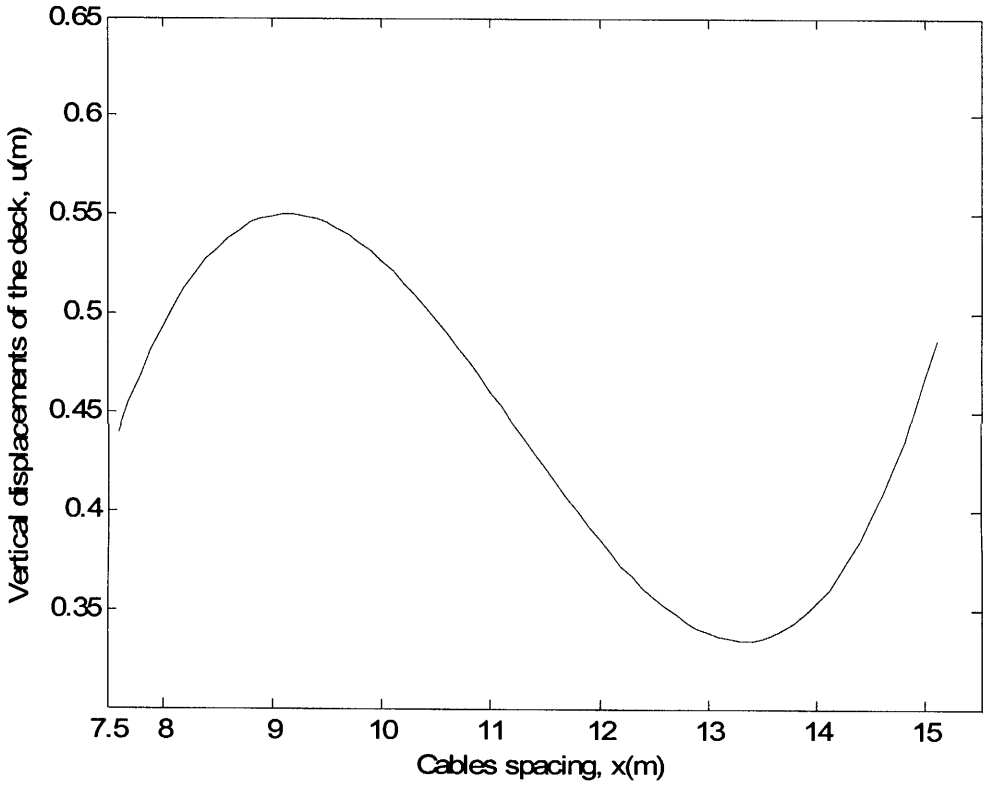

Figure 4.30 Function correlating cable spacing with vertical displacements for deck section type A

4.5.2 Type B models

All of the results from paragraph 4.3 and 4.4 are summarized in Table 4.22.

	Model 1	Model 3	Model 4	Model 5
Max vertical deflection of the deck (units in m):	0.5086	0.512	0.493	0.561
Max cable tension at the center of the main span (MN):	7.7	6.6	5.89	9.1
Max bending moment in the deck girder (MN-m):	39.4	38.4	39.7	31.4

Table 4.25 Performance of models 1-5 type B under longitudinal earthquake

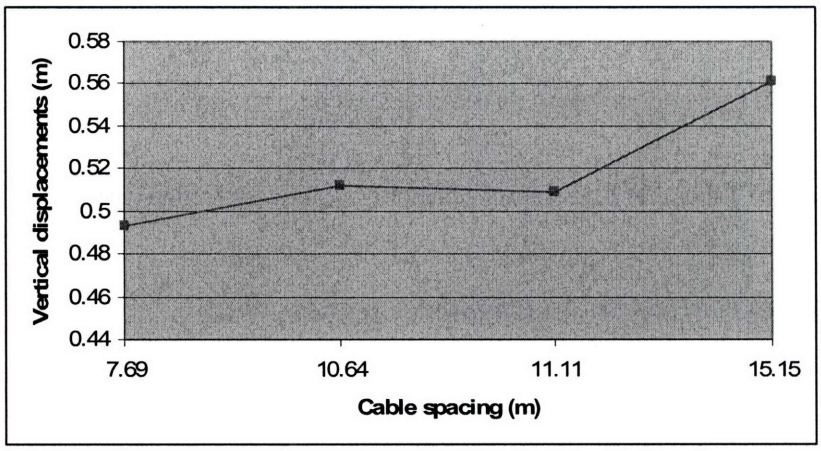

Figure 4.31 Experimental results of vertical displacements for deck section type B

MATLAB it once again used in order to derive an equation of a form similar to that of equation (4.6) that will relate the spacing between the cables to the vertical displacements of the deck. The system of four equations is formed by the values of Table 4.26 and can be solved for the constant parameters α, β, γ and δ.

u	x
0.508612	11.11111
0.511639	10.6383
0.493053	7.692308
0.560745	15.15152

Table 4.26 Vertical displacements for each cable spacing with deck section type B

The derived function for type B structures is equation (4.8), which is plotted in Figure 4.32. After differentiating once, we find that for a cable spacing of 12.39m the function appears to have a local minimum, u_3=0.5034m. Considering that a cable spacing less than 8.5m is too dense for such a long-span and greater than 15m is not possible, this number is the optimal solution of the equation (4.8). Translated in terms of bridge design, this means that 20 cables are needed on each side of every tower and that cable spacing in the main span should be of 12.195m. For this value, equation (4.8) gives a vertical displacement of u_3=0.505m.

Constant	Value
α	0.0011
β	-0.0353
γ	0.3805
δ	-0.8343

Table 4.27 Constants of equation (4.6) for deck section type B

$$u(x) = 0.0011 * x^3 - 0.0353 * x^2 + 0.3805 * x - 0.8343 \qquad (4.8)$$

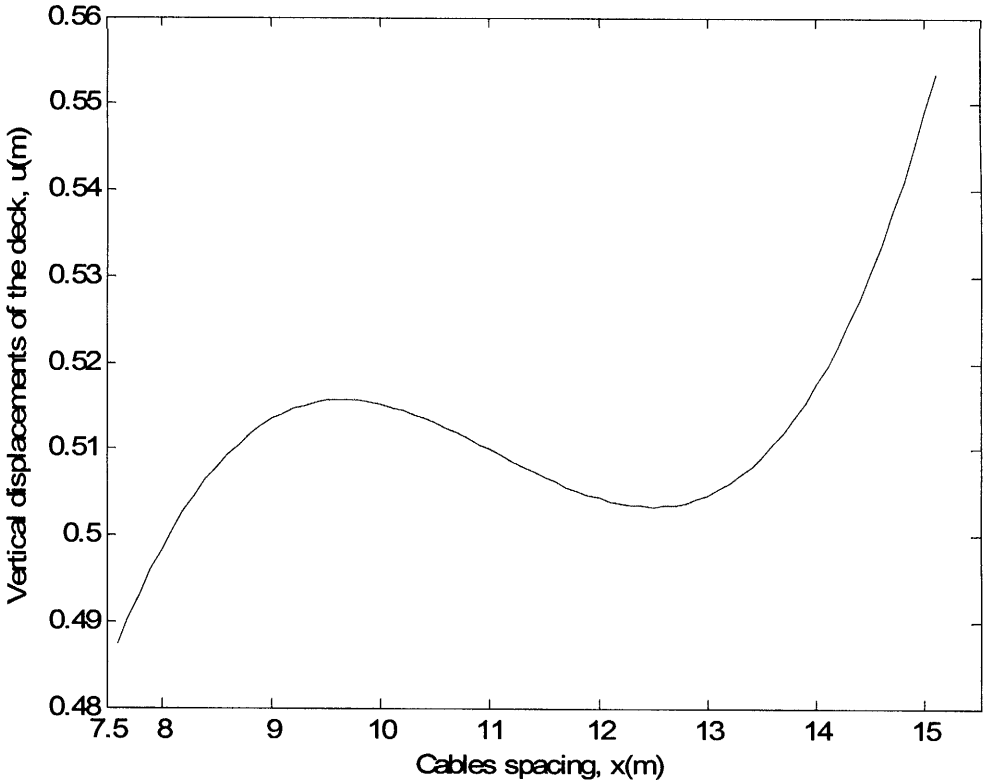

Figure 4.32 Function correlating cable spacing with vertical displacements for deck section type B

4.5.3 Further optimization

At this point, it would be ideal if a more general relationship could be determined, one that would relate the vertical deformations of the deck to both the cable spacing and the stiffness of the deck.

This relationship can be represented by equation (4.9).

$$u = c_{[0,0]}+c_{[1,0]}*x+c_{[2,0]}*x^2+c_{[0,1]}*y+c_{[1,1]}*x*y+c_{[2,1]}*x^2*y+c_{[0,2]}*y^2+c_{[1,2]}*x*y^2+c_{[2,2]}*x^2*y^2 \quad (4.9)$$

where u corresponds to the vertical displacement of the deck, x is the cables spacing and y is the bending rigidity (IE) of the steel frame girder of the deck. The solution to the system of equations that is created by Table 4.23 and Table 4.26 is reached with the help of MATLAB. Unfortunately, no constants that could satisfy equation (4.9) could be found.

Nevertheless, the process of finding a connection between bending rigidity (IE) of the deck girder and the optimum spacing does not end yet. The optimal cable spacing and the deck's bending rigidity, both already known, lead to the determination of the entire deck's equivalent bending rigidity, as if it were constructed solely out of steeel. For composite sections the following equations apply:

$$I_{equiv} = I_{steel} + \frac{I_{concrete}}{n} \quad (4.10)$$

$$E_s = 2.1*10^5 kPa \quad (4.11)$$

$$n = \frac{E_s}{E_c} \approx 10 \quad (4.12)$$

	I_{steel} (m^4)	$I_{concrete}$ (m^4)	I_{equiv} (m^4)	IE_{equiv} ($kN*m^2$)	$X_{Optimum\ cable\ spacing}$ (m)	Optimum ratio $\frac{X_{OptimumSpacing}}{IE_{equiv}}$	Dev
Type A	1.5346	0.13363	1.55	3.25E+05	13.2m	4.06 E-05	0%
Type B	1.0652	0.081126	1.07	2.25E+05	12.39m	5.5 E-05	35%

Table 4.28 Optimum ratio for the models

As can be seen from Table 4.28 the optimum ratio of type A design differs 35% from that of type B, a difference which does not permit us to draw conclusions about the role of the bending rigidity of the deck to the optimum spacing of the bridge.

4.5.4 Conclusions

After using several computer models with different cable spacing, it was possible to specify the optimum cable spacing, appropriate to the deck stiffness of the models.

In particular, in the type A model the optimal cable spacing appears to be 12.82m. On the other hand, for deck type B, the optimum cable spacing is 12.195m.

Unfortunately, it was not possible to determine a relationship that directly connects the optimal cable spacing to different deck stiffnesses.

4.6 Optimized bridges models

In this section, the two optimized models found in §4.5 are now checked.

4.6.1 Type A

4.6.1.1 Geometry

The geometry of the optimized model was imposed by the results of section §4.5. This model consists of 152 cables (19 cables on each side of every tower) that require a spacing of 12.82m with a minimum cable angle of 22.84° and a maximum cable angle of 68.4° (see Figure 4.33).

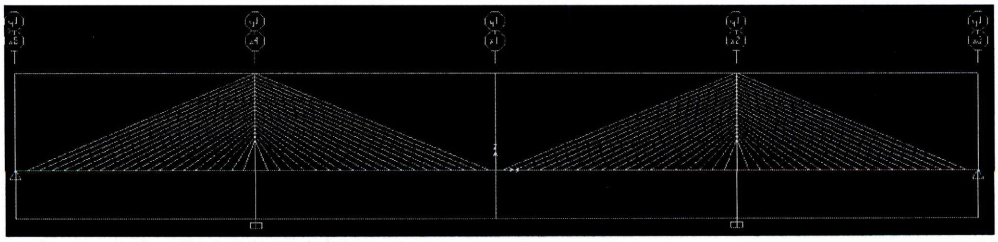

Figure 4.33 Side view of optimized model type A

4.6.1.2 Results

The modes of this bridge have exactly the same shape as the ones of Model 1. Table 4.29 summarizes the modal analysis for the optimized model of type A. Table 4.30 contains the performance criteria for optimized model type A. The comparison of Table 4.30 with the results in §4.5.1 depicts that the model created in this section performs better than any of the previous ones. Therefore, it is the optimum model. On the other hand, the 0.41m of the vertical deflection prove that the parameter of the deck's deflection is not so sensitive, with reference to the cable spacing, as shown in Figure 4.30.

Figure 4.34 and Figure 4.35 show the behavior of the model under earthquake.

Mode No.	T (sec)	Nature	Direction
1	7.000345	Symmetrical lateral movement of the towers	Y
2	7.000345	Anti-symmetrical lateral movement of the towers	Y
3	6.751179	X movement of the towers	Y
4	6.751168	X movement of the towers opposite of mode 3	Y
5	5.387757	Torsion of the deck	X
6	5.28286	Lateral (planar) bending of the deck	Y
7	3.888782	Bending of the deck	Z
8	3.813966	Anti-symmetrical torsion of the deck	X
9	1.774474	Anti-symmetrical bending of the deck	Z
10	1.465381	Lateral anti-symmetrical bending of the deck with torsion	Y
11	1.409266	Lateral symmetrical bending of the deck	Y
12	1.31981	Lateral anti-symmetrical bending of the deck	Y

Table 4.29 First 12 modes for optimized model type A

	Longitudinal earthquake
Max vertical deflection of the deck:	0.41m
Max cable tension at the center of the main span:	8MN
Max bending moment in the deck girder at the tower supports:	39.1MN-m

Table 4.30 Performance of optimized model type A under longitudinal earthquake

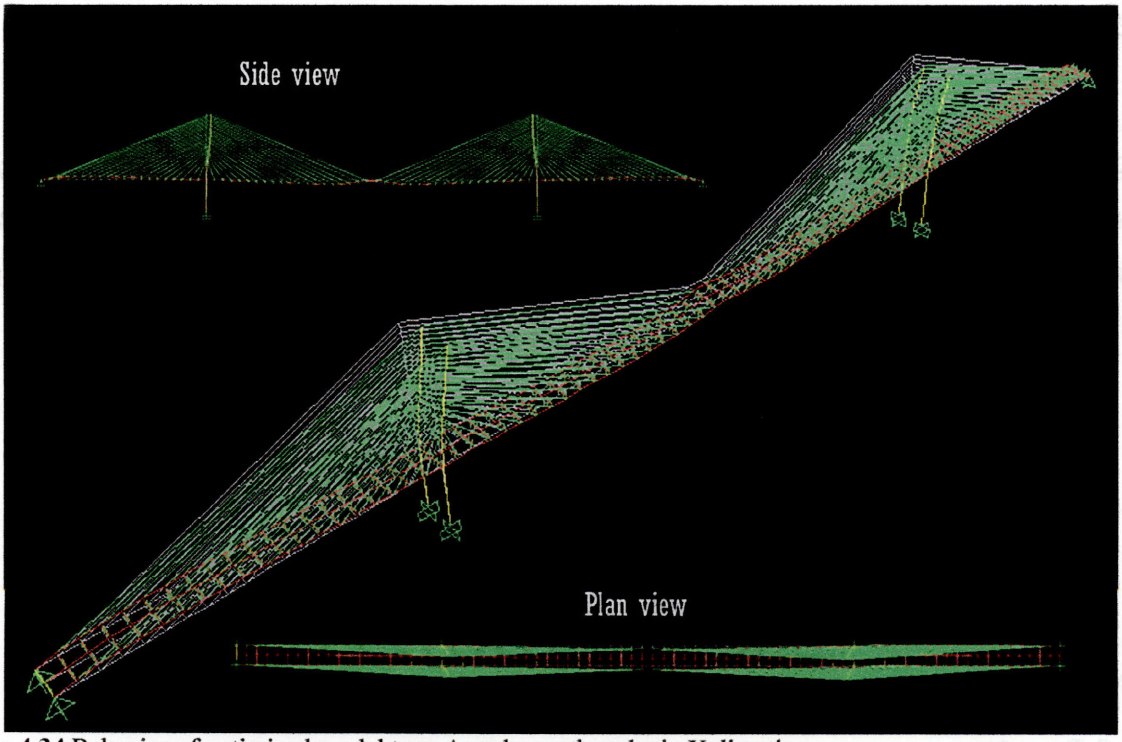

Figure 4.34 Behavior of optimized model type A under earthquake in X direction

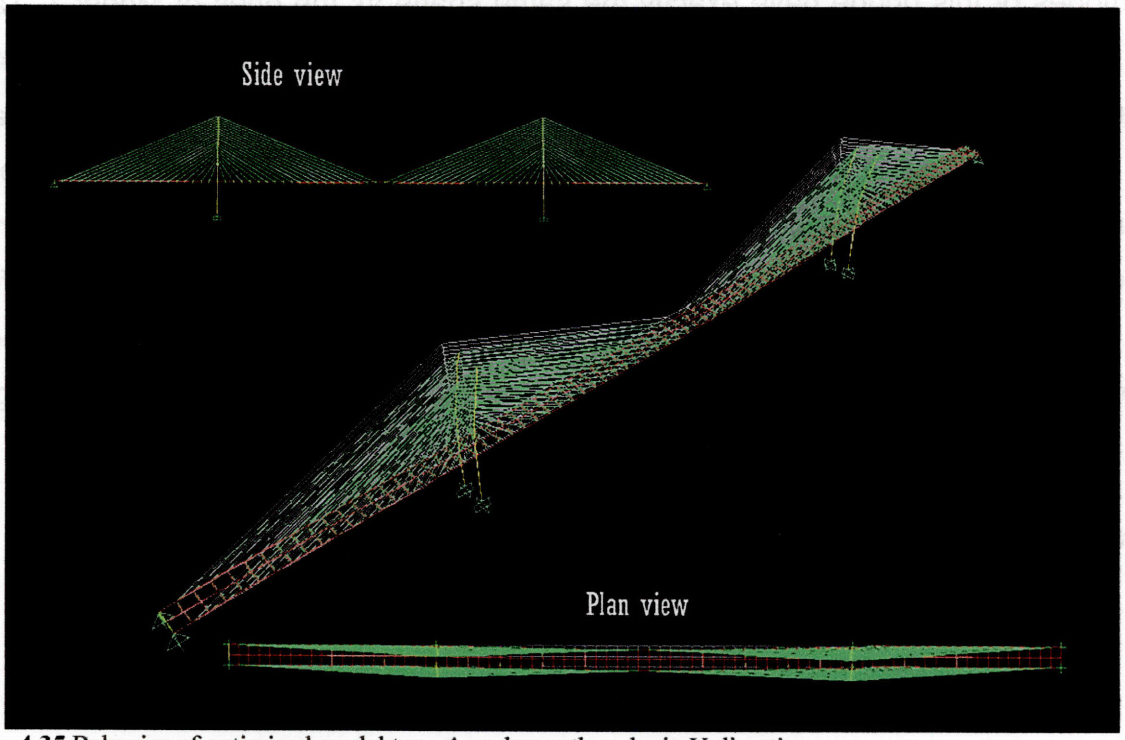

Figure 4.35 Behavior of optimized model type A under earthquake in Y direction

4.6.2 Type B

4.6.2.1 Geometry

The geometry of the optimized model was imposed again by the results of section §4.5. This model consists of 160 cables (19 cables on each side of every tower) that require a spacing of 12.195m with a minimum cable angle of 22.78° and a maximum cable angle of 66.8° (see Figure 4.36).

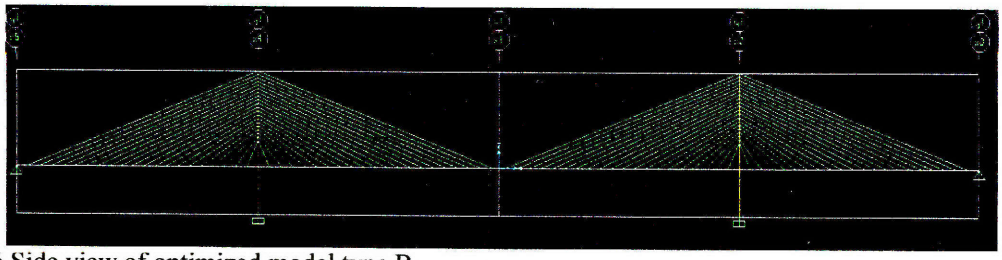

Figure 4.36 Side view of optimized model type B

4.6.2.2 Results

The modes of this bridge have exactly the same shape as the ones of Model 1. Table 4.31 summarizes the modal analysis for the type B optimized model. Table 4.32 contains the performance criteria for optimized model type A. The comparison of Table 4.32 with the results in §4.5.2 reveals that the model created in this section performs better than any of the previous ones, so it is the optimum one. However, the 0.507m of the vertical deflection is very close to the 0.5086 m of the model's 1 type B. Therefore, such a flexible deck like in bridge type B shows that the parameter of the deck's deflection is not as sensitive with reference to the cable spacing as shown in Figure 4.32.

Figure 4.37 and Figure 4.38 show the behavior of the model under earthquake.

Mode No.	T (sec)	Nature	Direction
1	7.127345	Symmetrical lateral movement of the towers	Y
2	7.127345	Anti-symmetrical lateral movement of the towers	Y
3	6.878179	X movement of the towers	Y
4	6.878168	X movement of the towers opposite of mode 3	Y
5	5.514757	Torsion of the deck	X
6	5.40986	Lateral (planar) bending of the deck	Y
7	4.015782	Bending of the deck	Z
8	3.940966	Anti-symmetrical torsion of the deck	X
9	1.901474	Anti-symmetrical bending of the deck	Z
10	1.592381	Lateral anti-symmetrical bending of the deck with torsion	Y
11	1.536266	Lateral symmetrical bending of the deck	Y
12	1.44681	Lateral anti-symmetrical bending of the deck	Y

Table 4.31 First 12 modes for optimized model type B

	Longitudinal earthquake
Max vertical deflection of the deck:	0.507m
Max cable tension at the center of the main span:	8.2MN
Max bending moment in the deck girder at the tower supports:	35.5MN-m

Table 4.32 Performance of optimized model type B under longitudinal earthquake

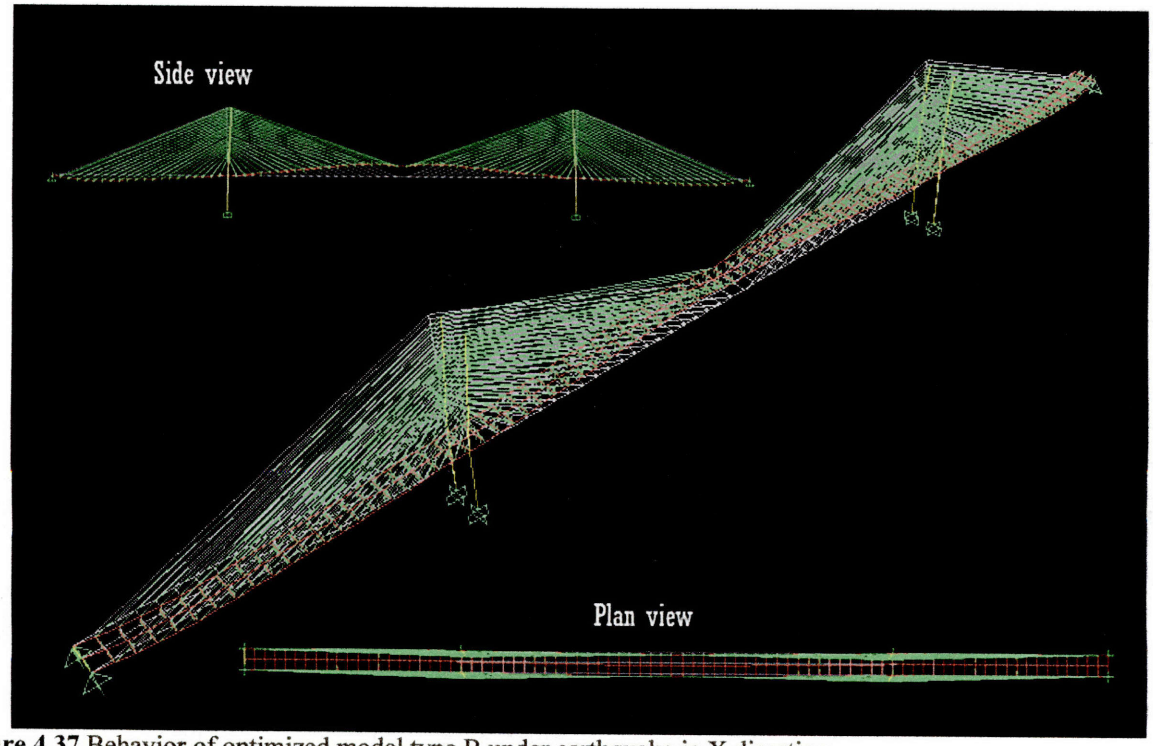

Figure 4.37 Behavior of optimized model type B under earthquake in X direction

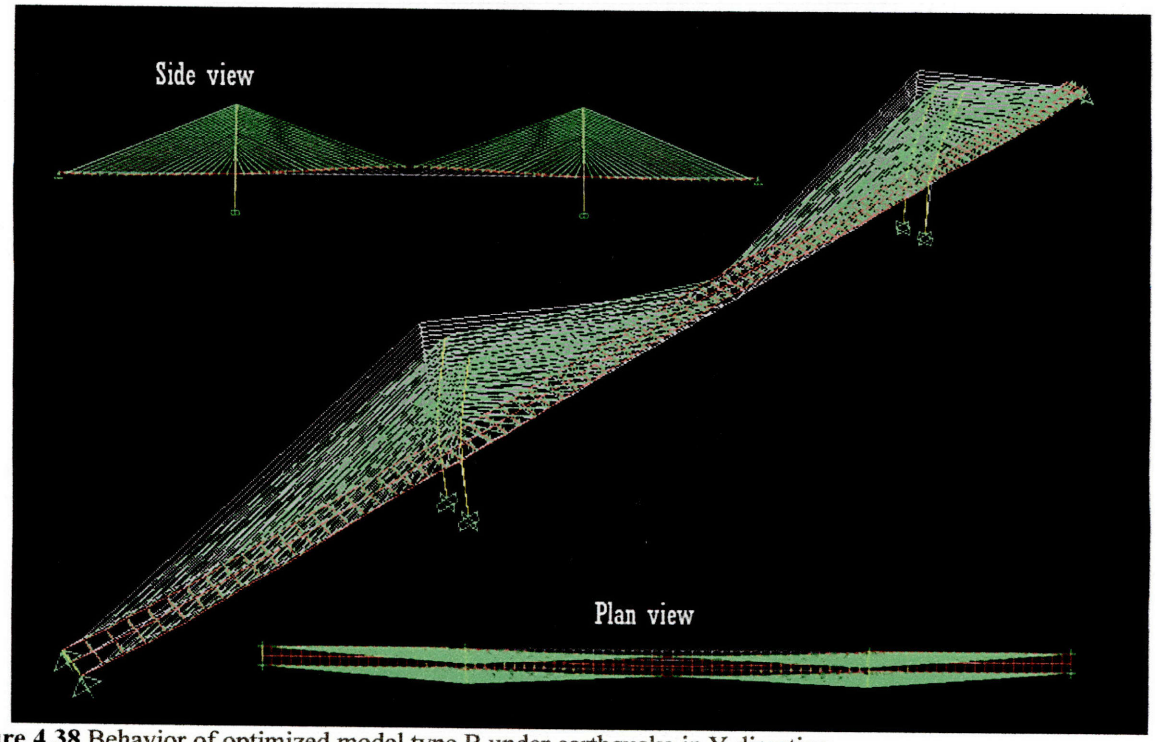

Figure 4.38 Behavior of optimized model type B under earthquake in Y direction

4.7 Further improvement of the typical bridge design

In order to improve the overall behavior of the type A cable-stayed bridge by remedying its fundamental weaknesses, braces are added to the towers of the model in section 4.6.1. The properties of the braces are shown in Figure 4.39.

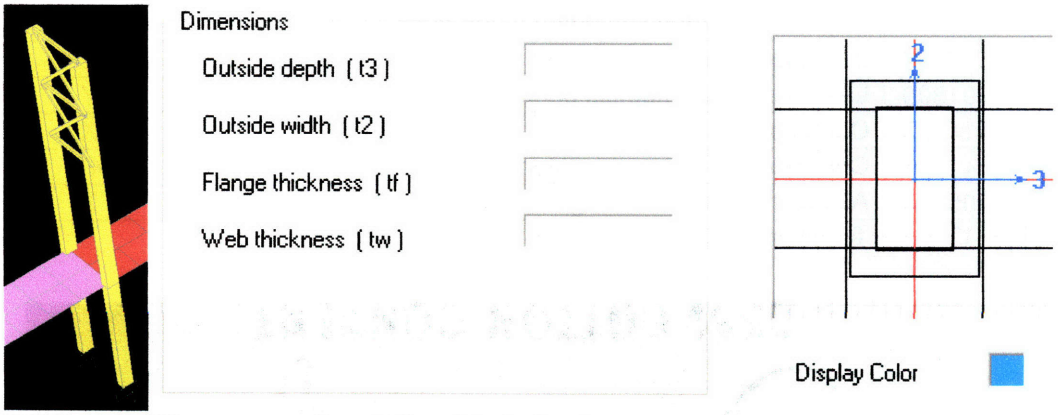

Figure 4.39 Braces of the towers made out of steel (units in m)

The computer simulation analysis, has proven the bridge's performance to have improved a lot. Table 4.33 summarizes the first twelve modes of this bridge while, Figure 4.40 to Figure 4.43 show the first 4 modes. The fundamental period of the structure has been reduced to 4.72sec. As far as the modes are concerned, the fundamental mode corresponds to the vertical bending of the deck. The second mode turned to be the planar bending of the deck. This is a much better response for a bridge 500m long, as the deck should be its weakest element. Rigid towers improve the response of the cable-stayed bridge as they provide stiffer support to the cables and consequently to the deck.

Mode No.	T (sec)	Nature	Direction
1	4.721911	Bending of the deck	Z
2	4.235708	Planar bending of the deck	Y
3	3.742041	Torsion of the deck	X
4	3.451909	Anti-symmetrical bending of the deck	Z
5	3.348404	Lateral anti-symmetrical bending of the deck with torsion	Y
6	3.28652	Anti-symmetrical torsion of the deck	X
7	2.776493	Lateral symmetrical bending of the deck	Y
8	1.544946	Bending of the deck	Z
9	1.501809	Lateral anti-symmetrical bending of the deck with torsion	Y
10	1.414933	Complex symmetrical torsion of the deck	X
11	1.341046	Complex anti-symmetrical torsion of the deck	XY
12	1.305164	Anti-symmetrical bending of the deck (higher mode)	Z

Table 4.33 First 12 modes for optimized braced model

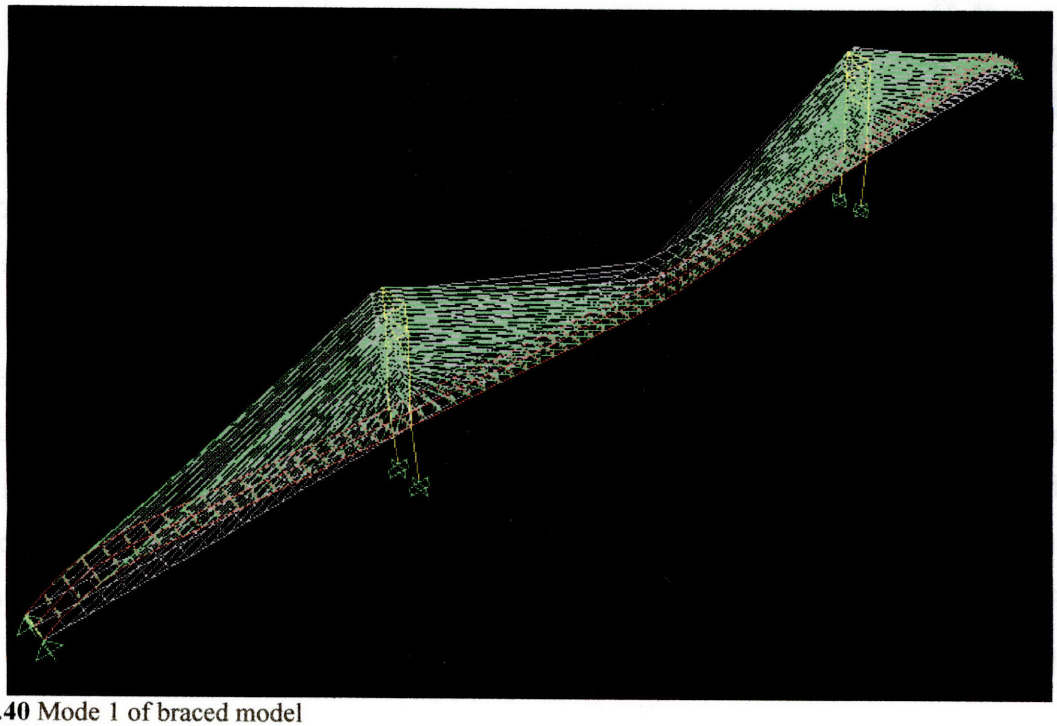

Figure 4.40 Mode 1 of braced model

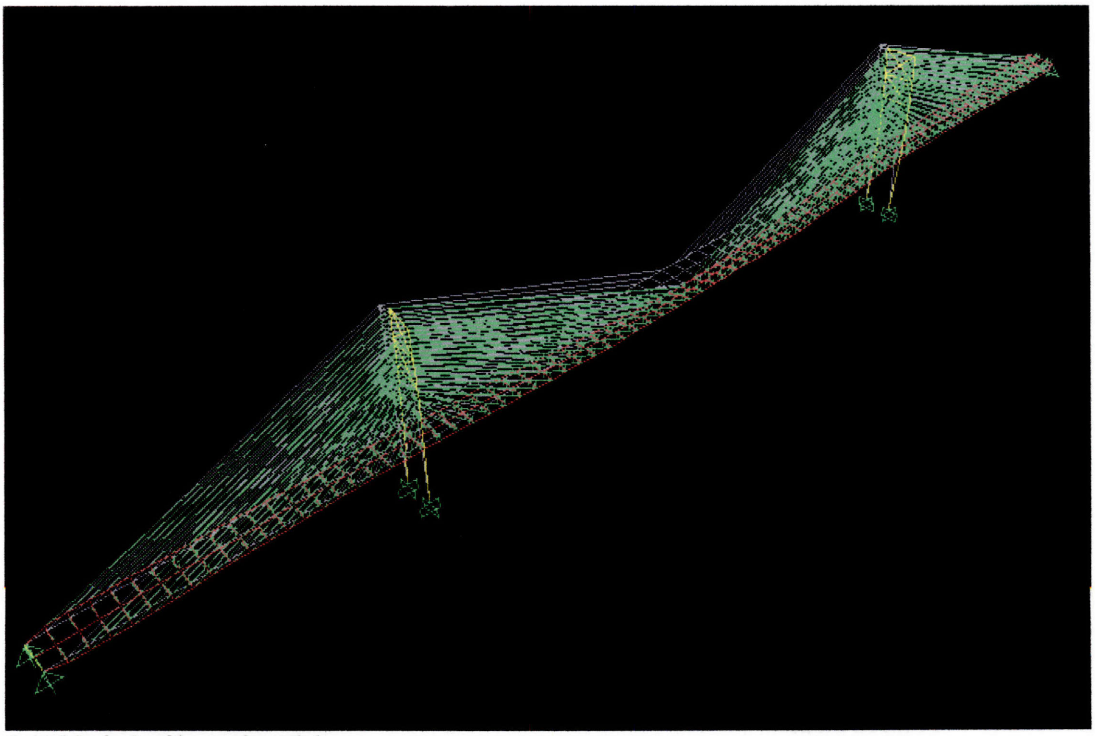

Figure 4.41 Mode 2 of braced model

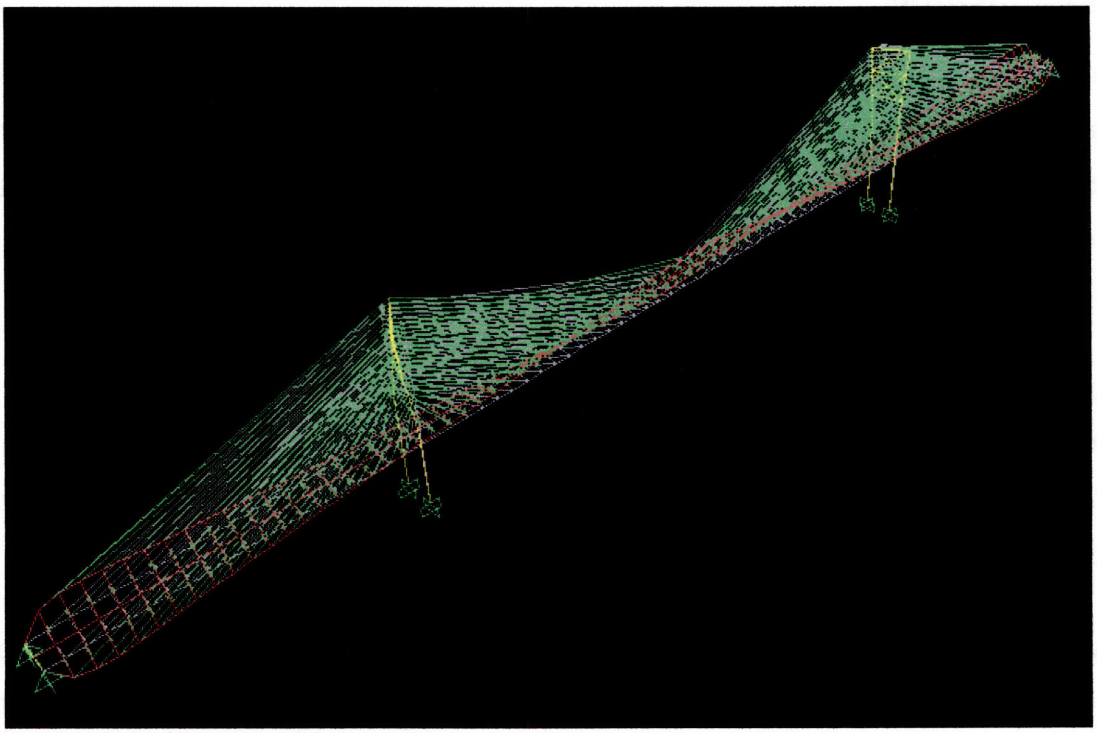

Figure 4.42 Mode 3 of braced model

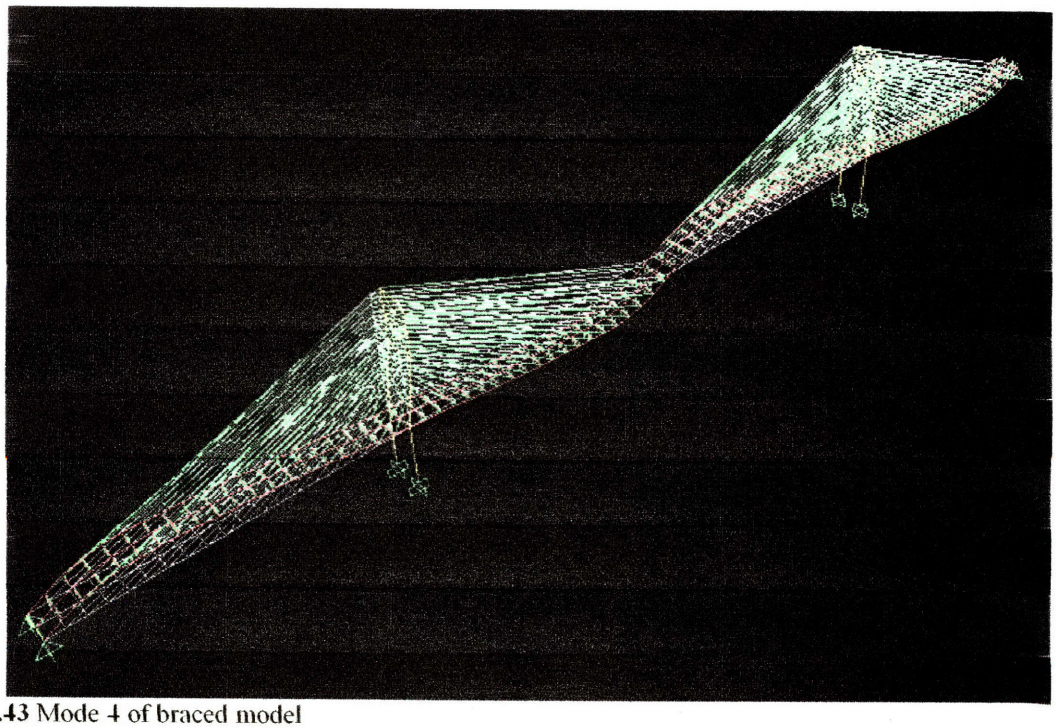

Figure 4.43 Mode 4 of braced model

4.8 Conclusions

The present research, made it possible to determine the optimum cable spacing for a very specific bridge design. The analyses gave optimum cable spacing of 12.82m and 12.195m, for type A and Type B bridges respectively. It is obvious that for a bridge with a span of 500m a stiffer deck reduces the vertical displacements of the deck by a lot. The type B deck is very flexible in order to span such a large distance.

The ideal outcome of this research would be to produce a relationship that apart from the cable spacing, could also connect the bending rigidity of the deck with the optimum performance of the bridge. Unfortunately, the computer simulations conducted were too limited to perform such a task.

Finally, section §4.7 made clear that more rigid towers improve the response of the cable-stayed bridge as they provide stiffer support to the cables and consequently to the deck.

CHAPTER 5
CASE STUDY OF RION-ANTIRION CABLE-STAYED BRIDGE

This chapter focuses on an actual cable-stayed bridge, the Rion-Antirion Bridge. A finite element model has been created in order to study the behavior of the bridge, through static structural analysis. The loads applied to the model are dead loads, live loads and the design earthquake response spectrum.

5.1 Introduction to structure and site

The Rion-Antirion Bridge (see Image 5.1) is crossing the Gulf of Corinth near Patras in western Greece. It links two small villages called Rio and Antirio respectively. The name of the bridge can be encountered in many different versions, such as Rion-Antirrion or Rio-Antirio bridge, because of the many different ways translating the Greek name of the bridge[1]. It is part of the country's new west transportation axis called Ionia Odos, a major national transport project connecting Kalamata with Igoumenitsa and reaching till Kakkavia in the Greek-Albanian borders. The objective is to establish direct access to all major urban centers of Greece (Patras, Athens, Lamia, Larissa, Thessalonica) from the developing neighboring countries in the Balkan region, from the other European countries and from the east, too. Vital is also the connection to the network of the major harbors in Greece, one of which is Patras' harbor.

[1] Ζεύξη Ρίου-Αντιρρίου

Image 5.1 The Rion-Antirion Bridge, Greece completed in 2004 with a 2,252 m continuous deck[2]

The Rion-Antirion crossing consists of a cable-stayed bridge. It is located in an environment consisted of high water depths and rather weak soil deposits. Additionally, the seismic activity in the area is severe and improbable to occur in an area like Massachusetts. This severity has made the design even more challenging.

5.2 Description of the structure

The main part of the Rion-Antirion Bridge is a continuous multi-cable-stayed bridge, supported by four large pylon/pier structures named M1, M2, M3 and M4 resting on the sea bed. The method of erection was the free cantilever. The final span lengths are 286, 3 x 560 and 286 m (Figure 5.1). The bridge has two 9.50 m wide carriageways, separated by a 0.50m wide central separator with a double safety fence and bounded by lateral crash barriers.

Figure 5.1 Rion-Antirion Bridge openings

With a reference span of 560m, the Rion-Antirion bridge ranks in the top 10 list of the world longest span for cable-stayed bridges. However, with its 4 pylons (compared to the usual set of 2), it is the cable-stayed bridge with the longest suspended deck (2,252

[2] Captured by http://www.gefyra.gr

meters) in the world. Such outstanding deck length outperforms the total deck length of the well-known Golden Gate suspension bridge (1,966 meters)

The Rion-Antirion bridge is built to withstand a collision of a 180,000 tons tanker, wind speed of 250 km per hour and over 7 Richter scale earthquake. Absorbing up to 2 meters tectonic displacement between any of its piers, the bridge is definitely, one of the safest places to be, should a major earthquake happen in the Patras area (Gefyra website, 2006).

5.2.1 Physical data

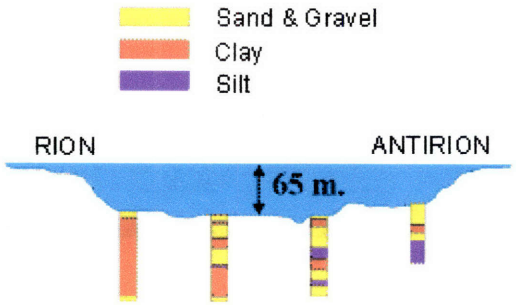

Figure 5.2 Rion-Antirion bridge physical data[3]

The bridge has to span a stretch of water of some 2,500 meters. Moreover the physical features of the strait present an exceptional combination of adverse conditions, which makes this project unique: water depth up to 65 meters, absence of stiff seabed subsoil, strong seismic activity and possible tectonic movements.

The seabed profile presents steep slopes on each side and a long horizontal plateau about 60m below sea level. No bedrock has been encountered during investigations down to a depth of 100 m below seabed. Based on a geological study, it is believed that the thickness of sediments made of thick layers of clay mixed in some areas with fine sand and silt is greater than 500 m.

[3] Captured by http://www.gefyra.gr

More information on the structure can be found in Marchetti et al. (2004), Morgenthal (1999), Papanikolas (2004) and Rion-Antirion Bridge, Design drawings and technical documentation.

5.3 Description of the finite element model

5.3.1 Geometry

The deck has a curvature in the longitudinal direction (see Figure 5.3 and Figure 4.2). There are four piers and 16 sets of 23 cables. The lengths of the three main spans are 560m and of the two side spans are 286m. The deck is fully suspended from the pylons without any direct shear connection. There are only dampers connecting the deck to the pylons.

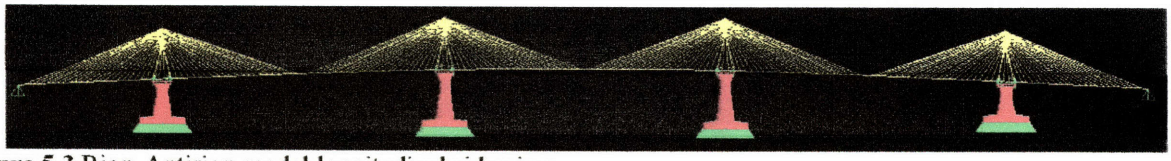

Figure 5.3 Rion-Antirion model longitudinal side view

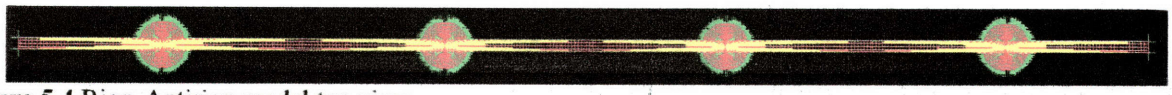

Figure 5.4 Rion-Antirion model top view

5.3.2 Foundations

The diameter of the foundations is 90m with a varying height starting at 9m in the outside and ending up to 13m in the inside of the diameter. The depth of the foundation varies from 47m at the outer piers (M1 and M4) to 63 m at the inner piers (M2 and M3). The foundations are pinned to the ground as the flexibility of the seabed is negligible. The quality of concrete used in the foundation is C60/75. More detailed description of the foundation is given in Figure 5.5.

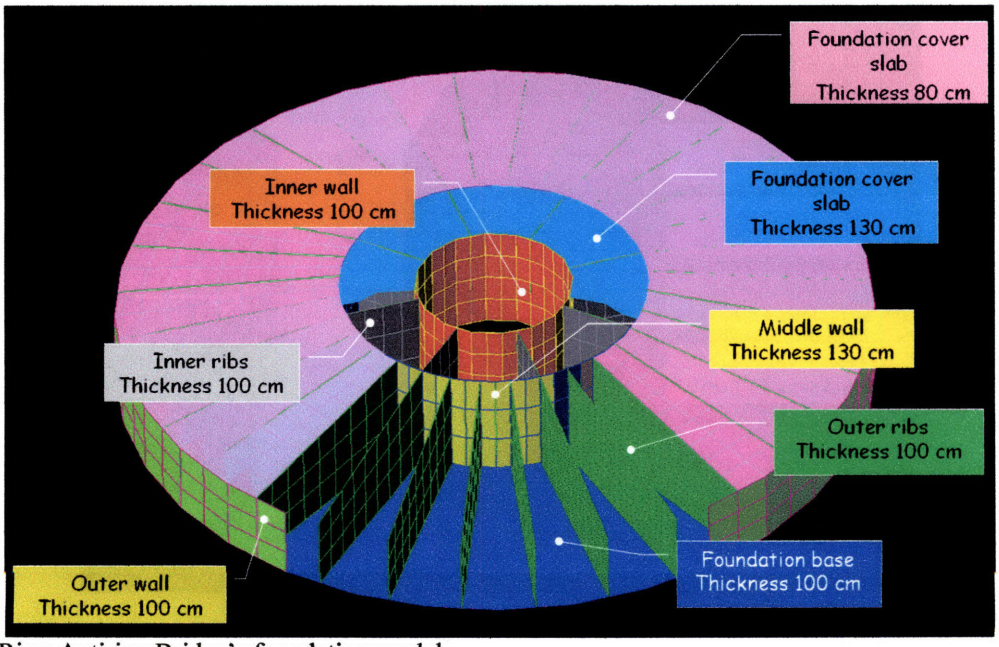

Figure 5.5 Rion-Antirion Bridge's foundation model

5.3.3 Piers

The height of the tall piers is 95.25m and of the short ones is 68.85m. The piers are sinked 35-50m below sea level and above the water level is 27-49m. The quality of the concrete varies from C45/55 to C50/60. A more detailed description of the piers is given in Figure 5.6.

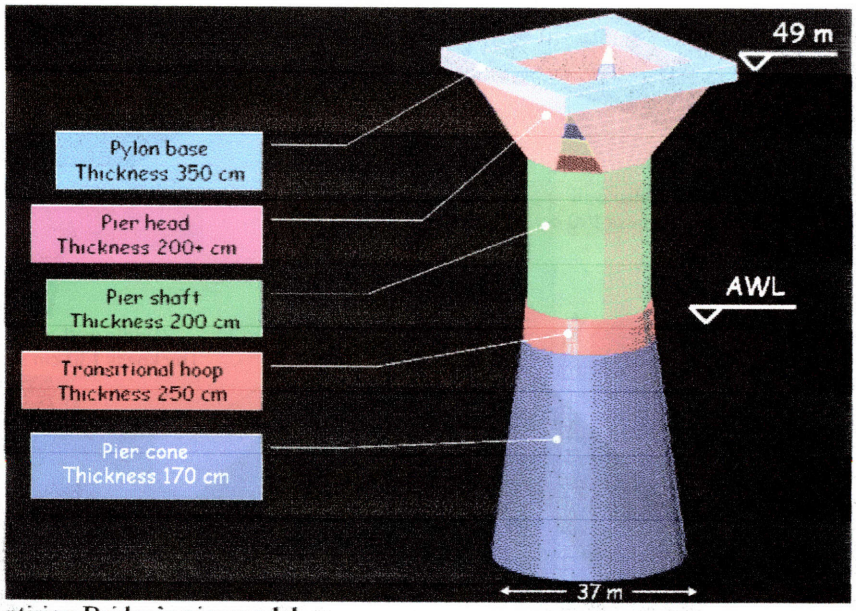

Figure 5.6 Rion-Antirion Bridge's pier model

5.3.4 Pylons

A detailed description of the finite element model of the pylon is given in Figure 5.7. The quality of concrete used here is C60/75 and of the structural steel is S460. The pylon starts at a height of 49m above sea level and goes up to 164m.

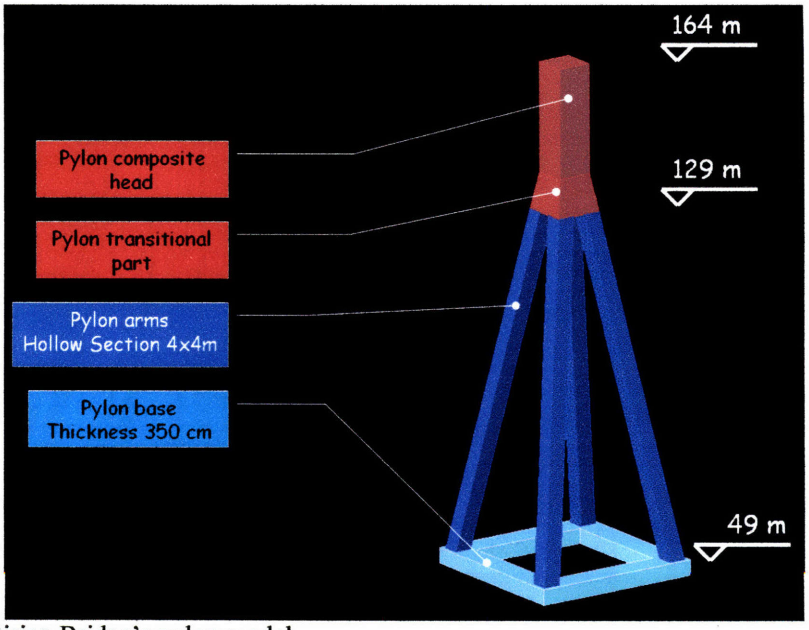

Figure 5.7 Rion-Antirion Bridge's pylon model

5.3.5 Deck and cables

The structural steel used for the deck is S460 while the stays are made out of steel T15S 1770MPa. The cable spacing is 12.22m with a minimum angle of 23° and a maximum angle of 81°. A more detailed description of the model is given in Figure 5.8. Shell elements assigned with the properties of concrete and with a thickness of 25cm are used for the simulation of the deck. Prestress was applied to all the cables in order to ensure small deformations of the deck after application of the factored self-weight and of the live loads of the structure. The initial displacements were gradually reduced after ten iterations.

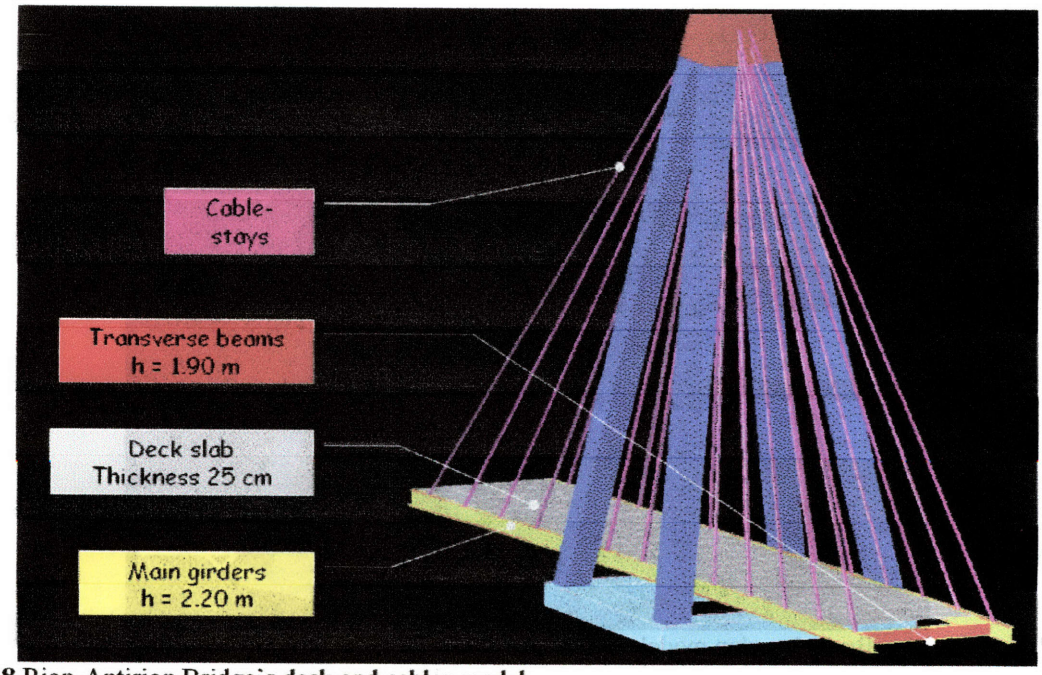

Figure 5.8 Rion-Antirion Bridge's deck and cables model

5.3.6 Earthquake excitation

In addition to the standard specifications, the Greek State has imposed stringent design seismic loading to the bridge design: a peak ground acceleration equal to 0.48g and a maximum spectral acceleration equal to 1.20g between 0.2 and 1.0sec. Figure 5.9 depicts the design earthquake response spectrum for the Rion-Antirion bridge and compares it to the Greek code design earthquake response spectrum that is anticipated in the area where the bridge is located. This response spectrum corresponds to an earthquake with a return period of 2000 years (Papanikolas, 2004). It is worth mentioning that these specifications are more severe than the accelerations recorded on August 17th, 1999, during the Izmit 7.4 Richter scale earthquake in Turkey. The actual acceleration of the Izmit earthquake was 0.399g.

The bridge's expected life span is 120 years which means that possibility for the design earthquake to take place during the bridge's life cycle is. 6%. It is interesting to point out that for the San Francisco-Oakland Bay Bridge's east span this possibility is 10%.

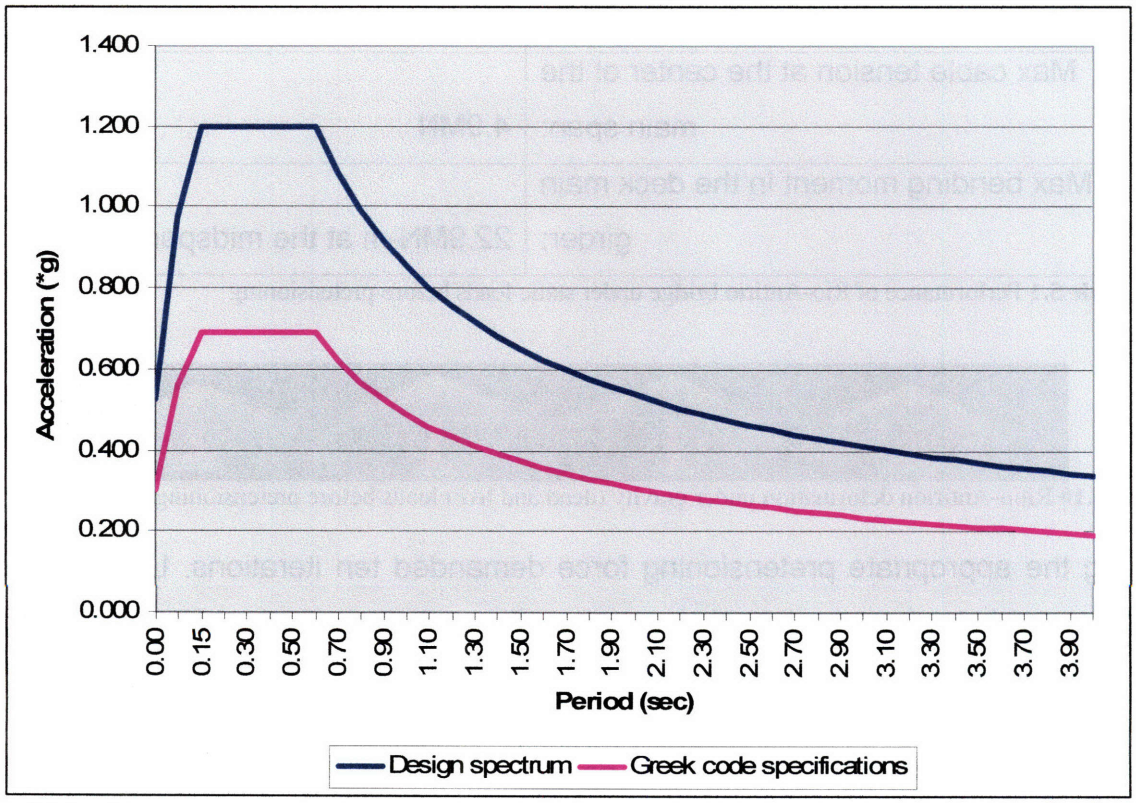

Figure 5.9 Design Response spectrum for Rion-Antirion bridge

5.4 Analytical Results

5.4.1 Static characteristics of the model

The results that derived after running the analysis of the model, are presented below.

Due to the dead and live loads of the bridge, the model deformed as shown in Figure 5.10. The condition of the bridge at this state has as follows:

Max vertical deflection of the deck:	2.98m
Max cable tension at the center of the main span:	4.9MN
Max bending moment in the deck main girder:	22.9MN-m at the midspan

Table 5.1 Performance of Rio-Antirio bridge under static loads before pretensioning

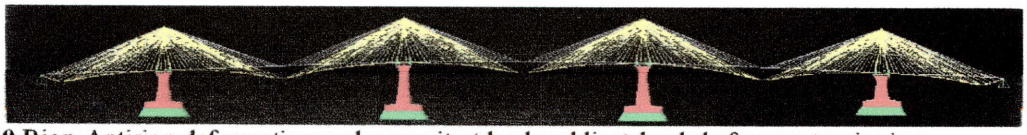

Figure 5.10 Rion-Antirion deformation under gravity (dead and live) loads before pretensioning

Finding the appropriate pretensioning force demanded ten iterations. Under the static loading of the bridge, the procedure led to the reduction of the deck deflections to ±1.5cm (see Figure 5.11). Table 5.2 depicts the results of the above process:

Max vertical deflection of the deck:	0.0153m
Max cable tension at the center of the main span:	5.8MN
Max bending moment in the deck girder:	5.1MN-m at the midspan

Table 5.2 Performance of Rion-Antirion bridge model after pretensioning

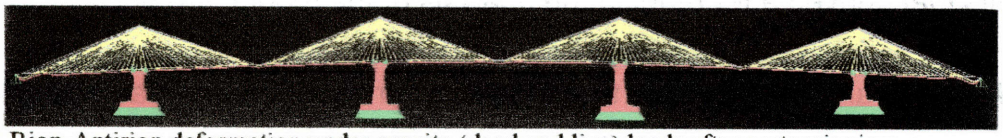

Figure 5.11 Rion-Antirion deformation under gravity (dead and live) loads after pretensioning

5.4.2 Dynamic characteristics – modal analyses

The modal analysis of the bridge revealed the weak points of the bridge. Mode 1 is shown in Figure 5.12. The fundamental period of the structure is 5.44sec and corresponds to the fundamental mode where there is symmetrical lateral movement of the deck. The first 6 modes of the bridge are shown in the following figures (Figure 5.12 to Figure 5.17), while Table 5.3 offers information on the first 12 modes.

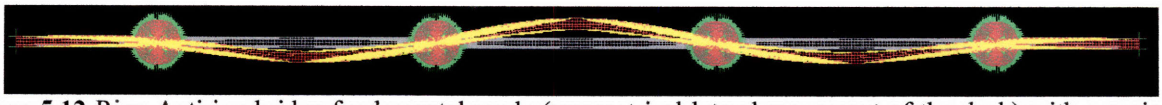

Figure 5.12 Rion-Antirion bridge fundamental mode (symmetrical lateral movement of the deck) with a period of T_1= 5.44sec

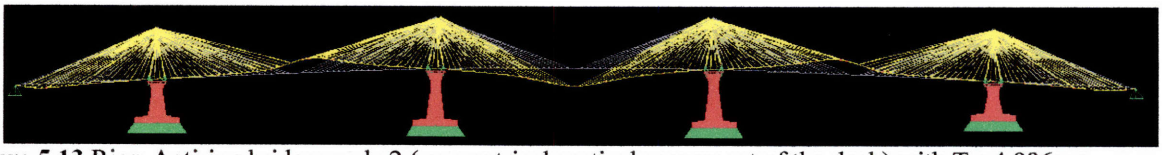

Figure 5.13 Rion-Antirion bridge mode 2 (symmetrical vertical movement of the deck) with T_2=4.986sec

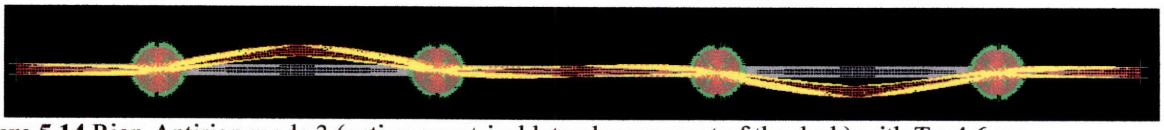

Figure 5.14 Rion-Antirion mode 3 (anti-symmetrical lateral movement of the deck) with T_3=4.6sec

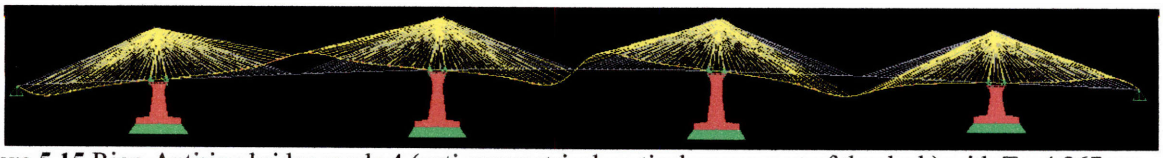

Figure 5.15 Rion-Antirion bridge mode 4 (anti-symmetrical vertical movement of the deck) with T_4=4.267sec

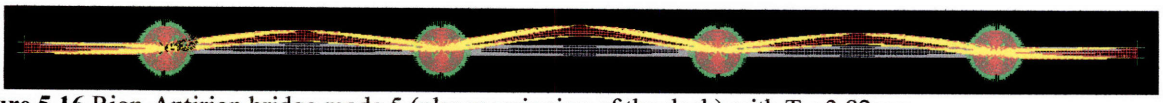

Figure 5.16 Rion-Antirion bridge mode 5 (planar swinging of the deck) with T_5=3.92sec

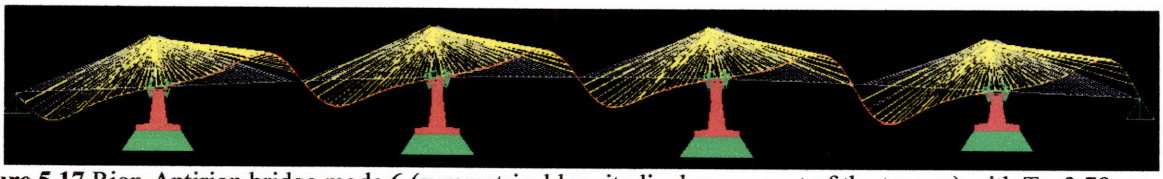

Figure 5.17 Rion-Antirion bridge mode 6 (symmetrical longitudinal movement of the towers) with T_6=3.78sec

Mode No.	T (sec)	Nature	Direction
1	5.441992	Symmetrical lateral movement of the deck	Y
2	4.986032	Symmetrical vertical movement of the deck	Z
3	4.602059	Anti-symmetrical lateral movement of the deck	Y
4	4.26657	Anti-symmetrical vertical movement of the deck	Z
5	3.920292	Planar swinging of the deck	Y
6	3.777919	Symmetrical vertical movement of the deck (3 crossing points)	Z
7	3.761501	Combination of mode 5 and 6	Y,Z
8	2.628126	Vertical fluttering of the deck	Z
9	2.443301	Anti-symmetrical fluttering of the deck	Z
10	2.252561	Higher mode of the deck	Z
11	2.126441	Higher mode of the deck	Z
12	2.109421	Torsion of the deck	X

Table 5.3 First 12 modes for Rion-Antirion bridge

5.4.3 Earthquake response

After analyzing the above characteristics of the bridge the response spectrum of section 5.3.6 is applied to the bridge as an excitation in both longitudinal and transverse direction. Figure 5.18 depicts the quasi-static behavior of the structure under seismic excitation.

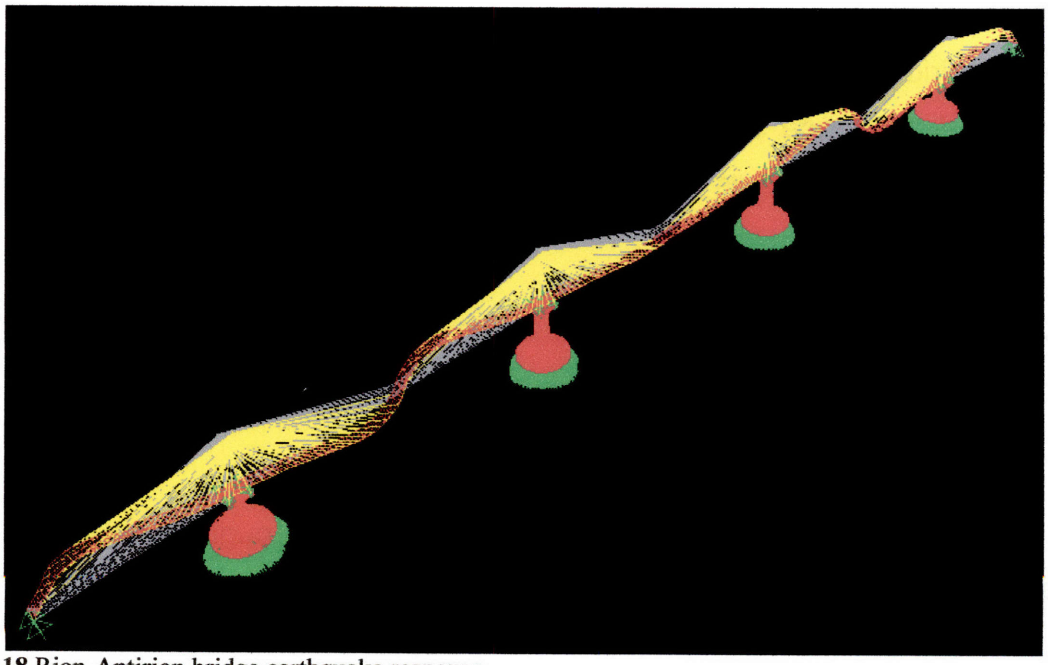

Figure 5.18 Rion-Antirion bridge earthquake response

The overall performance of Rion-Antirion bridge under seismic excitation is shown in Table 5.4.

Max vertical deflection of the deck:	0.49361m
Max cable tension at the center of the main span:	6.8MN
Max bending moment in the deck girder:	6.3MN-m at the midspan

Table 5.4 Performance of Rion-Antirion bridge model under earthquake

The 0.49361m vertical deflection of the deck corresponds to a deflection around $\frac{L}{1100}$ which satisfies the criteria according to which, the deck deflections should be less than $\frac{L}{800}$=0.7m.

5.5 Conclusions

The Rion-Antirion Bridge is an infrastructure project of major importance for the country. The technical challenge of completing the Rion-Antirion project within the planned schedule has been won, as the bridge opened about 3 months ahead the initially announced date.

The model developed in the present thesis describes the quasi-static behavior of the bridge with a very good precision. During, this study no analysis was performed for a tectonic displacement or the loss of some cables.

The present model definitely can be adjusted furthermore through a continuous process that demands more time and sources than available at the time.

CHAPTER 6
SUMMARY - CONCLUSIONS

Cable-stayed bridges are nowadays flourishing as they offer the most economical option for spanning distances from 200m to 1100m. The lightweight design and the aesthetical pleasure are also strong factors that place them among the most favorable alternatives for bridges' design. The incessant evolvement of technology as well as the enhancement of the engineers' knowledge on these indeterminate structures will undoubtedly draw the designers' attention even more in the future and the spans will not stop getting longer.

Specifically, the present research was able to find an optimum design for typical cable-stayed bridges with reference both to the cable spacing and the deck stiffness. Decks with two different stiffnesses for the steel frame were developed. For each different deck, five different computer models were created and analyzed. Numerical results were derived for the optimum cable spacing which corresponds to each one of the deck's stiffness.

In particular, a bridge of 500m main span with an equivalent steel deck of a bending rigidity $IE_{equiv}=3.25*10^5$ kN*m^2 demands a cable spacing of 13.2m. While, a bridge with the same main span but with an equivalent steel deck of a bending rigidity $IE_{equiv}=2.25*10^5$ kN*m^2 demands a cable spacing of 12.39m. Unfortunately, through this research it was not feasible to conclude to a more generic relationship that, besides the cable spacing, would also take into consideration the deck stiffness, in order to establish the optimum performance of the bridge.

As the results show a more flexible deck requires more closely spaced cables in order to provide to the deck the best possible support. However, for a cable-stayed bridge like the one modeled in this thesis with a 500m it is made clear that a deck with bending rigidity $IE_{equiv}=2.25*10^5$ $kN*m^2$ would make the deck much flexible with ultimate displacements of 0.505 m.

Furthermore, the present computer simulations demonstrate that more rigid towers can make a cable-stayed bridge function much better. Bracing the top of the towers can cause the towers' displacements to be reduced. This offers stiffer support to the cables and consequently to the deck of the bridge.

This thesis included also a case-study on Rion-Antirion cable-stayed bridge. The creation of a finite element model follows the brief description of the structure. The finite element model helped in the process of the structural analysis and in understanding of the quasi-static response of the bridge. The design earthquake response spectrum of the bridge was applied as a load case and produced displacements in the deck as high as 0.49m in the deck.

As a further contribution to this research, several improvements can be proposed. Firstly, running more than 10 different models (as it is done in this thesis) a rich library of results could be generated. In that case, it could maybe be possible to specify a relationship including both the cable spacing and the deck stiffness as dependent parameters of the bridge's performance. In addition, a dynamic analysis could reveal some of the models' weaknesses or even change its behavior. Finally, a denser mesh of finite element model of the Rion-Antirion Bridge that would offer a more accurate solution could not be created because of the constraints in the computational power of the available technology.

REFERENCES

Amornvivat, P., "Optimal Designs for Cable-Stayed Bridge", M.S. thesis, Massachusetts Institute of Technology, Cambridge, USA, 1996.

Billington D. P. and Deodatis G., "Form and Aesthetics in Cable-Stayed Bridges", Cable-Stayed Bridges: Recent Developments and their Future, Elsevier Science Publishers, New York, 1991.

Bridges Dictionary, http://www.nireland.com/bridgeman/Dictionary.htm, 03/15/2006.

Buonopane, S., "Nineteenth Century Cable-Supported Bridge Forms: The Roeblings and Beyond", Lecture at Massachusetts Institute of Technology, 2006.

Buonopane, S., "The Roeblings and the Stayed Suspension Bridge: Its Development and Propagation in 19th Century United States", Paper, Cambridge, 2006.

Caprani, C., "The history of Cable-Stayed bridges", Thesis.

EAK, "Greek Antiseismic Code", Athens, 2000.

Endo T., Iijima T., Ito M. And Okukawa A., "The Technical Challenge of Long Cable-Stayed Bridge – Tatara Bridge", Cable-Stayed Bridges: Recent Developments and their Future, Elsevier Science Publishers, New York, 1991.

Engineering.gr, http://www.engineering.gr, Torsional constant tables, 03/10/2006.

ESDEP lecture, http://www.kuleuven.ac.be/bwk/materials/Teaching/master/wg01b/l0440.htm, 02/25/2006.

Gefyra website, http://www.gefyra.gr/English/framesetbig.htm, 04/02/2006.

Gerasimidis, S, Medina-Andres, V., and Tsang, L., "The Bernice Bridge over the Cape Cod Canal", M.Eng Project, Massachusetts Institute of Technology, Cambridge, MA, 2006.

Grimsing and Neils, "Anchored and Partially Anchored Stayed Bridges", International Symposium on Suspension Bridges, 1966, pp 465-484.

Ito, M., "Cable-Stayed Bridges in Japan", Cable-Stayed Bridges: Recent Developments and their Future, Elsevier Science Publishers, New York, 1991.

Leonhardt F. and Zellner W., "Past, Present and Future of Cable-Stayed Bridges", Cable-Stayed Bridges: Recent Developments and their Future, Elsevier Science Publishers, New York, 1991.

Marchetti, M., Boudon, R., Monnerie, J., Bouve, P., Dupuis, D., Dadoun, F., Baechler, G., and Olsfors, J., "Adjustment of the Rion-Antirion Cable-Stayed Bridge: An Innovative Multidisciplinary Response to a Construction Challenge", France, 2004.

Morgenthal, G., "Cable-Stayed Bridges - Earthquake Response and Passive Control", MSc Dissertation, Imperial College of Science, Technology and Medicine, London, 1999.

Papanikolas, P., "Rion-Antirion Zeuksi", Dihmerida Ionia Odos, 14 May 2004.

Podolny, W. and Fleming, J. F., "Historical Development of Cable-Stayed Bridges", Journal of the Structural Division, Vol. 98, No. 9, 1972, pp. 2079-2095.

Ponaldy W. and Scalzi J., "Construction and Design of Cable-Stayed Bridges, second edition, Wiley-Interscience Publication, New York, 1986.

Prade, M., "Bridges & viaducts at the XIXe century: New techniques and great French achievements ", Wander Paris Brissaud Poitiers, 1988.

Reis J., "Brooklyn Bridge Gallery Postcards", http://www.endex.com/gf/buildings/bbridge/bbgallery/Jim%20Reis/bbgalleryJimReis.htm, 02/15/2006.

Rion-Antirion Bridge, Design drawings and technical documentation

Sobek, W., "Innovation in Structures", lecture at Harvard University during course GSD 6315, 03/21/2006.

Structurae website, http://en.structurae.de, 03/28/2006.

Tang, M.C. "Cable-Stayed Bridges in North America", Cable-Stayed Bridges: Recent Developments and their Future, Elsevier Science Publishers, New York, 1991.

Tang, M.C., "Design and Construction: Recent North American Experience", IABSE Symposium, Bridges: Interaction Between Construction Technology and Design, Leningrad, 1991.

Technique, http://www.gefyra.gr/English/framesetbig.htm, 04/24/2006

Troitsky, M.S., "Cable-Stayed Bridges", BSP Professional Books, Boston, 1988.

White, E. R., "Structural Aspects of Cable-Stayed Bridge design", M.S. thesis, Massachusetts Institute of Technology, Cambridge, USA, 1975.

APPENDIX A
SECTION EQUIVALENT PROPERTIES

In each type of section, finding the equivalent properties of the steel frames was needed. The way of modeling the deck section imposed the import of the geometrical properties of the steel frame equivalent cross-section into SAP2000 through the form shown in Figure A.1.

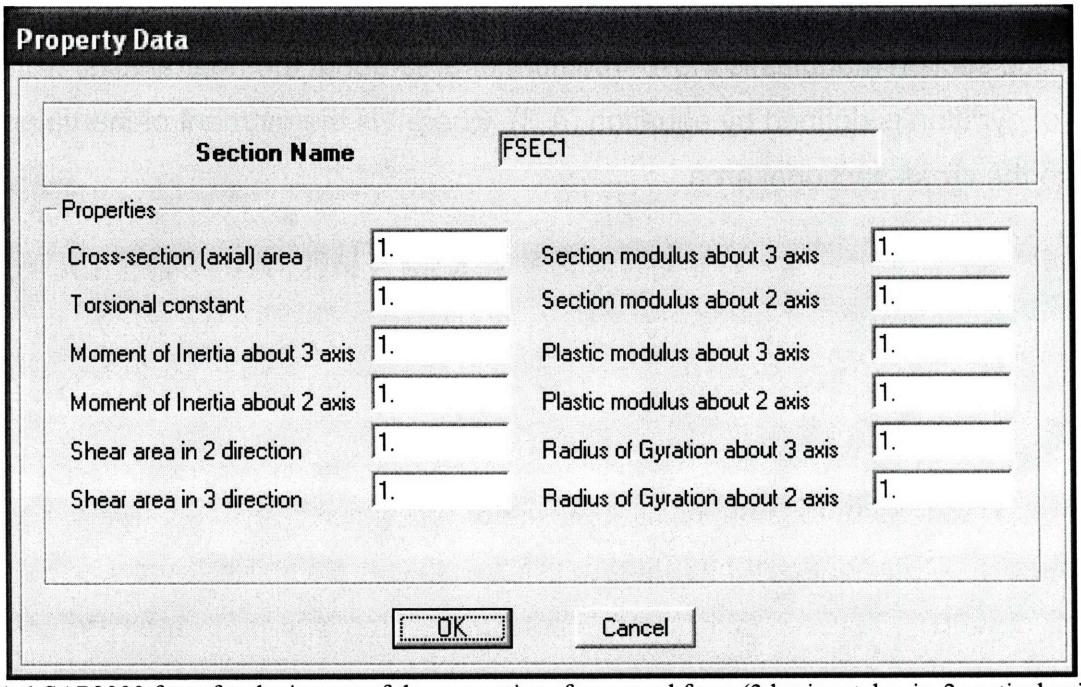

Figure A.1 SAP2000 form for the import of the properties of a general form (3 horizontal axis, 2 vertical axis)

Filling this input data requires the cross-sectional area of the frame. For an I-beam like the one in Figure A.2 we can easily calculate the torsional constant through formula (A.1):

$$J = \frac{1}{3} * \left(b_1 * t_1^3 + b_2 * t_2^3 + h * t_w^3 \right) \qquad \text{(A.1)}$$

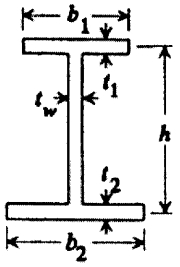

Figure A.2 A typical I-beam section

The moments of inertia are calculated as known for every rectangular area and then to find the elastic section modulus we divide each moment of inertia respectively by the distance from the neutral axis to the extreme fiber, c.

$$Z = \frac{I}{c} \qquad \text{(A.2)}$$

The plastic section modulus is the 1st moment of area about the neutral axis, while the radius of gyration is defined by equation (A.3), where I is the moment of inertia and A refers to the cross-sectional area.

$$r = \sqrt{\frac{I}{A}} \qquad \text{(A.3)}$$

GLOSSARY

Term	Explanation
Abutment	*The ground end-support of a bridge, especially to resist the horizontal thrust of an arch.*
Aerodynamic stability	*The ability of a bridge deck to withstand wind forces without damage from torsion, or oscillation: most relevant to cable-stayed and suspension bridges.*
Aerodynamic deck	*A bridge-deck with a cross-section tapering at each edge to provide aerodynamic stability.*
Air-spinning	*A modern method of constructing suspension bridge cables, in which wires are continuously unspooled back and forth across a span and bound into strands.*
Anchor arm	*The side-span, usually of a cantilever bridge, from abutment to pier, balancing the cantilever.*
Anchorage	*A secure fixing, usually in mass reinforced concrete, at the extremity of a side-span or anchor arm.*
Aqueduct	*A bridge or channel for conveying water, often over long distances.*
Aramid	*An artificial fibre whose exceptionally high tensile strength makes it potentially suitable for very long-spans.*
Arch	*A curved structural span.*
Art Deco	*A decorative style of the 1920s and 1930s, characterized by streamlined curves and geometrical forms.*
Backspan	*See side-span.*
Bar chain	*See eyebar.*
Bascule	*A form of moving bridge in which a hinged counterweight at one end of a span falls, causing the deck to rise.*
Batter	*An inclination from the vertical, as in the sloping side of a bridge pier.*
Beam	*A rigid, usually horizontal, structural element which may itself form an entire bridge.*
Bed joint	*The joint between the radiating elements of an arch.*
Bedrock	*The solid rock layer beneath sand or silt, especially in a river-bed.*
Bellman truss	*A patent design of overlapping wrought-iron king-post trusses plus further diagonal suspension ties.*
Bowstring arch	*An arch whose ends are linked to resist outward thrust.*
Box-girder	*A beam with a hollow square or rectangular section*
Brittle fracture	*The fracture of steel elements at low temperatures.*
Burr truss	*A timber design, combining king-post and arch.*
Cable-stayed bridge	*A bridge whose deck is directly supported from pylons by straight cables without vertical suspenders.*
Cable	*The staying or suspending bridge element; in modern suspension bridges, the main supporting cable is hung from towers, and formed from steel wire bound in strands.*

Term	Explanation
Caisson	A bridge foundation, usually embedded in a riverbed by continuously digging out the material within the bed, so that the caisson sinks.
Camber	A slight convexity on the road surface.
Cantilever	A horizontal member fixed at one end and free at the other.
Cantilever bridge	A bridge with rigid arms extending from both sides of a base, the inner ones usually supporting a central span.
Capital	The head of a column in Classical architecture.
Carbon fibre	Very high-strength filaments of near-pure carbon, suitable for reinforcement.
Cast iron	A brittle alloy with high carbon content: high compressive strength, low tensile strength.
Catenary	The curve into which a uniform rope or cable falls when suspended from two points, as in a suspension bridge.
Cellular construction	In early 20th century American suspension bridges, the method of constructing towers from relatively small welded steel box units.
Cement mortar	The mixture of sand, cement, water and lime that binds masonry and brick.
Centering	A temporary framework over which arch elements are assembled until they are self-supporting.
Chain	The principal supporting element of a now obsolete type of suspension bridge.
Chord	The top or bottom horizontal part of a truss.
Cladding	The outer, usually nonloadbearing, surface of a structure.
Clapper	A prehistoric type of stone slab bridge.
Cofferdam	A watertight structure allowing underwater foundations to be built in the dry.
Colonnade	A series of regularly spaced columns.
Composite construction	The use of different materials together in a single structure.
Compressed-air chamber	The space at the bottom of a caisson, into which air is introduced under pressure to exclude water so that excavation can take place.
Compression	The pushing force which tends to shorten a member; opposite of tension.
Compression zone	The area under compression in the upper part of a horizontal beam.
Compressive strength	The ability of a material to withstand compression.
Concrete	A mixture of water, sand, stone, and a binding element which hardens to a rock-like consistency.
Corbelling	Successive layers of masonry or brick projecting beyond each other.
Corinthian	A Classical architectural style, with leafy decoration at column-heads.
Corne de vache	A decorative feature in masonry bridge design, involving shaving the lower curving edge near the springing of an arch.
Counterweight	See bascule.
Creep	The slow permanent deformation of material under stress, as in shrinkage of concrete.
Creeper crane	The cranes used for building a steel cantilever bridge, moving slowly along the upper chord.
Crown	The highest part of an arch.

Term	Explanation
Cutout	The non-structural material removed from a spandrel, as in Maillart's bridges.
Cutwater	The end of a pier-base, pointed to cleave the water.
Dead load	A structure's own weight.
Deflection theory	An early 20th-century theory that very long suspension bridges would remain stable without deep stiffening trusses through a balance between flexibility and self-weight.
Doric	A Classical architectural style, with no decoration at column-heads.
Dovetail	A splayed piece of timber (or iron or stone) fitting tightly into a similarly shaped cutout.
Drawbridge	See bascule.
Dressing	The cutting of stone units to the required shape.
Dry-stone	Masonry laid without mortar.
Elliptical arch	An arch with a curve that becomes tighter towards the crown.
Entablature	In Classical architecture, the element that rests upon the capitals of the columns.
Environmental load	The external forces on a structure, such as wind and water. Extrados The outer surface of the curve of an arch.
Eyebar	The unit from which the chain of early suspension bridges was constructed, with a flattened ring at each end for linkage.
Falsework	Temporary scaffolding during construction.
Fan configuration	A cable-stayed bridge design in which the cables fan outwards as if from the handle of a fan.
Fender	A protective enclosure round a pier structure.
Fill	The material, usually rubble or earth, used to fill the space behind the outer surface of a masonry bridge structure.
Fin-back bridge	A very modern bridge type in which a vertical solid plane of prestressed concrete supports the spans above the deck.
Fink truss	A patent design of overlapping wrought-iron king-post trusses with additional diagonal bracing.
Flange	The flat top and bottom plates of a box-girder.
Formwork	Temporary boarding to hold concrete in shape while it hardens.
Galvanizing	The coating of metal with zinc for waterproofing.
Girder	A large beam, usually steel or concrete.
Glass fibre	A reinforcing material with high tensile strength.
Gradient of stress	The theoretically uniform change from purely compressive forces along the top of a beam to purely tensile along the bottom.
Granite	A hard crystalline rock, suitable for masonry bridges.
Hanger	See suspender.
Harp configuration	A cable-stayed bridge design in which cables radiate at a uniform distance from each other throughout their length.
Haunch	The part of an arch between the springing and the crown.
Horizontal thrust	The tendency of an arch to push outwards,
Howe truss	A patent design with vertical iron tension rods.
I-beam	A beam or girder with an 1-shaped cross-section.
Intrados	The inner surface of an arch ring. ionic A Classical architectural style with scroll decoration at the column-heads.
Jack-knife bridge	A form of moving bridge with a deck that hinges upwards at the centre.

Term	Explanation
Keystone	*The voussoir at the crown of an arch.*
King-post truss	*A truss consisting of a vertical post, connected to a horizontal beam by inclined tie-beams.*
Laminated timber	*Layers of timber clamped or glued face-to-face.*
Lift bridge	*See bascule.*
Lime mortar	*A non-waterproof binding material for masonry, consisting of lime, water and sand.*
Limiting span	*The maximum span possible for each particular type of bridge.*
Live load	*The weight of traffic passing over a bridge.*
Long truss	*A patent timber design based on overlapping king-post trusses.*
Mortar	*See lime mortar and cement mortar.*
Mortice	*A slot in a member, into which a projecting tenon is fixed to form a joint.*
Navigation span	*The part of a bridge with maximum clearance for shipping.*
Ogival arch	*A pointed arch*
Orthotropic deck	*A bridge deck which is stiffer in the direction of the span that it is laterally.*
Oscillation	*The movement, usually vertically, of a suspended bridge deck in the wind.*
Pier	*The support between two bridge spans, usually arches.*
Pinned arch	*An arch with hinges at the abutments and sometimes also at the crown.*
Plate girder	*A flat bridge deck with a shallow rectangular section.*
Pointed arch	*An arch with an angle at it~ crown.*
Pneumatic caisson	*A caisson with a compressed-air chamber.*
Pontoon bridge	*A bridge formed from floating units, sometimes boats, tied together in a series.*
Portal	*A-frame with side uprights connected by a horizontal member at the top.*
Post-tensioning	*The method of making prestressed concrete with steel strands tightened after the concrete has hardened.*
Pozzolana	*The volcanic dust first found at Pozzuoli, with which the Romans made waterproof concrete.*
Pratt truss	*A patent truss design with iron diagonals in tension.*
Pre-tensioning	*The method of making prestressed concrete with steel strands under tension as the concrete sets.*
Prefabrication	*The manufacture of structural units in an off-site factory.*
Prestressed concrete	*A modern type of concrete with stretched steel strands embedded in it to impart additional tensile strength.*
Pylon	*The vertical structural element from which stays radiate in a cable-stayed bridge.*
Reinforced concrete	*Concrete with steel bars or mesh embedded in it for increased tensile strength.*
Ripple	*The undulating motion of a suspended deck caused by wind.*
Scour	*The destructive effect on submerged piers from fast-flowing water.*
Segmental arch	*An arch formed from a segment of a circle.*
Semi-circular arch	*An arch forming a complete half-circle.*
Semi-fan configuration	*A style of cable-stayed bridge midway between the fan and harp.*
Shear	*The force acting across any beam or structural unit.*

Term	Explanation
Side-span	The outer suspended section of a suspension bridge from the tower to the anchorage, balancing the central suspended span.
Side-sway	The movement of a suspended bridge deck from side to side in wind.
Soffit	The under-surface of any piece of structure.
Spandrel	The area of an arch bridge above the extrados and below deck level.
Springing	The point where the end of an arch meets the abutment.
Stay	The staying or suspending bridge element; in modern suspension bridges, the main supporting cable is hung from towers, and formed from steel wire bound in strands.
Starling	The usually boat-shaped foundation for a masonry pier.
Steel	An alloy of iron with more carbon than wrought iron but less than cast iron, combining the tensile strength of the former with the compressive strength of the latter.
Stiffening truss	A truss usually beneath the entire deck of a suspension bridge.
Strand	A unit within a suspension bridge cable, itself formed from many individual wires.
Striking	The action of removing formwork, particularly centering, from beneath a completed arch.
Suspender	The vertical or zig-zag element on suspension bridges that links a cable with a deck.
Suspension bridge	A bridge with its deck supported from above by large cables or chains hanging from towers.
Swing bridge	A type of moving bridge in which the deck pivots sideways.
T-beam	A beam or girder with a T-shaped cross-section.
Tenon	A projecting piece of a member that fits into a mortise cut in another to form a joint.
Tensile strength	The ability of a material to withstand tension.
Tension	The pulling force that tends to lengthen a member.
Tied arch	See bowstring arch.
Torsion	The strain produced by twisting.
Tower	The vertical element in suspension bridges from which cables are hung.
Town truss	A patent truss design forming a wooden lattice.
Transporter bridge	A type of moving bridge in which a traveling gondola is suspended from an overhead frame.
Trapezoid	A four-sided figure with one pair of parallel sides.
Travertine	A pale form of limestone.
Truss	A frame of members in tension and compression.
Tuned mass damper	A counterweight to subdue a bridge deck's tendency to vibrate.
Voussoir	The wedge-shaped units, usually stone, from which an arch is formed.
Web	The side-plates of a box-gird r.
Whipple truss	Several patent designs by Squire Whipple: the most characteristic was a bowstring, with a curved cast-iron upper chord and lower members of wrought iron.
Wire cable	See cable.
Wrought iron	Soft and malleable alloy with very low carbon content; low compressive strength, high tensile strength.
Zig-zag bridge	Traditional Chinese bridge type, with deck elements at right angles to each other.

Term	Explanation
Zig-zag suspension	*The arrangement of suspension bridge cables first introduced on the Severn Bridge, as differing from vertical suspenders.*

Source: adapted by the author from Bridges Dictionary (2006)